

THESIS

HEMOCOMPATIBILITY OF POLYMERIC MATERIALS FOR BLOOD-CONTACTING
APPLICATIONS

Submitted by

Jodi Marie Woodbury

Graduate Degree Program in Bioengineering

In partial fulfillment of the requirements

For the Degree of Master of Science

Colorado State University

Fort Collins, Colorado

Spring 2015

Master's Committee:

Advisor: Ketul Popat

Prasad Dasi

Melissa Reynolds

Copyright by Jodi Marie Woodbury 2015

All Rights Reserved

ABSTRACT

HEMOCOMPATIBILITY OF POLYMERIC MATERIALS FOR BLOOD-CONTACTING APPLICATIONS

Hemocompatibility of a biomaterial plays a vital role in the overall success of the biomaterial in the body. Every implanted biomaterial tends to cause an immune response by the host tissue. The intensity of said response depends on many factors, including the properties of the material itself. In this study, we have assessed the hemocompatibility of expanded polytetrafluoroethylene (ePTFE), linear low-density polyethylene (LLDPE) and polyethylene terephthalate (PET); 3 potential materials for blood-contacting applications. The surface morphology was characterized using scanning electron microscopy (SEM), and surface wettability was characterized using contact angle goniometry. The cytotoxicity was investigated using lactate dehydrogenase (LDH) assay. The adsorption of key blood serum proteins was evaluated using micro-bicinchoninic acid (micro-BCA) assay. The results were visualized using SEM. Platelet adhesion and activation was investigated using live cell staining and SEM. Whole blood clotting kinetics were evaluated using a hemolysis assay and the results visualized using SEM. The results indicate that none of these materials are cytotoxic. Protein adsorption was highest on PET, and platelet adhesion was significantly higher on PET. However, the percentage of activated platelets and whole blood clotting kinetics was comparable on all materials. This work successfully creates a baseline against which the hemocompatibility of modified ePTFE, LLDPE and PET can be measured.

Keywords: hemocompatibility, platelets, biomaterial, implant, vascular graft, heart valve

ACKNOWLEDGEMENTS

I would like to thank the following individuals for their invaluable help which enabled me to complete this thesis. First and foremost, I would like to thank Dr. Ketul Popat, my teacher and advisor, for time spent mentoring me and helping me plan and execute experiments. Without his help, I would not have progressed as I did. I would especially like to thank him for his understanding and willingness to continue working with me when my circumstances required a drastic change in my program of study.

I wish to thank my fellow members in lab, Dr. Victoria Leszczak, Dr. Nathan Trujillo, and Jonathon Sorkin, MS. Thank you for teaching me the skills I would need to complete the work presented in this thesis. Thank you for all the tips, for the time spent helping me work through problems, and especially for the friendship you gave me.

Thanks are in order for Dr. Sue James, Dr. David Prawel, and Dr. Prasad Dasi. These are people provided direction when I needed it, whose mastery of subjects outside of the scope of this thesis helped me to understand my own work a little better.

I especially want to thank Nicole Lewis. She worked very closely with me when I first started at CSU, and without her help I could not have learned as quickly as I did.

Finally, thank you to John Cavicchia, Rachael Walker and Ryan Oba, for the close friendship and the comic relief. I'm immensely grateful to you for all the hours spent studying for classes and for the grip on reality you helped me maintain when the stress of school got to be overwhelming.

DEDICATIONS

I would like to dedicate this work to my family, without whom none of this would have been possible.

To my heroes, my parents, John and Corrina Emch, thank you for teaching me that little girls can play with Legos and to never give up on my dreams. Thank you for being happy for my successes and for never accepting anything less than my best. You taught me strength and confidence and how to find my own path. I would not be who I am and I could not have achieved what I have achieved without you.

To my parents-in-law, Mark and Rebecca Woodbury, thank you for all the dinners, game nights and words of advice you have given me. Those wonderful meals and late-night conversations helped me more than you can ever know.

To my husband, Nathan Woodbury, thank you for the love and encouragement you have given me throughout the duration of my work at CSU. Thank you for your patience and your kindness, and especially for giving me your last name. I could not have found the strength to keep pursuing this degree without you by my side.

Finally, to my sisters and brothers, and to the rest of my family who are too numerous to mention by name, thank you for the memories. You have helped me to finish this degree in ways that I cannot describe.

TABLE OF CONTENTS

ABSTRACT.....	ii
ACKNOWLEDGEMENTS.....	iii
DEDICATIONS.....	iv
LIST OF FIGURES	vii
INTRODUCTION	1
SPECIFIC AIMS	3
CHAPTER 1	5
LITERATURE REVIEW.....	5
1.1 Introduction	5
1.2 Physiological Response to Implanted Blood-Contacting Biomaterials.....	6
1.3 Artificial Heart Valve Applications for Blood-Contacting Biomaterials.....	15
1.4 Polymeric Materials for Blood-Contacting Applications.....	35
1.5 Effect of Material Surface Characteristics on Blood-Material Interactions.....	37
1.6 Conclusion.....	39
REFERENCES	40
CHAPTER 2	52
MATERIALS AND METHODS	52
2.1 Introduction	52
2.2 Fabrication of Substrates	53
2.3 Surface Characterization.....	57
2.4 Collection of Whole Blood.....	59
2.5 Cytotoxicity	60
2.6 Protein Adsorption.....	61
2.7 Platelet and Leukocyte Adhesion and Activation.....	63
2.8 Whole Blood Clotting.....	67
2.9 Statistical Analysis	68
2.10 Conclusion.....	69
REFERENCES	70

CHAPTER 3	73
RESULTS AND DISCUSSION	73
3.1 Introduction	73
3.2 Analysis of the Effect of the Carbon Tape and PTFE Disc	73
3.3 Surface Characterization.....	79
3.4 Cytotoxicity	83
3.5 Protein Adsorption.....	85
3.6 Platelet and Leukocyte Adhesion	89
3.7 Platelet and Leukocyte Activation.....	94
3.8 Whole Blood Clotting Kinetics	100
3.9 Conclusion	103
REFERENCES	105
 CHAPTER 4	 110
OVERALL CONCLUSIONS AND RECOMMENDATIONS FOR FUTURE WORK	110
4.1 Summary and Overall Conclusions	110
4.2 Recommendations for Future Work	115
REFERENCES	117

LIST OF FIGURES

- Figure 1.2.1:** Summary of the immune response toward biomaterials. The response consists of an inflammatory response, which can be intensified to the point of causing a foreign body response. 7
- Figure 1.2.2:** The possible interactions between the coagulation and complement systems and platelets and other immune cells. Reprinted from *Biomaterials*, Vol. 25, Maud B. Gorbet and Michael V. Sefton, *Biomaterial Associated Thrombus: Role of Coagulation Factors, Complement, Platelets and Leukocytes*, 5681-5703, Copyright 2004, with permission from Elsevier. 8
- Figure 1.2.3:** Simplified diagram of the intrinsic and extrinsic pathways of coagulation, showing the point at which both pathways intersect. Reprinted from *Biomaterials*, Vol. 25, Maud B. Gorbet and Michael V. Sefton, *Biomaterial Associated Thrombus: Role of Coagulation Factors, Complement, Platelets and Leukocytes*, 5681-5703, Copyright 2004, with permission from Elsevier. 9
- Figure 1.2.4:** Diagram showing the approximate time scale of protein adsorption, platelet adhesion and leukocyte adhesion during an immune response to an implanted biomaterial. Reprinted from *Biomaterials*, Vol. 25, Maud B. Gorbet and Michael V. Sefton, *Biomaterial Associated Thrombus: Role of Coagulation Factors, Complement, Platelets and Leukocytes*, 5681-5703, Copyright 2004, with permission from Elsevier. 11
- Figure 1.2.5:** Illustration of the events and timing of the foreign body response. Reprinted with permission from the *Annual Review of Biomedical Engineering*, Vol. 6, Buddy D. Ratner and Stephanie J. Bryant, *Biomaterials: Where Have We Been and Where Are We Going*, 41-75, Copyright 2004. 14
- Figure 1.3.1:** Diagram of the heart interior with colored arrows representing blood flow. Blue arrows represent blood flow to the lungs and red arrows represent blood flow through the body. Reprinted with permission from the National Heart, Lung and Blood Institute; National Institutes of Health; U.S. Department of Health and Human Services. 16

- Figure 1.3.2:** Depiction of stenosis in the aortic valve, characterized by a dramatically reduced open valve area. Reprinted with permission from the MayoClinic.com article “Aortic Valve Stenosis.” (<http://www.mayoclinic.org/normal-heart-and-aortic-valve-stenosis/img-20007788>) 17
- Figure 1.3.3:** Regurgitation due to mitral valve prolapse. Reprinted with permission from the National Heart, Lung and Blood Institute; National Institutes of Health; U.S. Department of Health and Human Services 19
- Figure 1.3.4:** Images of caged-ball valves. (a) Hufnagel valve, the original mechanical heart valve and (b) the Starr-Edwards mechanical heart valve. Reprinted from Medical Engineering and Physics, Vol. 33, Issue 2, Hadi Mohammadi and Kibret Mequanint, Prosthetic Aortic Heart Valves: Modeling and Design, 131-147, Copyright 2011, with permission from Elsevier 21
- Figure 1.3.5:** Images of three different caged-disc valves. Reprinted from The Annals of Thoracic Surgery, Vol. 76, Iss. 6, Vincent L. Gott, Diane E. Alejo, and Duke E. Cameron, Mechanical Heart Valves: 50 Years of Evolution, S2230-S2239, Copyright 2003, with permission from Elsevier. 22
- Figure 1.3.6:** Images of different types of tilting disc valves. Reprinted from The Annals of Thoracic Surgery, Vol. 76, Iss. 6, Vincent L. Gott, Diane E. Alejo, and Duke E. Cameron, Mechanical Heart Valves: 50 Years of Evolution, S2230-S2239, Copyright 2003, with permission from Elsevier. 23
- Figure 1.3.7:** Images of four different bileaflet mechanical heart valves. Reprinted from The Annals of Thoracic Surgery, Vol. 76, Issue 6, Vincent L. Gott, Diane E. Alejo, and Duke E. Cameron, Mechanical Heart Valves: 50 Years of Evolution, S2230-S2239, Copyright 2003, with permission from Elsevier. 24
- Figure 1.3.8:** Images of (A) a porcine xenograft valve, (B) a bovine pericardial valve and (C) a human allograft/homegraft valve. Reprinted from Circulation Research, Vol. 97, Ivan Vesely, Heart Valve Tissue Engineering, 743-755, Copyright 2005, with permission from Wolters Kluwer Health. 27
- Figure 1.3.9:** Images of the three most widely used stentless heart bioprosthetic valves, produced by Baxter, Medtronic, and St. Jude, from left to right. Reprinted from Cardiovascular Pathology, Vol. 12, Issue 5, Ivan Vesely, The Evolution of Bioprosthetic Heart Valve Design and its Impact on Durability, 277-286, Copyright 2003, with permission from Elsevier. 28

Figure 1.3.10: Schematic of a bileaflet mechanical heart valve showing damage to the blood components. Reprinted from Clinical and Experimental Pharmacology and Physiology, Vol. 36, Issue 2, Lakshmi P. Dasi, Helene A. Simon, Philippe Sucosky and Ajit P. Yoganathan, Fluid Mechanics of Artificial Heart Valves, 225-237, Copyright 2008, with permission from John Wiley and Sons.	31
Figure 1.3.11: Hypothetical models for the structural deterioration of bioprosthetic valves. Reprinted from Circulation, Vol. 119, Philippe Pibarot and Jean G. Dumesnil, Prosthetic Heart Valves: Selection of the Optimal Prosthesis and Long-Term Management, 1034-1048, Copyright 2009, with permission from Wolters Kluwer Health.	32
Figure 2.2.1: Images of the carbon tape circles and PTFE discs used to create the substrates. ..	55
Figure 2.3.1: ramé-hart Model 250 Standard Goniometer used to obtain contact angle measurements.	57
Figure 2.3.2: Illustration of contact angles corresponding to hydrophobicity and hydrophilicity. Reprinted with permission from Colorado State University, Figure 2.3.7 from the thesis of Jonathon Sorkin, “Titania Nanotube Arrays as Potential Interfaces for Neurological Prostheses.”	58
Figure 2.3.3: Scanning Electron Microscope (SEM) used to obtain SEM images, model JEOL JSM SEM 6500F	59
Figure 2.5.1: Plate reader – FLUOstar Omega	61
Figure 2.7.1: Fluorescent Microscope – Zeiss Imager.A2.....	64
Figure 3.2.1: The cytotoxicity of the 3 groups of TCPS. The results indicate no statistical difference between the control group and the test groups.....	75
Figure 3.2.2: Fluorescence microscopy images of platelets stained with calcein AM on different groups, showing visual difference between the control and test groups.....	76
Figure 3.2.3: Platelet coverage of the different groups. There are significantly less platelets adhered to the control group as compared to the test groups (* → p<0.05).	77

Figure 3.2.4: SEM images of adhered platelets, showing a similar trend to that found in the fluorescence microscopy images..... 78

Figure 3.2.5: Percentage of activated platelets on the substrates in each of the three groups. No statistical differences exist. 78

Figure 3.3.1: SEM images showing the surface structure of different materials..... 80

Figure 3.3.2: Contact angle measurements on different surfaces. The contact angle of TCPS is statistically different than that of ePTFE, LLDPE and PET (* \rightarrow $p < 0.05$) and that of LLDPE was statistically different than that of ePTFE and PET (# \rightarrow $p < 0.05$). 82

Figure 3.4.1: Cytotoxicity analysis of different materials using LDH assay. The results indicate no statistical differences in the cytotoxicity of all the materials. 84

Figure 3.5.1: ALB, IgG and FIB adsorption on different materials measured with micro-BCA assay. The results indicate no statistical difference in FIB adsorption on all the materials; however, FIB adsorption was statistically higher compared to ALB and IgG adsorption on all the materials (statistical symbol for this is not shown on the graph). ALB and IgG adsorption on PET was significantly higher than that on PS, ePTFE, and LLDPE (* \rightarrow $p < 0.05$). ALB and IgG adsorption on PS was significantly higher than that on ePTFE and LLDPE (# \rightarrow $p < 0.05$)..... 86

Figure 3.5.2: SEM images of ALB, IgG and FIB adsorbed to the surfaces of TCPS, ePTFE, LLDPE and PET. 88

Figure 3.6.1: Fluorescence microscopy images of platelets stained with calcein AM on different materials. 90

Figure 3.6.2: Platelet coverage on different surfaces calculated using ImageJ software and fluorescence microscopy images. Platelet coverage on PET is significantly higher than that on TCPS, ePTFE and LLDPE (* \rightarrow $p < 0.05$). 91

Figure 3.6.3: Fluorescence microscopy images of platelets and leukocytes stained with actin and DAPI on different materials. 92

Figure 3.6.4: Leukocyte coverage on different surfaces calculated using ImageJ software and fluorescence microscopy images. Leukocyte coverage on TCPS is significantly higher than that on ePTFE, LLDPE and PET (* → p<0.05). 93

Figure 3.7.1: SEM images of platelet adhesion and activation on different materials. 95

Figure 3.7.2: Percentage of activated platelets on different materials. PET has significantly higher percentage of activated platelets compared to LLDPE (*→ p<0.05). No other statistical difference exist. 96

Figure 3.7.3: Fluorescence microscopy images of P-selectin and CD45 expression on different materials. The images do not indicate an obvious visual difference between the materials. 98

Figure 3.7.4: P-selectin and CD45 coverage on different surfaces calculated using ImageJ software and fluorescence microscopy images. No statistical differences exist for either P-selectin or CD45 on any of the materials. 99

Figure 3.8.1: Absorbance due to amount of free hemoglobin in DI water after 15, 30, 45 and 60 minutes of clotting time. No statistical differences exist between the materials at any time point. 101

Figure 3.8.2: SEM images of blood clots on the surfaces of TCPS, ePTFE, LLDPE and PET 103

INTRODUCTION

This research seeks to evaluate the baseline hemocompatibility of three polymeric materials that have a potential for use in various blood-contacting applications, specifically, heart valve leaflet applications. Artificial heart valves have been used since the 1950s to treat heart valve disease. Mechanical heart valves are extremely durable, although they require the use of lifelong anticoagulant therapy to prevent thromboembolism complications. Bioprosthetic heart valves, in contrast, do not require anticoagulant therapy due to superior hemodynamics as compared to mechanical valves. However, the durability of bioprosthetic valves is far inferior to that of mechanical valves. Generally, these valves require replacement within 10-15 years due to mechanical failure. In an effort to combine the durability of mechanical valves with the compatibility of a bioprosthetic valve, research has been evaluating the feasibility of creating heart valve leaflets using polymeric materials. These types of heart valves show promising hemodynamics, although they are susceptible to tearing of the leaflet. Furthermore, no type of prosthetic heart valve has been able to completely overcome the immune response from the host tissue. This response consists of an inflammatory response that can eventually become a foreign body response, which can ultimately result in failure of the implant. Several attempts have been made at modification of material properties to mitigate this complication, although further research is needed before a truly biocompatible material is created. In this research, the physiological response of blood to the three polymeric materials was investigated. Expanded polytetrafluoroethylene (ePTFE), linear low density polyethylene (LLDPE) and polyethylene terephthalate (PET) were studied and compared to tissue culture polystyrene (TCPS), a material known to promote cell adhesion.

This work is divided into two specific aims. The first aim focuses on developing a technique with which to conduct the hemocompatibility studies that would overcome the floatation of the materials. It includes the determination of any effects on the results which may occur as a result of using the technique.

The second aim seeks to characterize the baseline hemocompatibility of ePTFE, LLDPE and PET. Adsorption of key blood proteins, albumin, immunoglobulin G, and fibrinogen were studied because this is generally accepted as the first event that occurs after implantation of biomaterial. This layer of protein directly influences all other steps in the inflammatory response. Next, platelet and leukocyte adhesion and activation on each of the materials was studied. These are the cells which initiate and intensify the coagulation cascade, which eventually leads to thrombus formation. The whole blood clotting kinetics were investigated, to determine which, if any, of the materials promote faster rates of blood clotting. Finally, the surface properties were characterized in the hopes of explaining the hemocompatibility of these materials in terms of their properties.

The work in this master's thesis establishes the baseline hemocompatibility of ePTFE, LLDPE and PET. The conclusion of this research indicates that the hemocompatibility of ePTFE, LLDPE and PET are comparable in their unmodified form to TCPS. The baseline established herein can then be used to evaluate any improvement in hemocompatibility future modifications of these materials may promote.

SPECIFIC AIMS

Fundamental Motivation: Establish a baseline hemocompatibility of ePTFE, LLDPE and PET against which any future modifications these materials can be compared.

Specific Aim 1: Development of a technique with which to conduct hemocompatibility experiments that addresses the issue of floatation of the test materials. This specific aim is discussed in detail in chapters 2 and 3 and will address the following:

- (a) Design of a well-controlled, reproducible method which enables consistency of exposure time in all liquids required in these studies.
- (b) Determination of the effect, if any, that the use of the method determined in part (a) will have on the results of the studies.

Specific Aim 2: Investigate the hemocompatibility of ePTFE, LLDPE and PET in comparison to that of TCPS. This specific aim is discussed in detail in chapters 2 and 3 and will include the following:

- (a) Characterization of surface structure and properties of these materials
- (b) Characterization of key blood proteins onto the surfaces of these materials.

(c) Evaluation of platelet and leukocytes adhesion and activation in response to these materials.

(d) Evaluation of whole blood clotting kinetics on these materials.

CHAPTER 1

LITERATURE REVIEW

1.1 Introduction

The need for blood-contacting biomaterials is urgent. These biomaterials are used in applications such as artificial heart valves, vascular grafts, kidney dialysis, and vascular stents. Heart disease which requires heart valve replacement has an extremely high occurrence, and the need is only expected to increase. The current options on the market are plagued either by a need for lifelong anticoagulants, or durability issues. Commercially available heart valves are either mechanical or bioprosthetic. Mechanical heart valves are extremely durable, but require lifelong anticoagulants. Bioprosthetic valves have better hemodynamics than mechanical valves, but are susceptible to tearing and calcification of the leaflets. Despite the prevalent use of these implants and the improvements that have been made, a truly biocompatible blood-contacting material has yet to be developed. Every implanted material causes a response by the host into which they are implanted. This includes an inflammatory response which can ultimately result in thrombosis or complete encapsulation of the implant. A great deal of research has gone into the development and improvement of new polymeric materials with which to make blood-contacting biomaterials. These materials include expanded polytetrafluoroethylene (ePTFE) and polyethylene terephthalate (PET). A third material, linear low density polyethylene (LLDPE) is not yet used as an implantable biomaterial, but has promising mechanical properties and initial biocompatibility results that suggest it could be used as such. The development of these materials as implantable biomaterials could improve the quality of life of the recipients, if issues with biocompatibility and durability are overcome.

1.2 Physiological Response to Implanted Blood-Contacting Biomaterials

The immune response is the defense mechanism through which the human body protects itself from unfamiliar organisms or other foreign entities. There are two types of immune response. The innate, or non-specific, immune response reacts almost immediately to any foreign entity or injury. The adaptive, or specific, immune response involves immunological memory, through which pathogen-specific antibodies are formed¹. Although the immune response is normally used to defend against foreign organisms, it has been hypothesized that it plays a role in biocompatibility of implanted biomaterials².

The process of implanting a biomaterial results in injury to tissues or organs. Because of this, the innate immune response is activated. Thus, any material will initiate a response reminiscent of tissue repair upon implantation into a living host^{3, 4}. The response that occurs can be grouped into two overall phases: the inflammatory response and the foreign body response. There has been a large amount of research that has studied the mechanisms through which these physiological responses occur, which include the intrinsic and extrinsic pathways of coagulation, the complement system, and interactions of platelets and other immune cells. The phases of the biological response to implanted biomaterials are summarized in **Figure 1.2.1**.

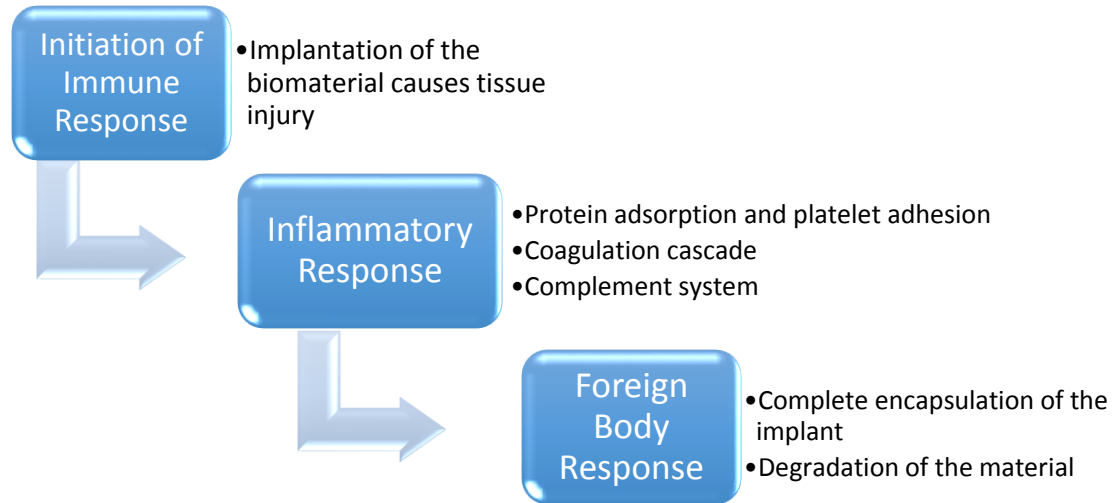


Figure 1.2.1: Summary of the immune response toward biomaterials. The response consists of an inflammatory response, which can be intensified to the point of causing a foreign body response.

1.2.1 *The Inflammatory Response*

The inflammatory response begins with blood-material interactions, which include protein adsorption, platelet/leukocyte adhesion, and activation of the coagulation and complement systems⁵. Within seconds of implantation, blood serum proteins adsorb non-specifically to the surface of the material. In normal physiological wound healing, the non-specific adsorption of blood proteins does not occur, which suggests that this step in the response to biomaterials may instigate all subsequent events⁶. The adsorption is controlled by the concentration of proteins in the blood and their diffusion coefficients. Initially, albumin is the protein which interacts most with the material surface. Over time, protein desorption followed by adsorption of different proteins may occur, which is known as the Vroman effect⁷. The layer of protein can vary many ways, including the types, amounts and conformation of the proteins which adsorb. The conformation of the proteins is critical, as this is what determines if the host cell response will be constructive or destructive⁸. It is through this layer of protein that cells sense the biomaterial, thus it is this layer that directly influences the activation of the coagulation cascade, complement

system, platelets and immune cells³. Furthermore, the interaction between the various systems in also influenced by the layer of protein adsorption³. The arrows shown in **Figure 1.2.2** summarize the possible interactions that can occur between the various systems in the physiological response to biomaterials.

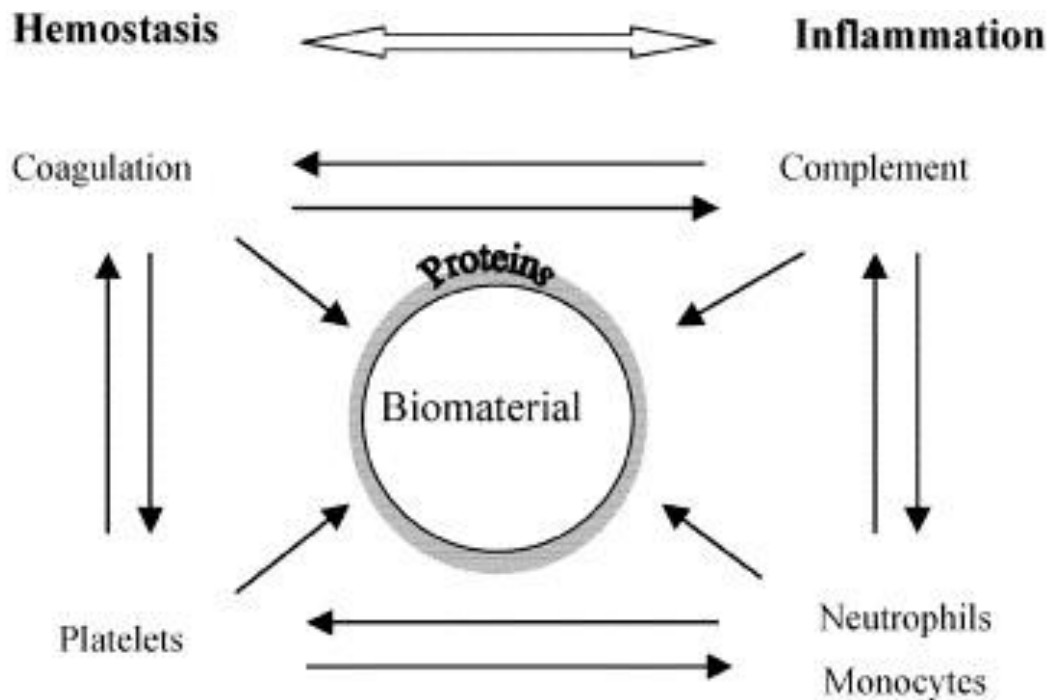


Figure 1.2.2: The possible interactions between the coagulation and complement systems and platelets and other immune cells. Reprinted from *Biomaterials*, Vol. 25, Maud B. Gorbet and Michael V. Sefton, *Biomaterial Associated Thrombus: Role of Coagulation Factors, Complement, Platelets and Leukocytes*, 5681-5703, Copyright 2004, with permission from Elsevier.

Coagulation can occur through either the intrinsic or extrinsic pathways, depicted in **Figure 1.2.3**. Factor XII (FXII) and tissue factor (TF) initiate the intrinsic and extrinsic pathways, respectively. FXII is a protein which is activated upon contact with a biomaterial surface, followed by a series of protein reactions which result in release of thrombin. The amount of thrombin released by the intrinsic pathway is insufficient to induce thrombus formation, suggesting the

interaction of this pathway with other systems is required to generate a clot³. TF is expressed by damaged cells at the site of vascular injury, thereby activating the extrinsic system of coagulation. Hence, activation of the extrinsic pathway is also implicated to play a role in the physiological response to implanted biomaterials⁵.

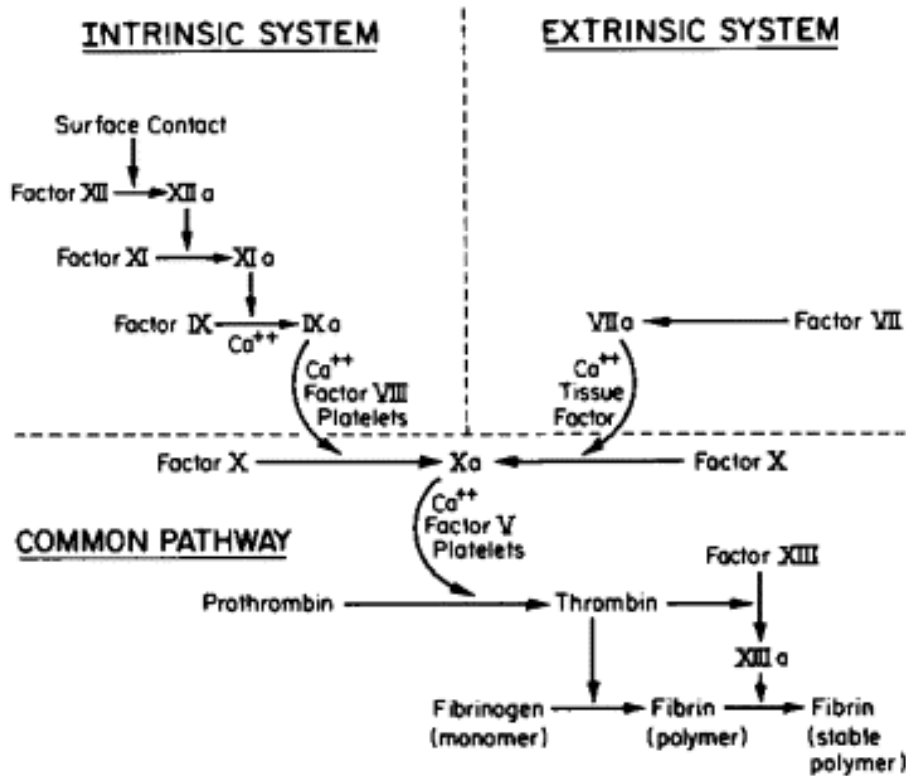


Figure 1.2.3: Simplified diagram of the intrinsic and extrinsic pathways of coagulation, showing the point at which both pathways intersect. Reprinted from Biomaterials, Vol. 25, Maud B. Gorbet and Michael V. Sefton, Biomaterial Associated Thrombus: Role of Coagulation Factors, Complement, Platelets and Leukocytes, 5681-5703, Copyright 2004, with permission from Elsevier.

The two different pathways of coagulations are not independent of each other. When coagulation is induced by the extrinsic pathway, the intrinsic pathway will still contribute to thrombin formation, playing a significant role in propagation of the response⁵.

Platelet adhesion rapidly follows protein adsorption. This is heavily influenced by the amount of fibrinogen adsorption, which is known to occur spontaneously on biomaterials³. Activation of platelets occurs due to calcium signaling^{9, 10}. Platelets that have adhered to a surface can be activated by molecules such as adenosine diphosphate (ADP), thromboxane A₂ (TXA₂), and thrombin, which bind to specific receptors on the surface¹¹. Thrombin is one of the most potent activators of platelets¹². Once activated, the shape of the platelet changes drastically, promoting platelet-platelet adhesion and increasing platelet recruitment. Additionally, the platelets release alpha granules upon activation, which contain signaling factors such as platelet factor 4 (PF-4) and P-selectin^{5, 13}. PF-4 increases platelet aggregation and circulating proteases, while P-selectin mediates adhesion of leukocytes to platelets¹⁴. Activated platelets also have a high affinity to bind to monocytes, which induces expression of TF by monocytes¹⁵. This in turn intensifies the coagulation pathway. Thus, the activation of platelets and the coagulation pathways are directly influenced and intensified by one another.

Leukocytes are immune cells which circulate in the blood. This class of cell consists of several different types of cells, but neutrophils and monocytes are the types of leukocytes which play the biggest role in the inflammatory response⁴. As with platelets, leukocyte adhesion is influenced by the layer of adsorbed proteins, but they are also recruited by the signals released by activated platelets and injured cells^{3, 16}. Leukocyte adhesion and activation is a complicated process, which involves many steps. These include rolling, activation and arrest¹⁷. Leukocyte rolling is mediated by L-selectin, E-selectin and P-selectin, all of which interact with glycosylated ligand receptors^{18, 19}. The interaction of these selectins with their ligands enable leukocytes to adhere to surfaces under blood flow conditions, since they form and break bonds at exceptionally high rates¹⁹. While rolling, the leukocyte remains in contact with the surface for prolonged periods

of time, which allow chemokines such as interleukin-8 (IL8) and platelet activating-factor (PAF) to stimulate activation¹⁷. Integrins mediate leukocyte arrest, enabling firm adhesion between the leukocyte and the surface¹⁹. **Figure 1.2.4** illustrates the time scale related to protein adsorption and platelet and leukocyte adhesion. Leukocytes and platelets co-stimulate each other. Activated leukocytes promote increased platelet aggregation, which in turn increases leukocyte activation¹⁶. Thus, adhesion and activation of leukocytes affects platelet adhesion and activation, which in turn affects the coagulation cascade. Once activated, leukocytes present a phagocytic response, which would normally result in removal of the pathogen. With biomaterials, however, this reaction elicits degradation of the material and a prolonged inflammatory response¹.

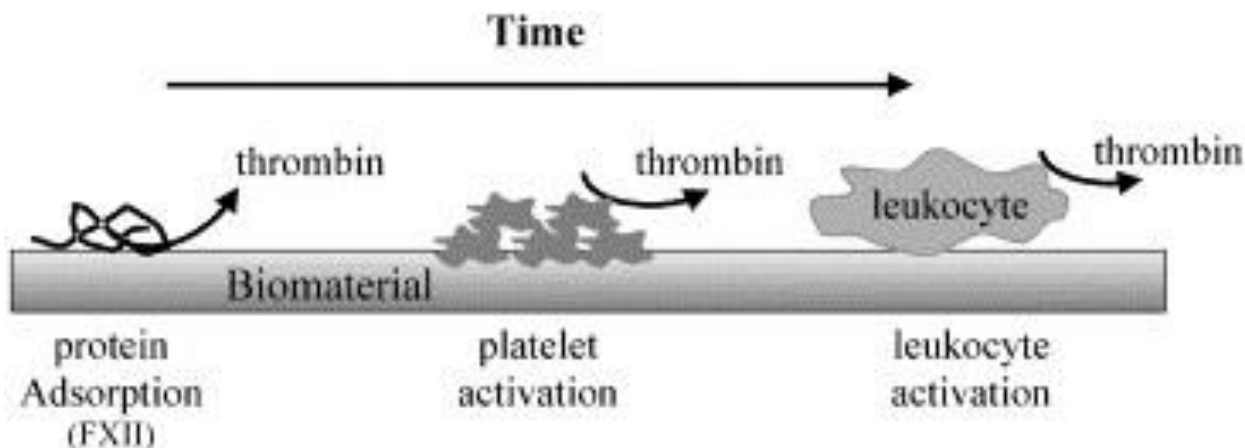


Figure 1.2.4: Diagram showing the approximate time scale of protein adsorption, platelet adhesion and leukocyte adhesion during an immune response to an implanted biomaterial. Reprinted from *Biomaterials*, Vol. 25, Maud B. Gorbet and Michael V. Sefton, *Biomaterial Associated Thrombus: Role of Coagulation Factors, Complement, Platelets and Leukocytes*, 5681-5703, Copyright 2004, with permission from Elsevier.

Complement is a system of 30 plasma and membrane-bound proteins that primarily function to get rid of foreign entities²⁰. Activation is achieved by the enzymatic cleavage of C3 into C3a and C3b by C3 convertases. The convertases are assembled via one of three pathways –

the classical, mannose-binding lectin or alternative pathway²⁰. The alternative pathway is relevant to biomaterials, as it is this pathway that is triggered directly by foreign surfaces. Once activated, the complement system plays a role in platelet and leukocyte recruitment and activation²⁰. Furthermore, activated complement proteins can also promote TF expression by monocytes³. Thus, the systems in the inflammatory response are all linked and the cross-talk between them plays a significant role in the response to implanted biomaterials.

1.2.2 The Foreign Body Response

The inflammation response described above can further be broken down into two phases. The acute inflammation phase is relatively short, lasting minutes to days, depending on the extent of the injury. This phase is characterized by the highest concentrations of monocytes, macrophages and neutrophils⁴. The chronic inflammation phase occurs when macrophages become the predominant cell type in the tissue surrounding the implant. This type of inflammation lasts much longer than acute inflammation⁴. The foreign body response occurs when the inflammatory response is intensified to the point of creation of foreign body giant cells¹. The fibrous capsule that walls off implants is the ultimate result of a foreign body response, illustrated in **Figure 1.2.5**. Scarring of the heart valve sewing rings and fibrous layers surrounding vascular grafts are two examples of this phenomenon⁶. One study has shown a direct link between plasma fibronectin and the foreign body response, suggesting fibronectin may be a modulator of the foreign body response²¹. Undoubtedly, the macrophage plays a key role in this response. Macrophages originate as monocytes, and play a pivotal role in perpetuating the inflammatory response through the cytokines they release²². Eventually, macrophages at the biomaterial interface will fuse together to form multinucleated foreign body giant cells (FBGC). These cells will attempt to degrade and

remove the foreign entity²³. Of the cytokines released by macrophages, transforming growth factor β (TGF β) is the most commonly expressed. This has been linked to chronic fibrosis and has been found abundantly in the fibrous capsules surrounding biomaterial implants, thus implicating a critical role of macrophages in the formation of the capsule surrounding biomaterials²².

Upon implantation in a mammal:

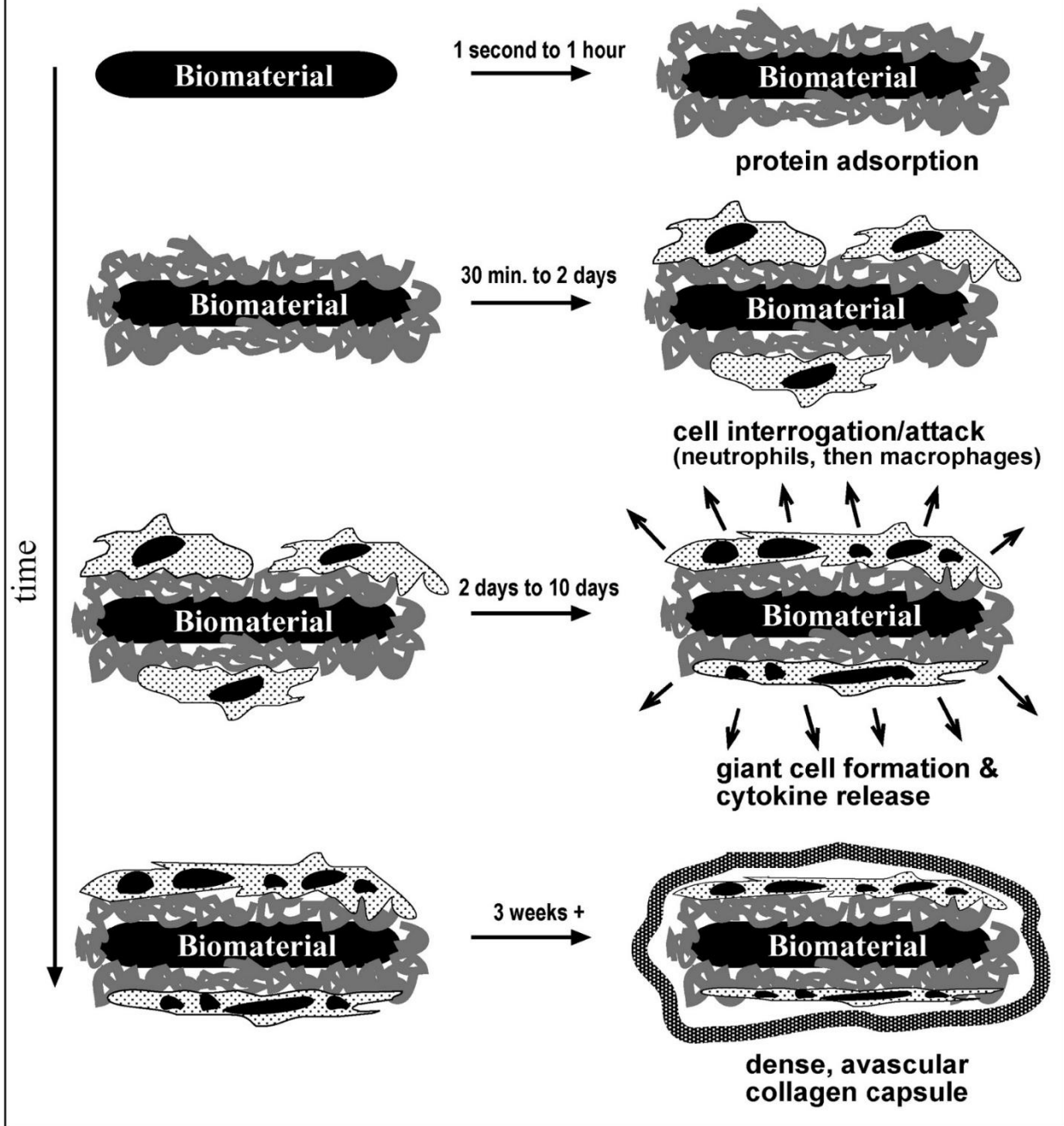


Figure 1.2.5: Illustration of the events and timing of the foreign body response. Reprinted with permission from the Annual Review of Biomedical Engineering, Vol. 6, Buddy D. Ratner and Stephanie J. Bryant, Biomaterials: Where Have We Been and Where Are We Going, 41-75, Copyright 2004.

1.3 Artificial Heart Valve Applications for Blood-Contacting Biomaterials

1.3.1 The Need for Artificial Heart Valves

The heart is a muscular organ which is responsible for pumping blood throughout the body²⁴. Its major anatomical features include the left and right atriums, the left and right ventricles, the valves, and several arteries and veins²⁵. The left and right heart can be considered two separate pump systems. The pulmonary pump, or right heart, is a relatively low-pressure system²⁶. It receives de-oxygenated blood from the body through two major veins: the superior and inferior vena cava. The blood from these veins enter the right atrium, which acts as a staging area for the right ventricle. It enters the right ventricle via the tricuspid valve, and is then pumped via the pulmonary valve into the pulmonary arteries to be oxygenated by the lungs²⁵⁻²⁷. The systematic pump, or left heart, is a high pressure system²⁶. The left side of the heart requires a higher pressure than the right side, because it pumps the blood through the entire body and not just to the lungs²⁵. From the lungs, the oxygenated blood travels to the left atrium via the pulmonary veins. It enters the left ventricle through the mitral valve. The left ventricle then pumps the blood into the aorta through the aortic valve, and from there it is pumped throughout the body²⁵⁻²⁷. **Figure 1.3.1** depicts the interior anatomy of and blood flow through the heart.

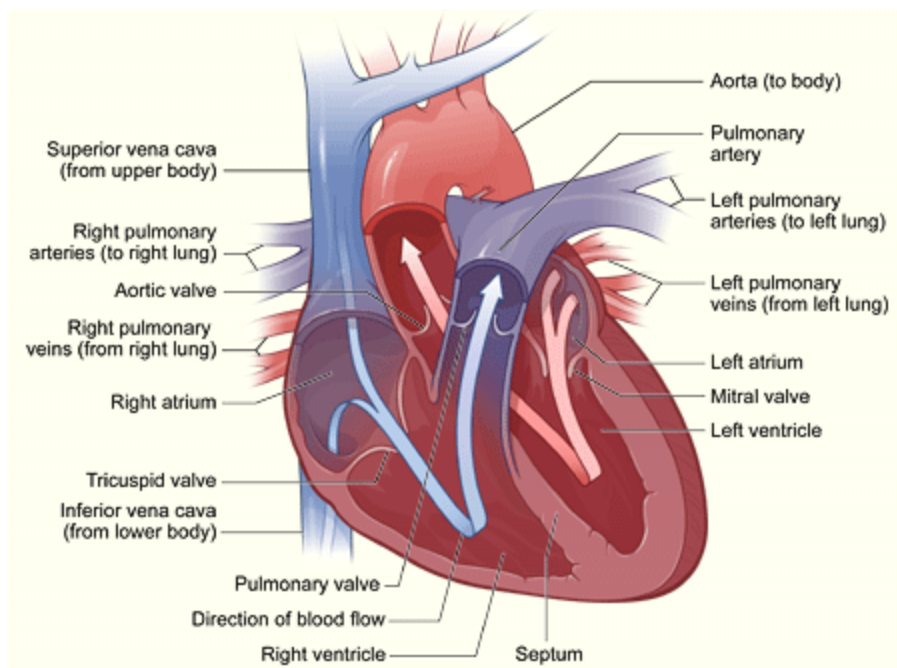
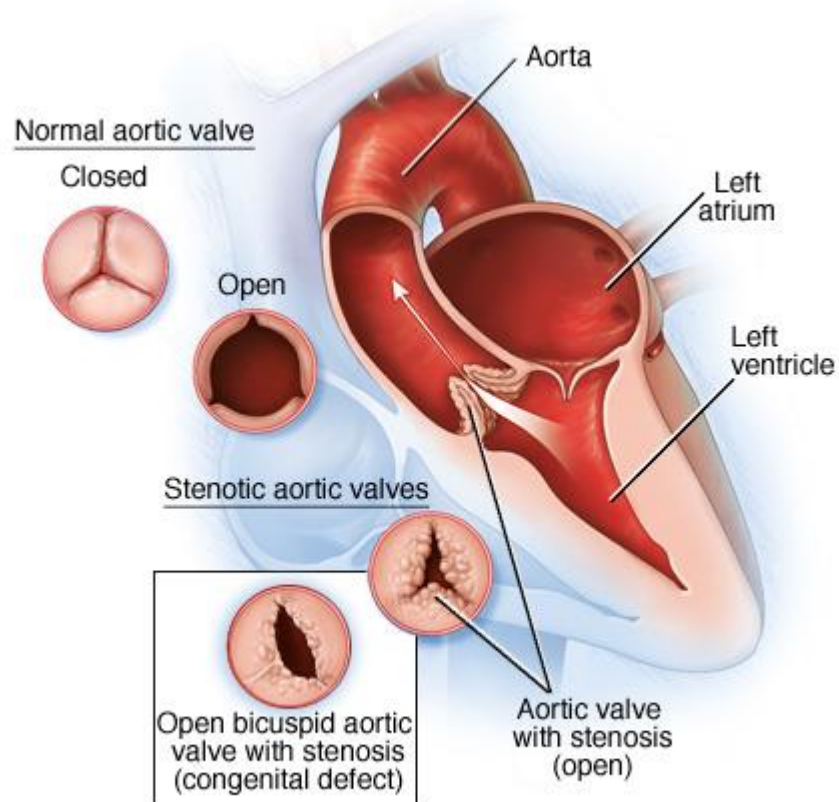


Figure 6.3.1: Diagram of the heart interior with colored arrows representing blood flow. Blue arrows represent blood flow to the lungs and red arrows represent blood flow through the body. Reprinted with permission from the National Heart, Lung and Blood Institute; National Institutes of Health; U.S. Department of Health and Human Services.

In a healthy heart, the valves are essential in turning the muscular chambers of the heart into unidirectional pumps²⁸. However, valve disease can occur quite frequently, especially in the older subset of the population. A malfunctioning heart valve has dire effects on the heart, as the heart is required to work much harder to maintain the required cardiac output²⁹. Valve disease generally strikes the aortic or mitral valves, and is characterized by the lack of proper opening and closing of the valve²⁹. The aortic valve is the most susceptible to disease, because the aortic valve is subject to the largest pressure difference of all the heart valves. This ensures the oxygenated blood is distributed effectively throughout the body³⁰. However, the prevalence of mitral disease is much higher than average in developing countries, due to the high occurrence of rheumatic fever³¹. There are two general manifestations of valve disease, no matter what the underlying cause

is. Stenosis (see **Figure 1.3.2**) is defined by a decreasing valve area, which ultimately causes increased velocity across the valve and increased pressure in the left atrium (mitral valve stenosis) or the left ventricle (aortic valve stenosis)^{31, 32}.



© MAYO FOUNDATION FOR MEDICAL EDUCATION AND RESEARCH. ALL RIGHTS RESERVED.

Figure 1.3.7: Depiction of stenosis in the aortic valve, characterized by a dramatically reduced open valve area. Reprinted with permission from the MayoClinic.com article “Aortic Valve Stenosis.” (<http://www.mayoclinic.org/normal-heart-and-aortic-valve-stenosis/img-20007788>)

Regurgitation occurs when the valve does not entirely close, which allows blood to flow back through. An example of this is shown in **Figure 1.3.3**. This increases the volume of blood in the chamber immediately preceding the valve (left ventricle for aortic regurgitation, left atrium for mitral regurgitation), which inherently increases the pressure^{31, 32}. Symptoms of valvular stenosis

or regurgitation include breathlessness, fainting, and a reduced ability to perform activities that require mild exertion. This occurs because the decreased amount of oxygenated blood that is able to be supplied to the body through malfunctioning valves. Furthermore, the heart attempts to compensate for the reduced cardiac output by working harder, thereby thickening the walls of the ventricles. Once this happens, the volume of the ventricles decrease, which further exacerbates the reduction of blood flow through the heart. Eventually, both stenosis and regurgitation, if left untreated, will result in heart failure. In certain cases, symptomatic mitral stenosis can be treated with balloon mitral valvuloplasty (BMV), although this treatment only delays the need for a valve replacement by about 10 years³¹. In contrast, the only effective method of treating symptomatic aortic stenosis, aortic regurgitation or mitral regurgitation is total valve replacement^{31, 32}.

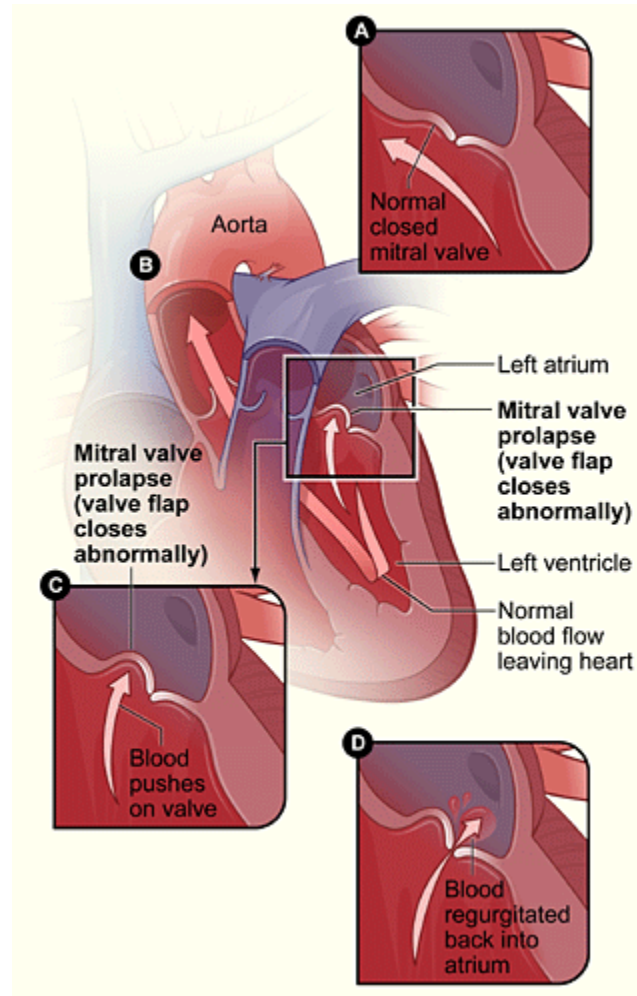


Figure 1.3.8: Regurgitation due to mitral valve prolapse. Reprinted with permission from the National Heart, Lung and Blood Institute; National Institutes of Health; U.S. Department of Health and Human Services.

Valve disease is extremely common. Aortic stenosis is present in up to 4% of adults over the age of 65, and aortic sclerosis, a precursor to aortic stenosis, is present in up to 25% of older adults³². The occurrence of valve disease is expected to increase drastically as the world's population ages. By the year 2050, nearly 21% of the world's population will be over the age of 60. As a result, the estimated number of necessary heart valve replacements is expected to triple

from approximately 300,000 to nearly 900,000³³. Currently, the mortality of valve replacement is less than 5% in younger patients, but that mortality rate doubles in elderly patients³¹. Additionally, while a valve replacement does increase the life expectancy of the patient with valve disease, it will not increase the life expectancy back to what it would be in an age-matched, healthy individual³³. Despite the phenomenal advancements that have been made in the field of heart valve engineering, there is much work to be done to reduce the mortality rates and increase the life expectancy associated with artificial heart valves.

1.3.2 Mechanical Heart Valves

Commercially available prosthetic heart valves are either mechanical or bioprosthetic. There are several different types of mechanical valves, including caged-ball valves, caged-disc valves, single tilting disc valves and bileaflet valves^{34, 35}. Caged-ball valves consist of a silastic ball, a circular sewing ring and metal arches which form the cage³⁶. The ball is seated in the circular sewing ring until the pressure in the chamber of the heart exceeds the pressure outside of the chamber. At this point, the ball is pushed up into the cage, allowing blood to flow³⁷. The first caged ball valve was designed by Dr. Charles Hufnagel, who initially implanted it in 1952³⁵. The most widely used version of the caged ball valves was the Starr-Edwards valve, approved by Food and Drug Administration (FDA) in 1965³⁸. Since then, more than 250,000 Starr-Edwards valves have been implanted³⁵. Images of the Hufnagel and Starr-Edwards valves are seen in **Figure 1.3.4**.

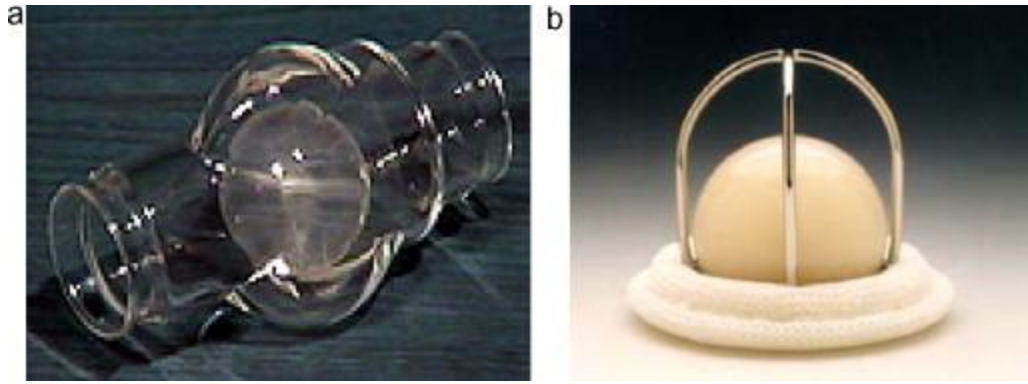


Figure 1.3.9: Images of caged-ball valves. (a) Hufnagel valve, the original mechanical heart valve and (b) the Starr-Edwards mechanical heart valve. Reprinted from Medical Engineering and Physics, Vol. 33, Issue 2, Hadi Mohammadi and Kibret Mequanint, Prosthetic Aortic Heart Valves: Modeling and Design, 131-147, Copyright 2011, with permission from Elsevier

Although these valves are demonstrated to be extremely durable, their hemodynamic properties are undesirable. Caged ball valves have been linked to the highest levels of thrombosis and thromboembolic complications, with nearly five times the incidence rate of major embolism than that of tilting disc valves³⁹. Because of this, patients who receive this type of valve are required to undergo extremely intense, lifelong anticoagulant therapy which drastically increases risk of hemorrhage in patients⁴⁰. As a result, the caged ball valve is generally no longer implanted. The emergence of artificial heart valves with superior hemodynamic properties are what ultimately caused the widespread use of caged ball valves to be discontinued.

Caged-disc valves, seen in **Figure 1.3.5**, are similar to the caged-ball valves, except a disc is contained within the cage in place of a ball²⁸. The caged-disc valves exhibited hemodynamics that were inferior to even the caged-ball valves, and they were removed from production shortly after their conception^{28, 35}.

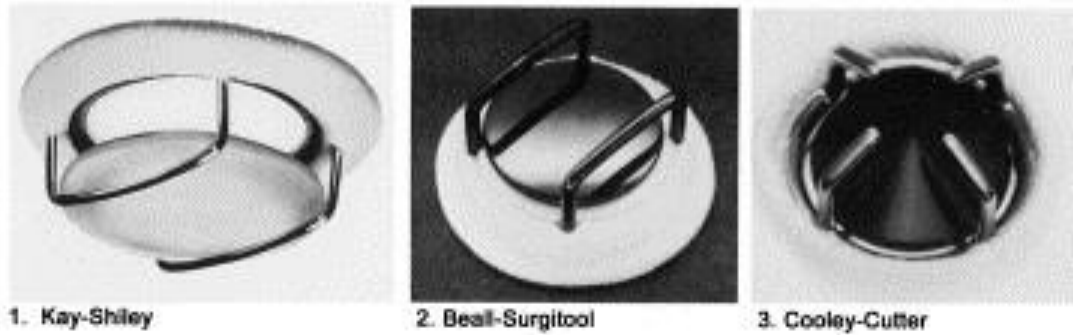


Figure 1.3.10: Images of three different caged-disc valves. Reprinted from *The Annals of Thoracic Surgery*, Vol. 76, Iss. 6, Vincent L. Gott, Diane E. Alejo, and Duke E. Cameron, *Mechanical Heart Valves: 50 Years of Evolution*, S2230-S2239, Copyright 2003, with permission from Elsevier.

Tilting disc valves are comprised of a disc secured to circular ring by lateral or central struts³⁶. The disc rotates about the strut between the closed and open positions during normal function, which prevents the contact wear from the strut components on one region of the disc. When closed, the disc should completely obstruct the valve opening²⁸. Images of several tilting disc valves can be seen in **Figure 1.3.6**.

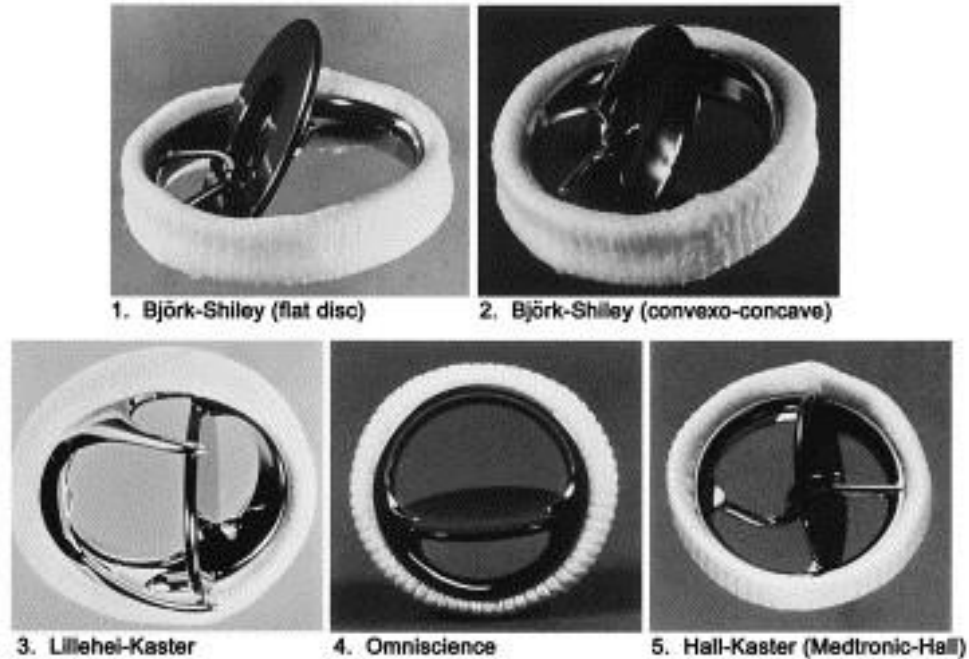


Figure 1.3.11: Images of different types of tilting disc valves. Reprinted from *The Annals of Thoracic Surgery*, Vol. 76, Iss. 6, Vincent L. Gott, Diane E. Alejo, and Duke E. Cameron, *Mechanical Heart Valves: 50 Years of Evolution*, S2230-S2239, Copyright 2003, with permission from Elsevier.

The first iteration of this type of valve was a collaborative project involving Dr. Viking Bjork and Donald Shiley⁴¹. This valve, released in 1969, featured a flat disc and was extremely successful. More than 300,000 of these valves have been implanted worldwide³⁵. The Medtronic-Hall valve (originally Hall-Kaster valve) is the most successful of the tilting disc valves. It features a unique disc with a central perforation for a thin metal strut, which acts as a guide during opening and closing⁴¹. Anticoagulant therapy is still required with these heart valves, despite the fact that the hemodynamics of these valves are superior to the caged-ball valves³⁹. These valves are still widely implanted today³⁷.

The most recent mechanical heart valve designs are the bileaflet heart valves, seen in **Figure 1.3.7**.

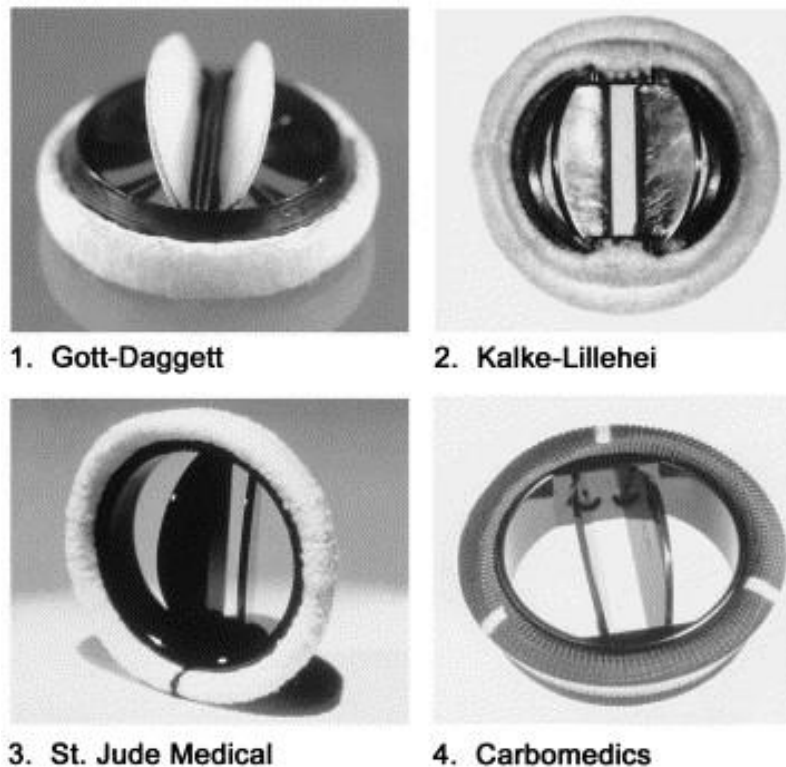


Figure 1.3.12: Images of four different bileaflet mechanical heart valves. Reprinted from *The Annals of Thoracic Surgery*, Vol. 76, Issue 6, Vincent L. Gott, Diane E. Alejo, and Duke E. Cameron, *Mechanical Heart Valves: 50 Years of Evolution*, S2230-S2239, Copyright 2003, with permission from Elsevier.

This type of valve consists of two semicircular leaflets which pivot about a hinge recessed into the ring-shaped housing. While open, the leaflets are away from the plane of the housing. This allows the blood to flow through three openings – a center rectangular orifice and two lateral semicircular orifices. When closed, the leaflets occlude the opening, preventing the blood from flowing through²⁸. The St. Jude Medical bileaflet valve was made entirely of pyrolytic carbon, with the exception of the sewing ring⁴¹. The design of this valve has changed in very minor ways since its introduction in 1977. It is the most widely used artificial heart valve, with over 1.3 million valves implanted³⁵. The bileaflet valves offer the best hemodynamic properties of any of the mechanical

valves^{39, 42}. For this reason, they remain the most popular mechanical heart valve design, accounting for 80% of implanted mechanical valves²⁸.

1.3.3 Bioprosthetic Heart Valves

Despite the widespread and frequent use of mechanical heart valves, their thrombogenic nature has led to a focus on finding a suitable substitute in the form of bioprosthetic heart valves. The design of these valves are meant to mimic the anatomy and function of the native heart valves³⁶. Bioprosthetic valves function due to the pressure gradient across the valve, similar to natural heart valves. When the blood pressure in the left atrium is greater than in the left ventricle (mitral valve), or the pressure in the left ventricle is greater than in the aorta (aortic valve), the leaflets of the valves open outwards, allowing blood to flow. The valves close once their respective pressure gradients reverse³⁰.

Bioprosthetic valves are currently available in three general forms: porcine xenograft valves, bovine pericardial valves, or human allograft/homograft valves⁴³. The first alternative approaches to heart valve replacement made use of human aortic valves from cadaveric tissue (homografts). Direct replacement of a diseased valve with a homograft was first performed in 1962²⁸. The Ross procedure, initially performed in 1967, entailed the surgical replacement of a patient's aortic valve with their pulmonary valve (allograft), and the replacement of the pulmonary valve with a homograft^{28, 43}. This procedure is particularly suited to improving the prognosis of children with valve disease. A major disadvantage of mechanical heart valves is their inability to grow, repair and remodel, and in children, this is especially poignant^{44, 45}. Replacement of the aortic valve with their own pulmonary valve avoids those complications⁴⁶. Despite the clinical success of these procedures, they are not an acceptable replacement for current artificial heart

valves. Their use depends on cadaveric valve supply, which cannot produce nearly enough valves to support the current and future demand for heart valves²⁸.

The porcine xenograft valve was made possible by the development of a tissue-fixation procedure using glutaraldehyde by Carpentier in 1969²⁸. This new procedure provided relatively inert biological tissue which allowed the development of a new artificial heart valve design. Porcine xenograft valves originally consisted of an intact porcine aortic valve, which had been preserved with glutaraldehyde and mounted to a rigid ring with flexible posts⁴³. This configuration was released as the Hancock Porcine Xenograft by Medtronic in 1970, and its use remains quite prevalent today²⁸. In 1976, Edwards Lifesciences released the Carpentier-Edwards Bioprosthesis. This was a porcine valve mounted on an entirely flexible frame²⁸. Since then, porcine valves are prepared in various ways, to maximize either ease of implantation or effective orifice area⁴³.

Bovine pericardial valves, or pericardial valves, are essentially sheets of preserved bovine pericardium mounted on supports³⁰. The design is meant to mimic the look and function of porcine valves⁴⁷. In 1991, the Carpentier-Edwards pericardial valve was approved for commercial use in the US. This valve provided better durability and hemodynamics than its predecessors²⁸. Since then, only a few other pericardial valves have been approved for commercial use in the US. Images of all three types of bioprostheses are shown in **Figure 1.3.8**.

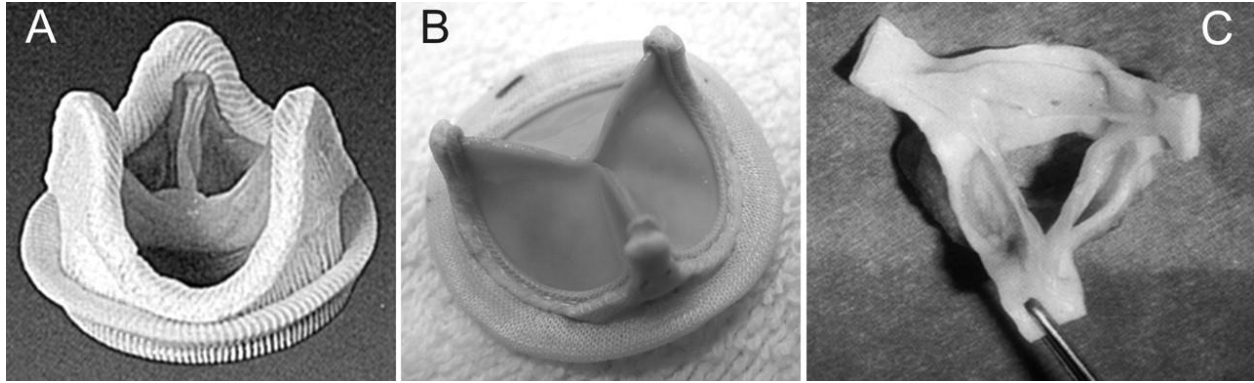


Figure 1.3.13: Images of (A) a porcine xenograft valve, (B) a bovine pericardial valve and (C) a human allograft/homegraft valve. Reprinted from *Circulation Research*, Vol. 97, Ivan Vesely, Heart Valve Tissue Engineering, 743-755, Copyright 2005, with permission from Wolters Kluwer Health.

The biggest challenge in the design of pericardial valves is selecting the leaflet shape that will maximize the effective orifice area, but will still provide adequate coaptation area when the valve is closed⁴⁷. The coaptation area of a valve is the area where the leaflets meet. A larger coaptation area ensures that the leaflets seal when they close, preventing any regurgitation of the valve⁴⁸. Porcine valves naturally have this coaptation area, but it must be engineered in a pericardial valve. This is accomplished by shaping the three leaflets as three segments of a cylinder and orienting them nearly parallel to the direction of blood flow⁴⁷. This design ensures that pressure forces the leaflets together when the valve is closed. It also provides a large, nearly circular orifice area when the valve is open. This characteristic gives the pericardial valves better hemodynamics than the porcine valves, which are the stiffer of the two valves due to the fixation procedure⁴⁷. Unfortunately, the design of the pericardial valves contains an inherent weakness. The stresses at the free edge of a pericardial valve leaflet are much higher than the stresses at the free edge of a porcine valve leaflet. If a single leaflet prolapses slightly, the stress loading experienced by the other leaflets is increased, which can eventually lead to tearing of the leaflets⁴⁷.

The most recent change in bioprosthetic heart valve design is the development of stentless valves. Stentless valves are available in both porcine and pericardial varieties³⁶. Images of this type of bioprosthetic valve are shown in **Figure 1.3.9**. The purpose of the stent is to maintain the geometry of the valve, which makes handling and implantation easier. It also ensures the valve functions as well in a patient as it does in the test fixture. The consequence of the stent is that it reduces the effective orifice area of the valve. Thus, without the stent, a larger valve could be placed in the same patient⁴⁷.

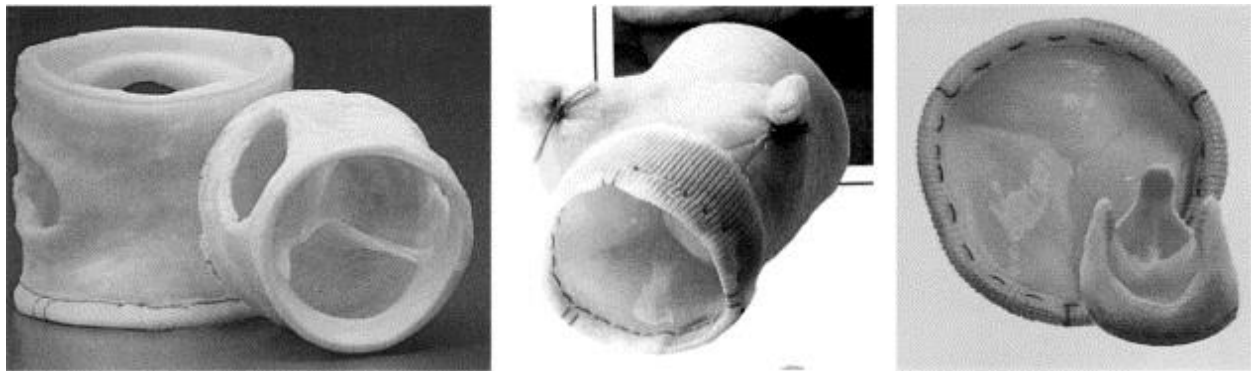


Figure 1.3.14: Images of the three most widely used stentless heart bioprosthetic valves, produced by Baxter, Medtronic, and St. Jude, from left to right. Reprinted from *Cardiovascular Pathology*, Vol. 12, Issue 5, Ivan Vesely, *The Evolution of Bioprosthetic Heart Valve Design and its Impact on Durability*, 277-286, Copyright 2003, with permission from Elsevier.

The successes and failures of the stentless valves are debatable. The durability of stentless valves should theoretically be better than that of stented valves, since the stresses should be distributed to the aortic tissue, instead of focuses on the leaflet material near the stent²⁸. However, several studies have shown that the durability of stentless valves is no different than the durability of stented valves. The two types of valves degenerate and fail at the same rates⁴⁹⁻⁵¹. Furthermore, the hemodynamics of stentless valves are purported to be superior to those of stented valves. Several

studies have analyzed the late clinical outcomes of aortic valve replacement with both stented and stentless bioprosthetic valves. The results indicate that stentless valves promote better long-term survival of patients, and the cause is attributed to the superior hemodynamics^{49, 50}. This is especially true in elderly patients with small aortic roots⁵². Unfortunately, widespread use of stentless valves could eventually increase the probability of reoperation due to valve failure. Superior hemodynamics increases survival time, but the same durability would cause many patients to outlive their bioprosthesis⁴⁹.

1.3.4 The Complications Associated with Artificial Heart Valves

The complications associated with artificial heart valves can be categorized into six groups: (1) thrombosis and thromboembolism, (2) anticoagulant-related hemorrhage, (3) tissue (pannus) overgrowth, (4) infection, (5) paravalvular leaks due to healing effects and (6) valve failure due to fatigue or chemical change⁵³. Thrombosis and hemorrhage are especially pertinent to mechanical heart valves. The hemodynamics of these valves are such that high shear stresses can be produced. In all types of mechanical heart valves, the blood flow is obstructed in some way, forcing the blood to flow around the component of the valve. In the case of the caged-ball valves, blood must flow around the ball. Tilting disc and bileaflet valves form a major and minor orifice when open, with blood being forced to flow around the disc or leaflet²⁸. Large forward flow jets occur in blood flow around the obstructions formed by the valve components. This high velocity causes high shear stress. This can cause platelet activation, which is one of the first few steps in the immune response described above^{28, 40, 53}. Areas of recirculating flow forms in regions where two different velocity flows interact. This flow stagnation and separation that occurs with mechanical valves promote the deposition of the damaged blood elements, which increases the probability of thrombus formation⁵³. **Figure 1.3.10** illustrates how this occurs. During the forward flow phase, the non-

physiological flow that the red blood cells (RBC) and other blood components experience can lead to rupture²⁸. These damaged cells would then release signals such as tissue factor, which initiates the extrinsic pathway of coagulation. Two different types of thrombus can form due to two different flow conditions. The formation of white/arterial thrombi occur in regions of high shear, since that is the condition under which preferential recruitment of platelet occurs. A fibrin-and-RBC-rich thrombus occurs in regions of low flow, thus forming a red thrombus 'tail'¹². For these reasons, patients who receive these mechanical valves are required to undergo lifelong anticoagulant therapy, which drastically increases the likelihood of hemorrhage, especially in older patients⁵⁴.

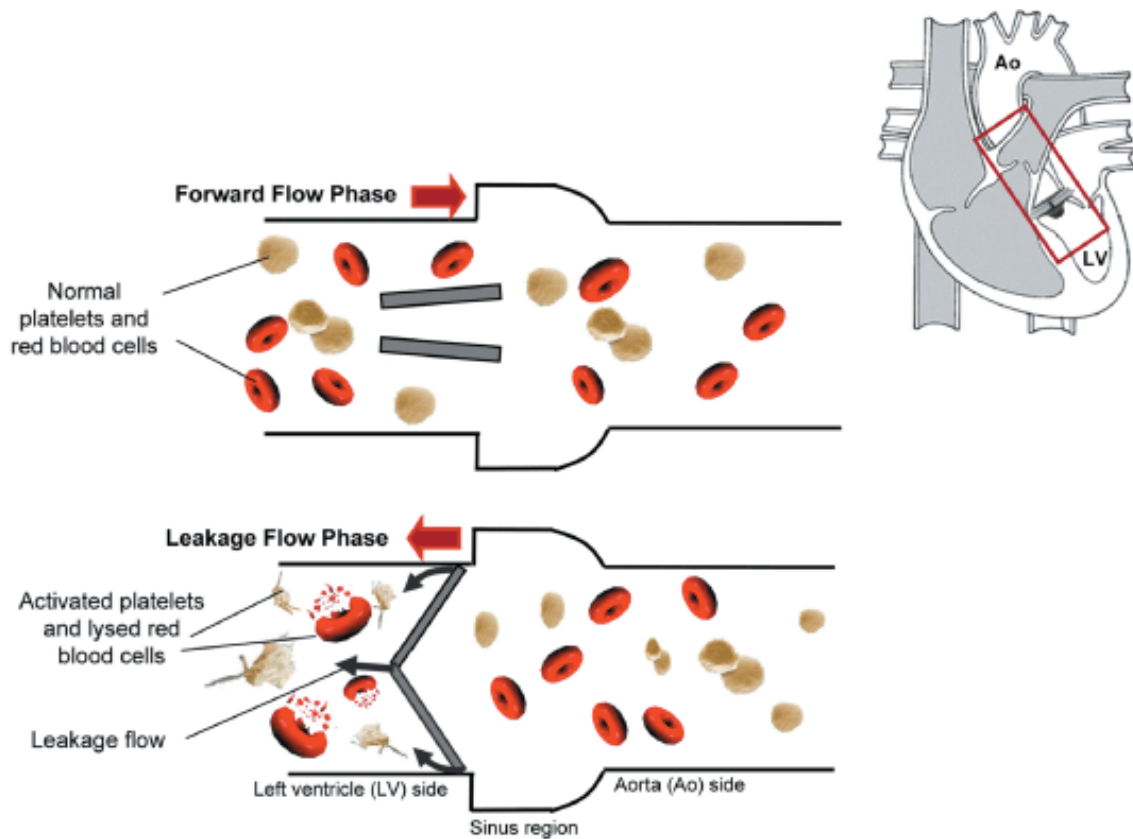


Figure 1.3.15: Schematic of a bileaflet mechanical heart valve showing damage to the blood components. Reprinted from *Clinical and Experimental Pharmacology and Physiology*, Vol. 36, Issue 2, Lakshmi P. Dasi, Helene A. Simon, Philippe Sucosky and Ajit P. Yoganathan, *Fluid Mechanics of Artificial Heart Valves*, 225-237, Copyright 2008, with permission from John Wiley and Sons.

Bioprosthetic heart valves do not have the same risk of thrombus as mechanical valves, but are highly susceptible to calcification and other forms of failure. Several possible mechanisms of failure are depicted in **Figure 1.3.11**.

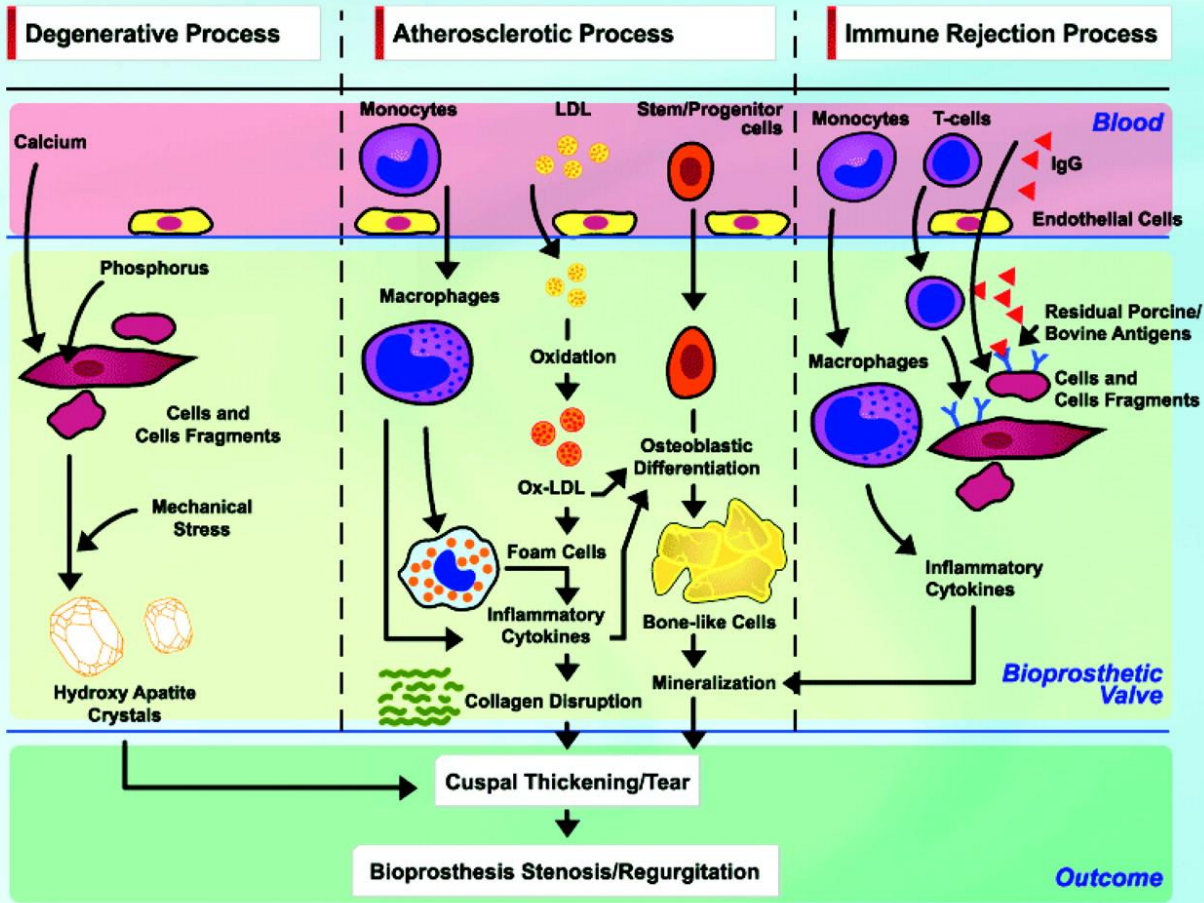


Figure 1.3.16: Hypothetical models for the structural deterioration of bioprosthetic valves. Reprinted from *Circulation*, Vol. 119, Philippe Pibarot and Jean G. Dumesnil, Prosthetic Heart Valves: Selection of the Optimal Prosthesis and Long-Term Management, 1034-1048, Copyright 2009, with permission from Wolters Kluwer Health.

The predominant failure mode is tearing of the leaflets, which occurs due to a variety of causes, including inflammation, collagen degradation and a lack of repair mechanisms⁴⁷. Originally, it was believed that tearing of the leaflets occurred due to calcification, however, recent discoveries suggest that these two phenomena have different causalities³⁶. Studies have demonstrated the link between inflammation and tissue degradation. In the majority of torn tissue valves, large amount of inflammatory cells are found covering the surface of and infiltrating into the material⁵⁵⁻⁵⁷. The

preservation of these bioprosthetic valves includes a crosslinking process, which results in the loss of a major means of stress distribution of the valve leaflets. Since these bioprosthetic valves cannot be repaired by the body, the loss of stress distribution often results in mechanical failure of the leaflets⁴⁷. However, it has been shown that by accounting for the orthotropy of the native valve during the design and construction of bioprosthetic valves, the stress distribution on the leaflets can be improved⁵⁸. Calcification is attributed to late failure of tissue valves. Although the exact mechanisms are uncertain, the calcium appears to originate in the mitochondria of dead cells, the dead porcine cells in the tissue being a likely source⁴⁷. Studies have linked the degree of calcification of the valve to the amount of glutaraldehyde present in the tissue⁵⁹. This suggests that the cell death caused by the presence of glutaraldehyde is another likely source of calcification of the valves⁴⁷. Many attempts at “anti-calcification” of the heart valves have been made, however, a successful method is yet to be found^{60, 61}. Despite their promising hemodynamics, patients who receive bioprosthetic heart valves will generally require a replacement within 10 to 15 years³⁴.

The major trade-off between mechanical and bioprosthetic heart valves is the durability and the hemocompatibility of the valve. Mechanical valves, while extremely durable, have low levels of compatibility and require lifelong anticoagulants as a result. In contrast, bioprosthetic valves do not require anticoagulants, but they fail rather quickly when compared to mechanical valves. Both types of valves have similar rates of infection and pannus overgrowth, and the survival rates associated with the two types of artificial heart valves are quite similar^{36, 62}. Therefore, mechanical valves are more suited to younger patients, who have much longer life expectancies than older patients. Bioprosthetic valves are almost exclusively used in older patients, who are not expected to outlive the shortened life span of the bioprosthetic valve, and thus would not require reoperation due to valve failure.

1.2.5 Recent Advances in Heart Valve Research

In 2002, a new method of implantation of heart valves was developed in which a bioprosthetic heart valve was implanted percutaneously in the pulmonary position²⁸. The percutaneous method has since been extended to include transcatheter aortic valve implantation (TAVI). Percutaneous methods of valve implantation are minimally invasive, and thus are critical for those patients who need valve replacements who cannot undergo open heart surgery⁶³. This method of implantation has been shown to reduce complications during implantation, such as major vascular bleeding and stroke⁶⁴. Furthermore, the functionality of the valves are improved with percutaneous implantation. The pressure gradient and orifice area are slightly better in bioprosthetic valve that were implanted percutaneously, likely due to the absence of the bulky support frame⁶⁵. Percutaneous implantation of artificial heart valves has shown promising initial results, but it is still a very new development. Before this method becomes common, an evidence base which analyzes the outcomes of those surgeries which utilized it must be created⁶³.

The most recent research into heart valves has been focusing on assessing the feasibility of using polymeric materials to create heart valve leaflets. Materials such as polytetrafluoroethylene (PTFE), silicone, polyurethane (PU) and polyethylene terephthalate (PET) have been attempted^{40, 66}. PTFE and silicone were quickly found to be inefficient leaflet materials⁶⁷. Further analysis of PU heart valve leaflets show that these valves have improved hemodynamic properties, but also have problems with tearing of the leaflets and thrombus formation around the stent⁴⁰. Promising work has been conducted with textile materials as heart valve leaflets. Studies have shown PET heart valve leaflets exhibit equivalent or better dynamics when compared to artificial heart valves currently in use⁶⁶. Despite the promising results, PET was demonstrated to have mechanical properties that varied with time when tested for fatigue under physiological conditions^{68, 69}. This

calls into question the suitability of this material for use in heart valve leaflet applications. Additionally, one study has shown that it is possible through tissue engineering to create a heart valve leaflet that has both morphological and histological similarity to a natural heart valve. However, it has yet to be tested *in vivo*, and it is unknown if the *in vitro* results will correlate to improved hemocompatibility and durability⁴⁴. Despite much research and many advances in the field of artificial heart valves, there is still much work to be done. Thus, additional work is necessary to develop artificial heart valves that not only prevent thrombus formation, but also have the durability to last a lifetime.

1.4 Polymeric Materials for Blood-Contacting Applications

1.4.1 Expanded Polytetrafluoroethylene (ePTFE) as a Biomaterial

ePTFE is currently used in a wide variety of applications, including soft tissue replacement, cardiovascular grafts and orthopedic applications. Its mechanical properties are such that it promotes biointegration due to its microporous structure, and also maintains high structural integrity⁷⁰. Furthermore, it is a hydrophobic, biostable material and does not undergo degradation when placed into the body^{71, 72}. When used for facial augmentation and rhinoplasty procedures, ePTFE has demonstrated high biocompatibility and increased stability over time⁷³. Due to the nature of the material, it cannot be used in situations where the implant is required to be rigid. However, it provided an excellent alternative to allografts in soft tissue replacement⁷⁴. Studies have demonstrated the potential of ePTFE for use in dura mater defects. When used to repair these defects in rats, ePTFE did not induce a foreign body reaction, and also became encased in a thin layer of connective tissue⁷⁵. ePTFE has been used to patch abdominal hernias and as an implant ring for urinary incontinence^{76, 77}. In vascular graft applications, ePTFE has demonstrated excellent biocompatibility and easier implantation as compared to other materials. Specifically, this material

showed little to no leukocyte adhesion and complement activation when studied in an *in vitro* perfusion system⁷⁸. Additionally, the growth of endothelial cells onto this material can be promoted when coated with certain molecules⁷⁹. The major drawback of ePTFE vascular grafts is their tendency to leak blood from the sutures used to sew the patch to the vessel wall, although much work is being done to mitigate this⁸⁰. This material has also shown promise in orthopedic applications. In rabbits, ePTFE has been shown to prevent restrictive adhesion following tendon repair with no apparent undesirable tissue reactions. It has also been implanted in sheep as a prosthetic ligament^{81, 82}. Overall, these studies have shown ePTFE to have excellent biocompatibility. When its biocompatibility is considered in conjunction with its biostability and excellent structural integrity, ePTFE becomes a promising candidate for many other applications.

1.4.2 Linear Low Density Polyethylene (LLDPE) as a Biomaterial

LLDPE is a linear copolymer of ethylene with propylene that has very high tear and puncture resistance as well as high tensile strength⁸³. It has many uses in the plastic industry, such as greenhouse films and stretch wrap^{84, 85}. Studies have shown it to be less hydrophobic than ePTFE or PET, although there are possible surface treatments that can increase its hydrophobic properties⁸⁶. It also has high potential of being used as a biodegradable plastic when blended with starch⁸⁷. It is not currently used as an implantable biomaterial, however, preliminary studies have shown that it has potential as a heart valve leaflet. Its high tear resistance gives it high durability, and it exhibited hemodynamics at least as good as bioprosthetic heart valves^{88, 89}. Thus, this work will assess the appropriateness of using LLDPE in biomaterial applications.

1.4.3 Polyethylene Terephthalate (PET) as a Biomaterial

PET is currently used in heart valve applications, as part of the stent and not as a leaflet material. It is a woven material with several possible fabrication techniques that provide a wide variability in its porosity. This material has good structural integrity, high flexibility and is kink-resistant⁷¹. Suture rings on artificial heart valves are often made out of PET, containing a water-repellent coating on the internal surface to ensure it doesn't result in thrombus⁹⁰. Studies have shown that this technique is effective at improving the host response to the PET suture ring⁹¹. PET has been used to create braided fabric prosthesis for the repair or replacement of tendons and ligaments⁹². It also is used in vascular graft applications. Although platelets and leukocytes tend to adhere in high numbers to this material, several studies have demonstrated that coating the material with substances such as albumin decreases the amount of platelets and leukocytes which adhere⁹³. Occasionally, only one side of the PET vascular graft is coated to ensure a non-thrombogenic blood-contacting side and a biocompatible outside surface⁹⁴. Studies have shown that spreading and proliferation of endothelial and smooth muscle cells onto PET is desirable, especially because the phenotype of the cells are preserved. This has promising implications for integration of the grafts into the host^{95, 96}. Thus far, the research into PET has identified it as a material with a biocompatibility that can be readily improved with surface treatments and excellent stability. This makes it useful in a wide variety of applications.

1.5 Effect of Material Surface Characteristics on Blood-Material Interactions

The interaction of blood with a foreign surface is influenced heavily by the material's surface characteristics. Factors such as surface charge, hydrophilicity/hydrophobicity, surface topography and chemical composition of the material all play a role in determining what the

interaction will be. Negatively charged surfaces have been correlated to higher potential of blood-material interactions⁹⁷. Several studies have demonstrated that adsorption of key blood serum protein occurs more preferentially onto hydrophobic surfaces than hydrophilic surfaces⁹⁸⁻¹⁰¹. Surface topography has also been shown to have an effect on cell adhesion and activation. In several studies, cell adhesion and activation increased as the surface roughness increased, especially in conditions of high blood flow rates^{102, 103}. This phenomenon has been attributed to the increase of available surface area that corresponds to an increased surface roughness¹⁰⁴. The combination of these studies show that blood-material interactions can be manipulated by changing the surface characteristics of the materials.

1.5.1 Modification of Polymeric Materials to Improve Hemocompatibility

Many techniques have been used to improve the hemocompatibility of polymeric materials. Grafting hydrophilic molecules onto the surface of polymeric materials has demonstrated reduced protein adsorption, increased *in vitro* clotting time, and the ability to create surfaces with selective adsorbability¹⁰⁵⁻¹⁰⁷. Coating material surfaces with thromboresistant polymers has also been shown to promote a reduction in fibrinogen adsorption¹⁰⁸. Perhaps the most well-known example of this type of modification are those materials coated with the anticoagulant heparin. Modification of material surfaces with plasma polymerization has demonstrated much promise with regards to improvement of biocompatibility¹⁰⁹. Introducing nanotopography to the surface of materials is a method that attempts to make the materials more biomimetic. It has been correlated to drastic improvements in hemocompatibility¹¹⁰. Another promising method used to modify polymeric materials is to create interpenetrating polymer networks (IPN). An IPN is a combination of two or more polymers in network form, with one polymerized or cross-linked in the presence of the

other¹¹¹. Many studies have demonstrated their usefulness in biomaterial applications. IPN combinations have been used in vascular tissue engineering, urinary biomaterial applications, and ophthalmic biomaterial applications¹¹²⁻¹¹⁴. They are very versatile. An IPN can be made with a variety of combinations of polymers that would result in different porosities, wettability characteristics, and surface structures. They can also be helpful in stabilizing biodegradable materials¹¹⁵. They are known to reduce platelet adhesion by decreasing protein adsorption, thus increasing hemocompatibility of the material^{116, 117}. IPNs are of particular interest in heart valve engineering applications, as they create more stable results than surface coatings¹¹⁸.

1.6 Conclusion

Current commercially available biomaterials have a wide variety of applications. One of the most frequent uses of these materials are artificial heart valve applications. Despite their frequent use, they are still plagued by issues such as thrombosis and calcification. Additionally, every implanted material elicits a reaction from the host tissue which can ultimately lead to rejection of the implant. The first steps in this response, namely protein adsorption and adhesion and activation of platelets and leukocytes, affect all subsequent events. Thus, the characterization of these events on different materials can aid in determining their biocompatibility.

REFERENCES

1. Loon, S.L.M.v., et al., *The Immune Response in In Situ Tissue Engineering of Aortic Heart Valves*. Calcific Aortic Valve Disease. 2013.
2. Remes, A. and D.F. Williams, *Immune response in biocompatibility*. Biomaterials, 1992. **13**(11): p. 731-743.
3. Franz, S., et al., *Immune responses to implants – A review of the implications for the design of immunomodulatory biomaterials*. Biomaterials, 2011. **32**(28): p. 6692-6709.
4. Anderson, J.M., *BIOLOGICAL RESPONSES TO MATERIALS*. Annual Review of Materials Research, 2001. **31**(1): p. 81-110.
5. Gorbet, M.B. and M.V. Sefton, *Biomaterial-associated thrombosis: roles of coagulation factors, complement, platelets and leukocytes*. Biomaterials, 2004. **25**(26): p. 5681-5703.
6. Ratner, B.D. and S.J. Bryant, *BIOMATERIALS: Where We Have Been and Where We are Going*. Annual Review of Biomedical Engineering, 2004. **6**(1): p. 41-75.
7. Greisler, H.P., *Interactions at the Blood/Material Interface*. Annals of Vascular Surgery, 1990. **4**(1): p. 98-103.
8. CAMERON J. WILSON, B.E., et al., *Mediation of Biomaterial–Cell Interactions by Adsorbed Proteins: A Review*. Tissue Engineering, 2005. **11**(1-2): p. 1-18.
9. Rink, T.J. and S.O. Sage, *Calcium Signaling in Human Platelets*. Annual Review of Physiology, 1990. **52**(1): p. 431-449.
10. Feinstein, M., *The Role of Calcium in Blood Platelet Function*, in *Calcium in Drug Action*, G. Weiss, Editor. 1978, Springer US. p. 197-239.

11. Jin, J., J.L. Daniel, and S.P. Kunapuli, *Molecular Basis for ADP-induced Platelet Activation: II. THE P2Y1 RECEPTOR MEDIATES ADP-INDUCED INTRACELLULAR CALCIUM MOBILIZATION AND SHAPE CHANGE IN PLATELETS*. Journal of Biological Chemistry, 1998. **273**(4): p. 2030-2034.
12. Jackson, S.P., *Arterial thrombosis[mdash]insidious, unpredictable and deadly*. Nat Med, 2011. **17**(11): p. 1423-1436.
13. Ruggeri, Z.M., *Platelets in atherothrombosis*. Nat Med, 2002. **8**(11): p. 1227-1234.
14. Esmon, C.T., *The interactions between inflammation and coagulation*. British Journal of Haematology, 2005. **131**(4): p. 417-430.
15. Levi, M. and T. van der Poll, *Two-Way Interactions Between Inflammation and Coagulation*. Trends in Cardiovascular Medicine, 2005. **15**(7): p. 254-259.
16. Courtney, J.M., et al., *Biomaterials for blood-contacting applications*. Biomaterials, 1994. **15**(10): p. 737-744.
17. Ley, K., *Molecular mechanisms of leukocyte recruitment in the inflammatory process*. Cardiovascular Research, 1996. **32**(4): p. 733-742.
18. Wan, S., J.-L. LeClerc, and J.-L. Vincent, *Inflammatory response to cardiopulmonary bypass : Mechanisms involved and possible therapeutic strategies*. Chest, 1997. **112**(3): p. 676-692.
19. Ley, K., et al., *Getting to the site of inflammation: the leukocyte adhesion cascade updated*. Nature Reviews Immunology, 2007. **7**(9): p. 678-689.
20. Nilsson, B., et al., *The role of complement in biomaterial-induced inflammation*. Molecular Immunology, 2007. **44**(1-3): p. 82-94.
21. Keselowsky, B.G., et al., *Role of plasma fibronectin in the foreign body response to biomaterials*. Biomaterials, 2007. **28**(25): p. 3626-3631.

22. Ward, W.K., *A Review of the Foreign-body Response to Subcutaneously-implanted Devices: The Role of Macrophages and Cytokines in Biofouling and Fibrosis*. Journal of Diabetes Science and Technology, 2008. **2**(5): p. 768-777.
23. Anderson, J.M., A. Rodriguez, and D.T. Chang, *FOREIGN BODY REACTION TO BIOMATERIALS*. Seminars in immunology, 2008. **20**(2): p. 86-100.
24. National Heart, L.a.B.I. *Anatomy of the Heart*. How the Heart Works 2011 November 17, 2011 [cited 2015 January 21, 2015].
25. Opie, L.H., *Heart Physiology: From Cell to Circulation*. 2004: Lippincott Williams & Wilkins.
26. Mahadevan, V., *Anatomy of the heart*. Surgery (Oxford), 2008. **26**(12): p. 473-476.
27. Whitaker, R.H., *Anatomy of the heart*. Medicine, 2010. **38**(7): p. 333-335.
28. Dasi, L.P., et al., *Fluid Mechanics of Artificial Heart Valves*. Clinical and Experimental Pharmacology and Physiology, 2009. **36**(2): p. 225-237.
29. Flanagan, T.C. and A. Pandit, *Living Artificial Heart Valve Alternatives: A Review*. European Cells and Materials, 2003. **6**: p. 28-45.
30. Mohammadi, H. and K. Mequanint, *Prosthetic aortic heart valves: Modeling and design*. Medical Engineering & Physics, 2011. **33**(2): p. 131-147.
31. Ray, S., R. Beynon, and A. Borg, *Mitral valve disease*. Medicine, 2010. **38**(10): p. 537-540.
32. Linefsky, J.P. and C.M. Otto, *Aortic valve disease*. Medicine, 2010. **38**(10): p. 541-544.
33. Yacoub, M.H. and J.J.M. Takkenberg, *Will heart valve tissue engineering change the world?* Nat Clin Pract Cardiovasc Med, 2005. **2**(2): p. 60-61.

34. Wanpen Vongpatanasin, M.D., M.D. L. David Hillis, and M.D. Richard A. Lange, *Prosthetic Heart Valves*. New England Journal of Medicine, 1996. **335**(6): p. 407-416.
35. Gott, V.L., D.E. Alejo, and D.E. Cameron, *Mechanical heart valves: 50 years of evolution*. The Annals of Thoracic Surgery. **76**(6): p. S2230-S2239.
36. Pibarot, P. and J.G. Dumesnil, *Prosthetic Heart Valves: Selection of the Optimal Prosthesis and Long-Term Management*. Circulation, 2009. **119**(7): p. 1034-1048.
37. Bloomfield, P., *Choice of heart valve prosthesis*. Heart, 2002. **87**(6): p. 583-589.
38. Vlahakes, G.J., *Mechanical Heart Valves: The Test of Time....* Circulation, 2007. **116**(16): p. 1759-1760.
39. Cannegieter, S.C., et al., *Optimal Oral Anticoagulant Therapy in Patients with Mechanical Heart Valves*. New England Journal of Medicine, 1995. **333**(1): p. 11-17.
40. Han, K.Y., et al., *Recent Advances in Polymeric Heart Valves Research*. International Journal of Biomaterials Research and Engineering, 2011. **1**(1).
41. DeWall, R.A., N. Qasim, and L. Carr, *Evolution of mechanical heart valves*. The Annals of Thoracic Surgery, 2000. **69**(5): p. 1612-1621.
42. Yoganathan, A.P., et al., *Bileaflet, tilting disc and porcine aortic valve substitutes: In vitro hydrodynamic characteristics*. Journal of the American College of Cardiology, 1984. **3**(2s1): p. 313-320.
43. Vesely, I., *Heart valve tissue engineering*. Circ Res, 2005. **97**(8): p. 743-55.
44. Zund, G., et al., *The in vitro construction of a tissue engineered bioprosthetic heart valve*. European Journal of Cardio-Thoracic Surgery, 1997. **11**(3): p. 493-497.
45. Schoen, F.J. and R.J. Levy, *Pathology of Substitute Heart Valves: New Concepts and Developments*. Journal of Cardiac Surgery, 1994. **9**: p. 222-227.

46. Laudito, A., et al., *The Ross procedure in children and young adults: A word of caution*. The Journal of Thoracic and Cardiovascular Surgery, 2001. **122**(1): p. 147-153.
47. Vesely, I., *The evolution of bioprosthetic heart valve design and its impact on durability*. Cardiovascular Pathology, 2003. **12**(5): p. 277-286.
48. McCarthy, K.P., L. Ring, and B.S. Rana, *Anatomy of the mitral valve: understanding the mitral valve complex in mitral regurgitation*. Vol. 11. 2010. i3-i9.
49. David, T.E., et al., *Aortic valve replacement with stentless and stented porcine valves: a case-match study*. The Journal of Thoracic and Cardiovascular Surgery, 1998. **116**(2): p. 236-241.
50. David, T.E., et al., *Aortic valve replacement with stentless porcine aortic valves: a ten-year experience*. J Heart Valve Dis, 1998. **7**(3): p. 250-4.
51. Zilla, P., et al., *Prosthetic heart valves: Catering for the few*. Biomaterials, 2008. **29**(4): p. 385-406.
52. Sintek, C.F., A.D. Fletcher, and S. Khonsari, *Stentless porcine aortic root: Valve of choice for the elderly patient with small aortic root?* The Journal of Thoracic and Cardiovascular Surgery, 1995. **109**(5): p. 871-876.
53. Yoganathan, A.P., Z. He, and S. Casey Jones, *FLUID MECHANICS OF HEART VALVES*. Annual Review of Biomedical Engineering, 2004. **6**(1): p. 331-362.
54. Beyth, R.J., *Hemorrhagic complications of oral anticoagulant therapy*. Clin Geriatr Med, 2001. **17**(1): p. 49-56.
55. Ferrans, V.J., et al., *Structural changes in glutaraldehyde-treated porcine heterografts used as substitute cardiac valves: Transmission and scanning electron microscopic observations in 12 patients*. The American Journal of Cardiology, 1978. **41**(7): p. 1159-1184.

56. Nistal, F., et al., *Comparative study of primary tissue valve failure between lonescu-shiley pericardial and Hancock porcine valves in the aortic position*. The American Journal of Cardiology, 1986. **57**(1): p. 161-164.
57. Schoen, J., R. Shemin, and L. Cohn, *Pathologic evaluation of a unileaflet pericardial bioprosthesis after implantation as tricuspid and mitral valve replacements in sheep*. Trans Soc Biomater, 1986. **9**: p. 76.
58. Arcidiacono, G., A. Corvi, and T. Severi, *Functional analysis of bioprosthetic heart valves*. Journal of Biomechanics, 2005. **38**(7): p. 1483-1490.
59. Levy, R.J., et al., *Biologic determinants of dystrophic calcification and osteocalcin deposition in glutaraldehyde-preserved porcine aortic valve leaflets implanted subcutaneously in rats*. The American Journal of Pathology, 1983. **113**(2): p. 143-155.
60. Levy, R., et al., *Inhibition of calcification of bioprosthetic heart valves by local controlled-release diphosphonate*. Science, 1985. **228**(4696): p. 190-192.
61. Páez, J.M.G. and E. Jorge-Herrero, *Assessment of Pericardium in Cardiac Bioprostheses: A Review*. Journal of Biomaterials Applications, 1999. **13**(4): p. 351-388.
62. Hammermeister, K.E., et al., *A comparison of outcomes in men 11 years after heart-valve replacement with a mechanical valve or bioprosthesis*. New England Journal of Medicine, 1993. **328**(18): p. 1289-1296.
63. Dworakowski, R., et al., *Valvular heart disease: percutaneous alternatives*. Medicine. **38**(10): p. 550-554.
64. Rozeik, M., D. Wheatley, and T. Gourlay, *Percutaneous heart valves; past, present and future*. Perfusion, 2014. **29**(5): p. 397-410.
65. Smith, C.R., et al., *Transcatheter versus Surgical Aortic-Valve Replacement in High-Risk Patients*. New England Journal of Medicine, 2011. **364**(23): p. 2187-2198.
66. Heim, F., B. Durand, and N. Chakfe, *Flexible textile heart valve prosthesis: an in vitro evaluation*. Res J Tex Apparel, 2004. **8**: p. 1-11.

67. Daebritz, S.H., et al., *Introduction of a flexible polymeric heart valve prosthesis with special design for mitral position*. *Circulation*, 2003. **108 Suppl 1**: p. II134-9.
68. Heim, F. and B.S. Gupta, *Textile Heart Valve Prosthesis: The Effect of Fabric Construction Parameters on Long-term Durability*. *Textile Research Journal*, 2009. **79**(11): p. 1001-1013.
69. Heim, F., B. Durand, and N. Chakfe, *Textile for heart valve prostheses: Fabric long-term durability testing*. *Journal of Biomedical Materials Research Part B: Applied Biomaterials*, 2010. **92B**(1): p. 68-77.
70. Catanese, J., et al., *Mechanical properties of medical grade expanded polytetrafluoroethylene: The effects of internodal distance, density, and displacement rate*. *Journal of Biomedical Materials Research*, 1999. **48**(2): p. 187-192.
71. Xue, L. and H.P. Greisler, *Biomaterials in the development and future of vascular grafts*. *Journal of Vascular Surgery*, 2003. **37**(2): p. 472-480.
72. Guidoin, R., et al., *Expanded polytetrafluoroethylene arterial prostheses in humans: chemical analysis of 79 explanted specimens*. *Biomaterials*, 1993. **14**(9): p. 694-704.
73. Maas, C.S., D.R. Gnepp, and J. Bumpous, *EXpanded polytetrafluoroethylene (gore-tex soft-tissue patch) in facial augmentation*. *Archives of Otolaryngology–Head & Neck Surgery*, 1993. **119**(9): p. 1008-1014.
74. Conrad, K. and G. Gillman, *A 6-Year Experience with the Use of Expanded Polytetrafluoroethylene in Rhinoplasty*. *Plastic and Reconstructive Surgery*, 1998. **101**(6): p. 1675-1683.
75. Viñas, F.C., et al., *Evaluation of expanded polytetrafluoroethylene (ePTFE) versus polydioxanone (PDS) for the repair of dura mater defects*. *Neurological research*, 1999. **21**(3): p. 262-268.
76. Bent, A.E., D.R. Ostergard, and M. Zwick-Zaffuto, *Tissue reaction to expanded polytetrafluoroethylene suburethral sling for urinary incontinence: Clinical and histologic study*. *American Journal of Obstetrics and Gynecology*, 1993. **169**(5): p. 1198-1204.

77. LeBlanc, K.A. and W.V. Booth, *Laparoscopic Repair of Incisional Abdominal Hernias Using Expanded Polytetrafluoroethylene: Preliminary Findings*. Surgical Laparoscopy Endoscopy & Percutaneous Techniques, 1993. **3**(1): p. 39-41.
78. Kottke-Marchant, K., et al., *Vascular graft-associated complement activation and leukocyte adhesion in an artificial circulation*. Journal of Biomedical Materials Research, 1987. **21**(3): p. 379-397.
79. Lord, M.S., et al., *The modulation of platelet and endothelial cell adhesion to vascular graft materials by perlecan*. Biomaterials, 2009. **30**(28): p. 4898-4906.
80. Berguer, R., et al., *Expanded polytetrafluoroethylene layer and nonporous elastomer coating for vascular patches*. 1992, Google Patents.
81. Bolton, C.W. and W.C. Bruchman, *The GORE-TEXTM Expanded Polytetrafluoroethylene Prosthetic Ligament An In Vitro and In Vivo Evaluation*. Clinical Orthopaedics and Related Research, 1985. **196**: p. 202-214.
82. Hanff, G. and L. Hagberg, *Prevention of restrictive adhesions with expanded polytetrafluoroethylene diffusible membrane following flexor tendon repair: An experimental study in rabbits*. The Journal of Hand Surgery, 1998. **23**(4): p. 658-664.
83. Turtle, B.L., *Linear low density polyethylene*. 1986, Google Patents.
84. Hong, Y., et al., *Film blowing of linear low-density polyethylene blended with a novel hyperbranched polymer processing aid*. Polymer, 2000. **41**(21): p. 7705-7713.
85. Basfar, A.A., K.M. Idriss Ali, and S.M. Mofti, *UV stability and radiation-crosslinking of linear low density polyethylene and low density polyethylene for greenhouse applications*. Polymer Degradation and Stability, 2003. **82**(2): p. 229-234.
86. Kim, Y., et al., *Improvement of hydrophobic properties of polymer surfaces by plasma source ion implantation*. Surface and Coatings Technology, 2006. **200**(16-17): p. 4763-4769.

87. Chandra, R. and R. Rustgi, *Biodegradation of maleated linear low-density polyethylene and starch blends*. *Polymer Degradation and Stability*, 1997. **56**(2): p. 185-202.
88. Prawel, D.A., et al., *Hemocompatibility and Hemodynamics of Novel Hyaluronan-Polyethylene Materials for Flexible Heart Valve Leaflets*. *Cardiovasc Eng Technol*, 2014. **5**(1): p. 70-81.
89. IV, H.D., *Development of Biopoly Materials for use in Prosthetic Heart Valve Replacements*, in *Department of Mechanical Engineering*. 2012, Colorado State University. p. 126.
90. Curcio, M., et al., *Suture ring for heart valve prostheses*. 1992, Google Patents.
91. Wang, J., et al., *Surface characterization and blood compatibility of poly(ethylene terephthalate) modified by plasma surface grafting*. *Surface and Coatings Technology*, 2005. **196**(1–3): p. 307-311.
92. Silvestrini, T.A. and J.E. Laptewicz, *Triaxially-braided fabric prosthesis*. 1989, Google Patents.
93. Kottke-Marchant, K., et al., *Effect of albumin coating on the in vitro blood compatibility of Dacron® arterial prostheses*. *Biomaterials*, 1989. **10**(3): p. 147-155.
94. Karwoski, T. and Y. Matsuzawa, *Polytetrafluoroethylene coated polyethylene terephthalate*. 1988, Google Patents.
95. Ma, Z., et al., *Surface engineering of electrospun polyethylene terephthalate (PET) nanofibers towards development of a new material for blood vessel engineering*. *Biomaterials*, 2005. **26**(15): p. 2527-2536.
96. Gupta, B., et al., *Plasma-induced graft polymerization of acrylic acid onto poly(ethylene terephthalate) films: characterization and human smooth muscle cell growth on grafted films*. *Biomaterials*, 2002. **23**(3): p. 863-871.
97. Deppisch, R., et al., *Blood material interactions at the surfaces of membranes in medical applications*. *Separation and Purification Technology*, 1998. **14**(1–3): p. 241-254.

98. Sigal, G.B., M. Mrksich, and G.M. Whitesides, *Effect of Surface Wettability on the Adsorption of Proteins and Detergents*. Journal of the American Chemical Society, 1998. **120**(14): p. 3464-3473.
99. Xu, L.-C. and C.A. Siedlecki, *Effects of wettability and contact time on protein adhesion to biomaterials surfaces*. Biomaterials, 2007. **28**: p. 3273-3283.
100. Wu, Y., et al., *The role of adsorbed fibrinogen in platelet adhesion to polyurethane surfaces: A comparison of surface hydrophobicity, protein adsorption, monoclonal antibody binding, and platelet adhesion*. Journal of Biomedical Materials Research Part A, 2005. **74A**(4): p. 722-738.
101. Ostuni, E., et al., *A Survey of Structure–Property Relationships of Surfaces that Resist the Adsorption of Protein*. Langmuir, 2001. **17**(18): p. 5605-5620.
102. Eriksson, C., J. Lausmaa, and H. Nygren, *Interactions between human whole blood and modified TiO₂-surfaces: influence of surface topography and oxide thickness on leukocyte adhesion and activation*. Biomaterials, 2001. **22**(14): p. 1987-1996.
103. Cumming, R.D., *IMPORTANT FACTORS AFFECTING INITIAL BLOOD-MATERIAL INTERACTIONS*. ASAIO Journal, 1980. **26**(1): p. 304-308.
104. Didisheim, P., et al., *RELATIVE ROLE OF SURFACE CHEMISTRY AND SURFACE TEXTURE IN BLOOD-MATERIAL INTERACTIONS*. ASAIO Journal, 1983. **29**(1): p. 169-176.
105. Elbert, D.L. and J.A. Hubbell, *Surface Treatments of Polymers for Biocompatibility*. Annual Review of Materials Science, 1996. **26**(1): p. 365-394.
106. Wesslén, B., et al., *Protein adsorption of poly(ether methane) surfaces modified by amphiphilic and hydrophilic polymers*. Biomaterials, 1994. **15**(4): p. 278-284.
107. Ikada, Y., *Surface modification of polymers for medical applications*. Biomaterials, 1994. **15**(10): p. 725-736.

108. Beugeling, T., *The interaction of polymer surfaces with blood*. Journal of Polymer Science: Polymer Symposia, 1979. **66**(1): p. 419-427.
109. Oehr, C., *Plasma surface modification of polymers for biomedical use*. Nuclear Instruments and Methods in Physics Research Section B: Beam Interactions with Materials and Atoms, 2003. **208**(0): p. 40-47.
110. Elsamny, M., *Biological NanoArchitecture: Architecture in the Age of Biomaterials*. Advance Materials Research, 2013. **671-674**: p. 2174-2179.
111. Sperling, L.H. and V. Mishra, *The current status of interpenetrating polymer networks*. Polymers for Advanced Technologies, 1996. **7**(4): p. 197-208.
112. Jones, D.S., et al., *Physicochemical characterisation and biological evaluation of hydrogel-poly(ϵ -caprolactone) interpenetrating polymer networks as novel urinary biomaterials*. Biomaterials, 2005. **26**(14): p. 1761-1770.
113. Liu, L. and H. Sheardown, *Glucose permeable poly (dimethyl siloxane) poly (N-isopropyl acrylamide) interpenetrating networks as ophthalmic biomaterials*. Biomaterials, 2005. **26**(3): p. 233-244.
114. Liu, Y. and M.B. Chan-Park, *Hydrogel based on interpenetrating polymer networks of dextran and gelatin for vascular tissue engineering*. Biomaterials, 2009. **30**(2): p. 196-207.
115. Soldani, G., et al., *Long term performance of small-diameter vascular grafts made of a poly(ether)urethane–polydimethylsiloxane semi-interpenetrating polymeric network*. Biomaterials, 2010. **31**(9): p. 2592-2605.
116. Morimoto, N., et al., *Physical properties and blood compatibility of surface-modified segmented polyurethane by semi-interpenetrating polymer networks with a phospholipid polymer*. Biomaterials, 2002. **23**(24): p. 4881-4887.
117. Ishihara, K., et al., *Hemocompatibility on graft copolymers composed of poly(2-methacryloyloxyethyl phosphorylcholine) side chain and poly(n-butyl methacrylate) backbone*. Journal of Biomedical Materials Research, 1994. **28**(2): p. 225-232.

118. Lee, F. and M. Kurisawa, *Formation and stability of interpenetrating polymer network hydrogels consisting of fibrin and hyaluronic acid for tissue engineering*. Acta Biomaterialia, 2013. **9**(2): p. 5143-5152.

CHAPTER 2

MATERIALS AND METHODS

2.1 Introduction

There are many polymeric materials used in many different blood-contacting applications. Despite the frequent use of these materials, they all tend to elicit an immune response when placed in contact with blood¹⁻³. These effects include inflammation, infection, or thrombosis, which can lead to failure of the biomaterial^{2,3}. Within seconds to minutes of implantation, several key blood serum proteins adsorb to the surface of the material and undergo conformational changes. This layer of protein promotes adhesion and subsequent activation of platelets^{2,3}. These initial events occur relatively quickly and characterize the short-term hemocompatibility of a biomaterial. Platelets that adhere to the surface of the material provide signals and cues that not only play a role in the formation of the fibrin clot and recruitment of leukocytes, but also initiate an immune response that results in complete encapsulation of the implant². These events take longer to occur, and thus define a material's long-term hemocompatibility. The initial events that occur will influence the subsequent events, thus the characterization of these initial events is important. Furthermore, the surface characteristics of a material can influence the initial events¹⁻⁴, therefore, characterization of the surfaces of materials is essential.

In this study, we have characterized the material surfaces and investigated the hemocompatibility of expanded polytetrafluoroethylene (ePTFE), linear low-density polyethylene (LLDPE) and polyethylene terephthalate (PET). The material surface morphology was characterized using scanning electron microscopy (SEM) and the surface wettability was characterized using contact angle goniometry. Prior to assessing hemocompatibility, the

cytotoxicity of the materials was determined, as any blood-contacting material should not cause cell death. Hemocompatibility of the materials was assessed by investigating protein adsorption, platelet and leukocyte adhesion, platelet and leukocyte activation and whole blood clotting kinetics. In order to quantitatively study protein adsorption, platelet adhesion, and adhered platelet activation, a static assay would give basic material chemistry and surface related information without the confounding effects from blood flow – structure interaction effects. Different materials are bound to result in different dynamics when exposed to blood flow, and this study aims to more specifically address the fundamental surface response characteristics in the absence of dynamic effects as a baseline.

2.2 Fabrication of Substrates

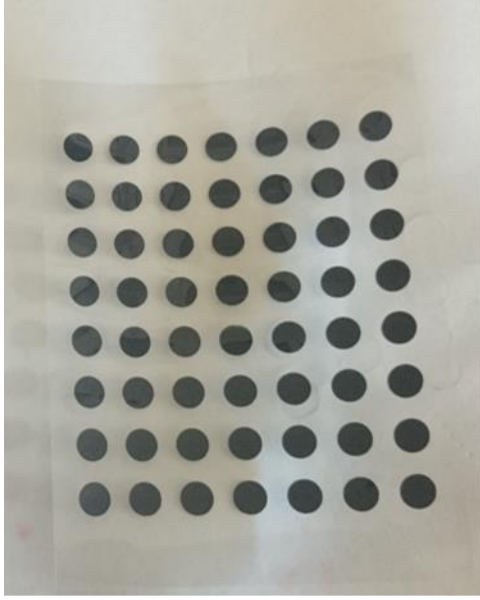
When these studies began, it was quickly discovered that two of the materials used, specifically ePTFE and LLDPE, tended to float in all of the liquids used in the experiments. This meant that these materials were not exposed to the plasma in the same way as TCPS and PET, as those materials sank. This was problematic, due to the drastic and inconsistent effect on the results. In order to remedy this issue, a method to sink ePTFE and LLDPE needed to be developed. Several methods were attempted by which to sink the ePTFE and the LLDPE without adhesives and additional materials. These methods largely revolved around varying the amount of liquid into which the substrates were being sunk. However, the success of these methods was minimal, as the materials did not sink consistently.

The focus then shifted, and methods were considered that required attaching the ePTFE and LLDPE to another material, one that would sink 100% of the time. Polytetrafluoroethylene (PTFE) was chosen as the additional material. Preliminary experiments showed that it does indeed

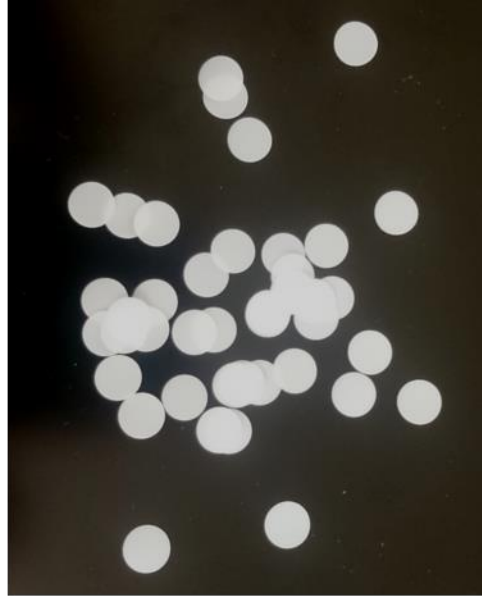
sink consistently, and research has demonstrated PTFE to be a hemocompatible material⁵⁻⁷. It was commercially available as a thin disc, which was the ideal shape, since the substrates themselves are 8-mm circles.

Several adhesives were considered during this stage of the process, although the options were quickly narrowed down to two, due to the potential toxicity of the others. The first was tissue adhesive. This option was the first choice because tissue adhesive is non-toxic and would not induce cell death⁸⁻¹¹. Unfortunately, the glue would not stick to the PTFE discs, ePTFE or the LLDPE. Even after the adhesive was allowed to dry for 24 hours, it still did not hold the materials to the PTFE discs. This ruled it out as a usable adhesive in these studies. The next option was double-sided carbon tape. Carbon tape was considered because of the strong and solvent-free adhesive. The tape was commercially available as double-sided tape, and it also came in pre-cut circles, which would allow for easier and more consistent assembly of the substrates.

In short, all substrates used in these studies were taped to an 8-mm-diameter PTFE disc (Qorpak) using 6 mm pre-cut double-sided carbon tape circles (Ted Pella, Inc.) to prevent sample floatation. **Figure 2.2.1** shows the carbon tape circles and the PTFE discs. The 6-mm diameter carbon tape circles were chosen to ensure the tape would be covered completely by the substrates.



Ted Pella Carbon
Tape Circles



Qorpak PTFE Discs

Figure 2.2.1: Images of the carbon tape circles and PTFE discs used to create the substrates.

The substrates and the PTFE discs were sterilized in 70% ethanol for 15 minutes. Then, the ethanol was aspirated and the substrates and PTFE discs were washed twice with phosphate buffered saline (PBS) and allowed to air dry. Once they were dry, one carbon tape circle was applied to each PTFE disc, and the tape-disc assemblies were exposed to UV light for 15 minutes. The substrates were then applied to the exposed side of the carbon tape, forming the substrate-disc assemblies that would be used in these experiments. Finally, the samples were again exposed to UV light for 30 minutes to further sterilize them.

2.2.1 Analysis of the Effect of the Addition of Carbon Tape and PTFE discs

In order to determine the effect, if any, that the chosen method of substrate preparation would have on the results of the experiments, several studies were completed. These studies involved only TCPS as a substrate material. Three groups of samples were made: No Tape, Tape 1 and Tape 2. The samples in the ‘No Tape’ group were 8-mm-diameter samples of TCPS, with no additional adhesive or other materials. ‘Tape 1’ consisted of samples created as described above. ‘Tape 2’ consisted of samples that were created as follows. The entire substrate assembly was formed by taping non-sterilized TCPS to non-sterilized PTFE. Then, the substrates were sterilized by a 30 minute bath in 70% ethanol, followed by two washes in PBS. After air drying, they were exposed to UV light for 30 minutes. The two different methods of creating the assembled substrates were used to determine if exposing the carbon tape to ethanol would have any negative effects, as the procedure for fixing samples for SEM would require ethanol baths.

The three sample groups were used to perform a cytotoxicity assay and to determine the platelet adhesion and activation. The procedure for these experiments will be described later in this chapter. TCPS was the only material used for these experiments for several reasons. First, TCPS sinks, and thus it was physically possible to use it. Second, TCPS is a known non-cytotoxic material, and it does not inhibit cell adhesion. Therefore, a substantial amount of platelets would be expected to adhere to the control (No Tape) surfaces, which would allow for some indication of whether the experiments worked.

2.3 Surface Characterization

2.3.1 Surface Wettability – Contact Angle Measurements

The surface wettability was characterized using contact angle measurements¹² (ramé-hart Model 250 Standard Goniometer, shown in **Figure 2.3.1**).



Figure 2.3.1: ramé-hart Model 250 Standard Goniometer used to obtain contact angle measurements.

Contact angles indicate the hydrophobicity or hydrophilicity of a material. Materials with contact angles greater than 90° are considered hydrophobic, while materials with contact angles less than 90° are hydrophilic¹³ (see **Figure 2.3.2**).

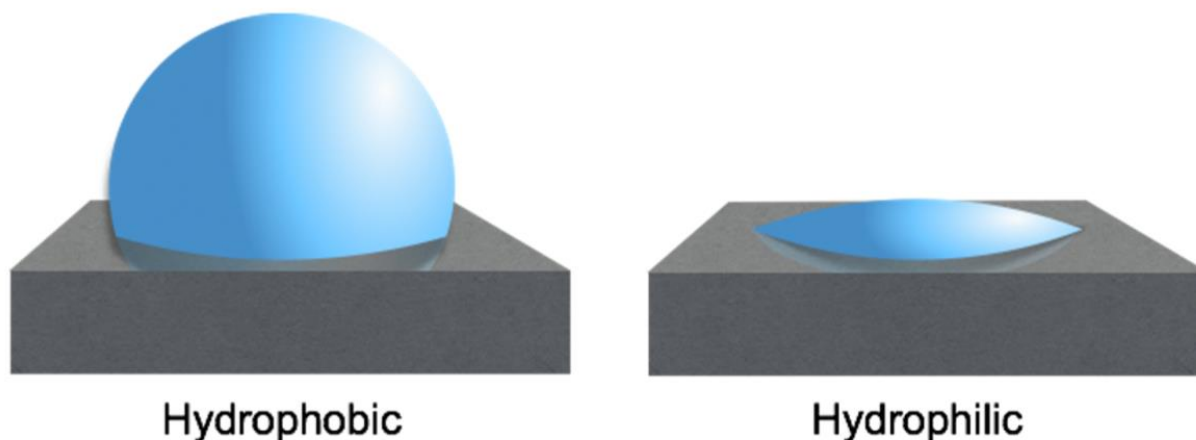


Figure 2.3.2: Illustration of contact angles corresponding to hydrophobicity and hydrophilicity. Reprinted with permission from Colorado State University, Figure 2.3.7 from the thesis of Jonathon Sorkin, “Titania Nanotube Arrays as Potential Interfaces for Neurological Prostheses.”

The substrates were cleaned by blowing air across the surface to remove any foreign material that might affect the contact angles. Approximately 1 μL droplet of DI water was dispensed onto each surface. The goniometer was used to find the angle of phase separation between the liquid-solid, and liquid-vapor interface, or the contact angle. The contact angle was measured within 5 seconds of droplet contact with the substrate surface. Images of the droplet on the substrate surface were taken and analyzed using the accompanying software (DROPImage advanced software) to determine the contact angle. Representative images were taken of a droplet on each sample.

2.3.2 SEM Imaging

The surface structure of each substrate was characterized using SEM. The substrates were coated with a 10 nm layer of gold and imaged at 15 kV. The microscope used is seen in **Figure 2.3.3**, model JEOL JSM SEM 6500F.

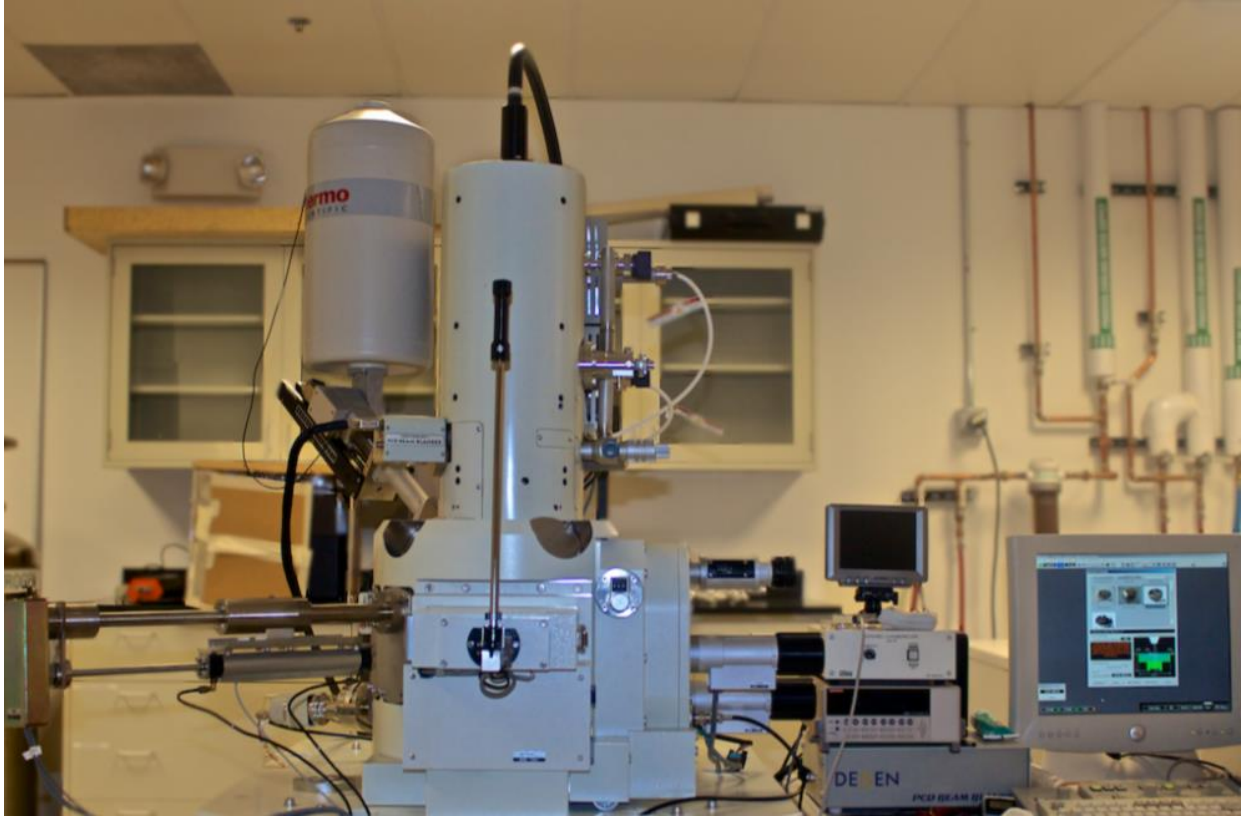


Figure 2.3.3: Scanning Electron Microscope (SEM) used to obtain SEM images, model JEOL JSM SEM 6500F

2.4 Collection of Whole Blood

Whole blood was collected from healthy individuals who were showing no signs of illness and had not taken pain medications within 2 weeks of donation. The blood was collected into 10 mL vacuum tubes (BD Medical) coated with ethylenediaminetetraacetic acid (EDTA) to prevent clotting. The first tube was discarded to account for the skin plug and the locally activated platelets caused by the needle insertion. The tubes were centrifuged within 30 minutes of blood collection at 150 g for 15 minutes to separate the plasma from the rest of the blood components. The plasma was then pooled and used within 15 minutes of isolation.

2.5 Cytotoxicity

The cytotoxicity of different materials was determined using the lactate dehydrogenase (LDH) assay (Cayman Chemical). The cytotoxicity of a material is a measure of the amount of cell death it causes when placed in contact with cells. Cell death can occur through two mechanisms: apoptosis or necrosis. Although the two mechanisms follow two different pathways, they both cause cell damage or lysis, resulting in increased membrane permeability. LDH is a soluble enzyme located within cells, which is released through the membrane upon cell death¹⁴. Therefore, measuring the amount of LDH in the substrate-exposed plasma can be an indication of membrane integrity, and thus an accurate measure of the cytotoxicity of the materials¹⁴. In order to complete this experiment, the substrates were placed in a 48 well plate and incubated in 500 μ L of plasma on a horizontal shaker plate at 100 rpm for 2 hours at room temperature. Upon completion of the incubation, the substrate-exposed plasma was used to measure the cytotoxicity per manufacturer instructions. In short, the substrates were placed on a shaker plate at 1,000 rpm for 5 minutes to dislodge any dead cells from the surfaces. The substrates were then removed from the plasma. The standards (provided in the assay kit), along with the substrate-exposed plasma, were transferred to a 96-well plate, with each well containing 150 μ L of either standards or substrate-exposed plasma. The reaction solution was created per manufacturer instructions (96% v/v assay buffer, 1% v/v NAD⁺, 1% v/v Lactic Acid, 1% v/v INT, and 1% v/v LDH Diaphorase), and 150 μ L was added to each well (1:1). The solutions were allowed to incubate further for 30 minutes at 100 rpm on a horizontal shaker plate. The absorbance of the solutions was then read at a wavelength of 490 nm, using the FLUOstar Omega plate reader, shown in **Figure 2.5.1**.



Figure 2.5.1: Plate reader – FLUOstar Omega

2.6 Protein Adsorption

2.6.1 *Micro-BCA Assay*

Albumin (ALB), immunoglobulin (IgG) and fibrinogen (FIB) adsorption was investigated on different materials. The substrates were placed in a 48-well plate and incubated in 500 μ L of 100 μ g/mL solutions of ALB (Sigma Aldrich), IgG (Sigma Aldrich) or FIB (Sigma Aldrich) in PBS. They were incubated on a horizontal shaker plate at 100 rpm for 2 hours at room temperature. After the incubation, the substrates were moved to a clean 48-well plate and washed twice with PBS to remove any non-adherent proteins. Subsequently, the substrates were incubated in 500 μ L

1% sodium dodecyl sulfate solution (SDS) solution in PBS on a horizontal shaker plate for 3 hours in order to solubilize the proteins. The substrates were then removed from the SDS solutions.

Once the SDS solutions with solubilized proteins were created, a micro-BCA assay (Thermo Scientific) was used to determine the protein concentration in the solutions. This assay is a detergent-compatible BCA formulation for the colorimetric quantification of total protein. It works by utilizing BCA as the detection reagent for Cu^{+1} , which is formed when Cu^{+2} is reduced by proteins¹⁵. When two molecules of BCA bond with one Cu^{+1} ion, a purple-colored reaction product is formed. The colored complex exhibits a strong absorbance at 562 nm, which is linear with increasing protein concentrations¹⁵. The manufacturer's instructions were followed to determine the protein concentration in each SDS solution. A set of 9 standards of each protein in PBS was created, with the following concentrations: 200 $\mu\text{g/mL}$, 40 $\mu\text{g/mL}$, 20 $\mu\text{g/mL}$, 10 $\mu\text{g/mL}$, 5 $\mu\text{g/mL}$, 2.5 $\mu\text{g/mL}$, 1 $\mu\text{g/mL}$, 0.5 $\mu\text{g/mL}$ and 0 $\mu\text{g/mL}$ (blank). The working reagent was prepared by mixing Reagent MA, Reagent MB and Reagent MC, all provided in the kit, in a ratio of 25:24:1 (MA:MB:MC). Then, 150 μL of each standard and SDS solutions were put into a 96-well plate, followed by the addition of 150 μL of the working reagent into each well containing a standard or SDS solution. The plate was incubated for 2 hours at 37°C and 5% CO_2 . After cooling to room temperature, the plate was placed in a plate reader and the absorbance was measured at 562 nm.

2.6.3 Visualization of Proteins Adsorbed to the Surfaces

In order to obtain a visualization of the proteins adsorbed to the surfaces of the materials, the substrates were incubated in 500 μL of 100 $\mu\text{g/mL}$ solutions of ALB, FIB and IgG for 2 hours at room temperature on a horizontal shaker plate at 100 rpm. They were then washed twice with

PBS and allowed to air dry. The substrates were then coated with a 10 nm layer of gold and imaged with SEM at 15 kV.

2.7 Platelet and Leukocyte Adhesion and Activation

2.7.1 Fluorescence Microscopy Imaging – Calcein-AM Live Stain

Platelet adhesion on different materials was investigated using fluorescence microscopy imaging of calcein-AM live staining. This stain serves as a viability probe for both enzymatic activity and cell membrane integrity, since the enzymatic activity of the cell is required to activate the fluorescence of the compound, and the membrane integrity is required to retain the fluorescent complexes. The electrically neutral esterase molecules can diffuse easily through the cell membrane. Once inside the cell, the initially non-fluorescent molecules are converted by intercellular esterases into fluorescent molecules, which are then retained by the cell membrane. In order to complete this experiment, the substrates were placed in a 48-well plate and incubated in 500 μ L of plasma on a horizontal shaker plate at 100 rpm for 2 hours. After incubation, the plasma was aspirated and the substrates were washed twice with PBS to remove any un-adhered platelets. They were then incubated in 5 μ M calcein-AM solution in PBS for 30 minutes at 37°C and 5% CO₂. After incubation, the substrates were rinsed with PBS and imaged using a fluorescence microscope (Zeiss Imager.A2, shown in **Figure 2.7.1**). The images were analyzed using ImageJ software to determine the percent coverage of adhered platelets on different substrates.

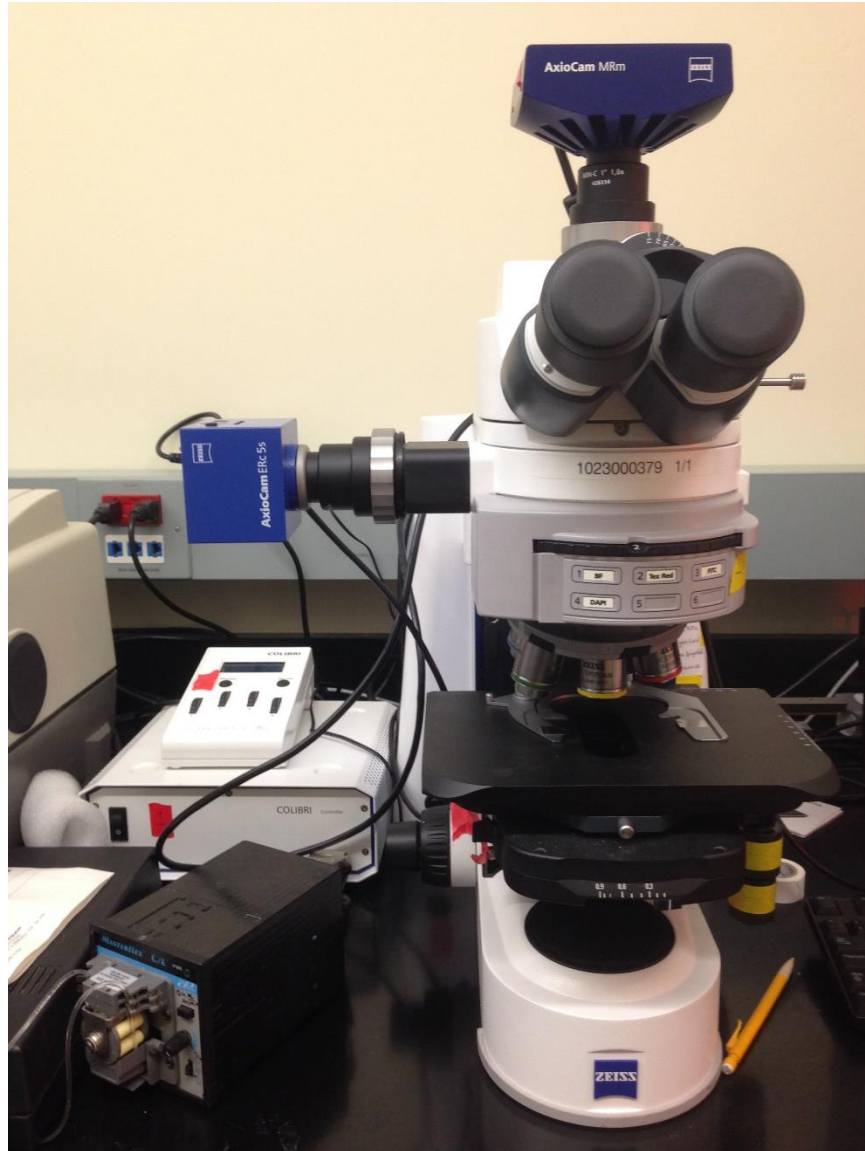


Figure 2.7.1: Fluorescent Microscope – Zeiss Imager.A2

2.7.2 Fluorescence Microscopy Imaging – Actin and DAPI Stains

Platelet adhesion was further analyzed to differentiate between platelets and leukocytes. This was accomplished using rhodamine conjugated phalloidin (Cytoskeleton, Inc.) stain for platelets (hereafter called actin) and 4',6-diamidino-2-phenylindole- dihydrochloride stain (DAPI, AnaSpec, Inc.) for leukocytes. Phalloidin is a toxin derived from the *Amanita*

phalloides mushroom. It binds to F-actin in cells, preventing its depolymerization. Thus, once conjugated with a fluorescent tag, it is a highly efficient probe for actin filaments. However, it cannot diffuse through most live cell membranes, so the cells must be fixed and permeabilized. Once this occurs, the stain can easily pass through. DAPI stain targets nucleic acids, preferentially binding to AT base pairs^{16, 17}. This makes it a probe for cells with nuclei, thus differentiating between platelets and leukocytes, as platelets do not have nuclei². The substrates were placed in a 48-well plate and incubated in 500 μ L of plasma on a horizontal shaker plate at 100 rpm for 2 hours. After incubation, the plasma was aspirated and the substrates were washed twice with PBS to remove any un-adhered platelets. The samples were transferred to new wells. The adhered cells were fixed with 3.7 % formaldehyde in PBS for 15 minutes at room temperature and washed 3 times for 5 minutes each in PBS. The cell membranes were then permeabilized with 1 % Triton-X in PBS at room temperature for 3 minutes and rinsed once with PBS. The samples were transferred to new wells and incubated in 500 μ L of 70 nM actin solution in PBS for 25 minutes at room temperature. Following this incubation, 500 μ L of 300 nM DAPI stain was added to each well. After 5 minutes, the wells were aspirated and the surfaces were rinsed with PBS. They were then imaged with a fluorescent microscope. The images were analyzed using ImageJ software to determine the percent coverage of adhered leukocytes on different substrates.

2.7.3 Visual Determination of Activated Platelets Using SEM

Adhered platelets on different materials were imaged using SEM. The substrates were placed in a 48-well plate and incubated in 500 μ L of plasma on a horizontal shaker plate at 100 rpm for 2 hours. After incubation, the plasma was aspirated and the substrates were washed twice with PBS to remove any un-adhered platelets. The cells adhered to the substrates were fixed by

incubation in a primary fixative consisting of 3% glutaraldehyde, 0.1M sodium cacodylate, and 0.1M sucrose for 45 minutes. They were then incubated in a buffer consisting of the primary fixative without glutaraldehyde for 10 minutes. This was followed by dehydration by incubation in increasing concentrations of ethanol (35%, 50%, 70%, 100%) for 10 minutes each. The substrates were further dehydrated in hexamethyldisilazane (HMDS) for 10 minutes. The substrates were allowed to air dry and placed in a dessicator until used for imaging with SEM. The substrates were coated with a 10 nm layer of gold and imaged at 15 kV. The SEM images were also used to semi-quantify platelet activation by determining the percentage of platelets with the morphology consistent with different levels of activation. The following criteria were used to characterize different levels of activation:

- Unactivated: platelets with no dendritic extensions and a spherical, compact bodies
- Activated: platelets with dendritic extensions and non-spherical bodies

2.7.4 Fluorescence Microscopy Imaging – P-selectin and CD45 Stains

Immunofluorescence staining was used to determine the expression of P-selectin and CD45, proteins exclusive to platelets and leukocytes, respectively. P-selectin is expressed upon the activation of platelets. It plays key roles in leukocyte recruitment and further deposition of fibrin^{2, 18, 19}. CD45 is expressed upon activation of leukocytes. It plays important roles in several immune pathways, and has not been found to be expressed by platelets^{20, 21}. Therefore, the expression of each of these proteins indicates the activation of platelets and leukocytes, and differentiates between the two. The substrates were placed in a 48-well plate and incubated in 500 μ L of plasma on a horizontal shaker plate at 100 rpm for 2 hours. After incubation, the plasma was aspirated and the substrates were washed twice with PBS to remove any un-adhered platelets. The

samples were transferred to new wells. The adhered cells were fixed with 3.7 % formaldehyde in PBS for 15 min at room temperature and washed 3 times for 5 minutes each in PBS. The cell membranes were permeabilized in 1 % Triton-X in PBS at room temperature for 3 minutes and washed 3 times for 5 minutes each with PBS. This was followed by incubation in a blocking solution of 10 % bovine serum albumin (BSA) in PBS for 30 minutes at room temperature to prevent non-specific immune reactions. The samples were washed 3 times for 5 minutes each in PBS. They were then incubated for 1 hour at room temperature in a 1:50 solution of primary antibodies in 2% BSA – P-Selectin for platelets and CD45 for leukocytes (Santa Cruz Biotechnology). The samples were transferred to fresh wells and then washed 3 times for 5 minutes each in PBS. This was followed by incubation for 1 hour at room temperature in a 1:100 solution of fluorescently-labeled secondary antibodies in 2% BSA – donkey anti-goat conjugated with Texas Red for P-Selectin and chicken anti-mouse conjugated with FITC for CD45 (Santa Cruz Biotechnology). Finally, the surfaces were washed 3 times for 5 minutes each in PBS and then imaged with a fluorescence microscope. All images were processed using ImageJ software to determine the percent coverage of P-selectin and CD45.

2.8 Whole Blood Clotting

2.8.1 Hemolysis Assay

Whole blood clotting kinetics on the surfaces of the materials was evaluated. The clotting kinetics play an important role in the ultimate success of a blood-contacting material. If a clot forms quickly, the material could be encapsulated, leading to failure of the implant¹. In order to characterize the whole blood clotting kinetics, sterilized samples were placed in a 12-well plate. Whole blood was drawn from healthy individuals using untreated (non-EDTA) 3 mL vacuum tubes

and 5 μ l of blood was dropped onto each surface. The free hemoglobin concentration was measured after the blood had clotted for 15, 30, 45 and 60 minutes, as free hemoglobin is an indication of the amount of clotting that has occurred. Larger amounts of free hemoglobin correspond to a smaller amount of clotting¹. In order to measure the free hemoglobin, the surfaces were transferred into a clean 12-well plate with 500 μ l of DI water in each well. The surfaces were then gently agitated for 30 seconds and left in the DI water for 5 minutes. The free hemoglobin was released from red blood cells that were not trapped in the thrombus in this manner. Finally, 300 μ l of the DI water was transferred to a 96-well plate. The absorbance of the water was measured at a wavelength of 540nm using a plate reader. The value of absorbance is directly proportional to the concentration of free hemoglobin in DI water, with higher absorbance corresponding to higher amounts of free hemoglobin¹. Therefore, the absorbance of the DI water is an indication of the amount of clotting caused by each of the materials.

2.8.2 Visualization of Blood Clots on Surfaces

The blood clots on the surface of each material was visualized. Whole blood was drawn from healthy individuals using untreated (non-EDTA) 3 mL vacuum tubes and 5 μ l of blood was dropped onto each surface. The blood was allowed to clot for 60 minutes. After 60 minutes, the clots were coated with a 10nm layer of gold and imaged with SEM at 15 kV.

2.9 Statistical Analysis

The contact angle measurements, platelet adhesion, immunofluorescence and platelet activation studies were conducted with 3 substrates of each material and were repeated with 3 different platelet populations ($n_{\min} = 9$). The cytotoxicity and protein adsorption studies were

conducted with 5 substrates of each material and were repeated with two different platelet populations ($n_{\min} = 10$). All the quantitative results were analyzed using ANOVA and Tukey's Post Hoc test, with statistical significance considered at $p < 0.05$.

2.10 Conclusion

Many polymeric materials are used today in many different blood-contacting applications. Despite their frequent use, they all still tend to elicit an immune response. There are several events that occur within seconds to minutes of exposure to blood, such as adsorption of blood serum proteins, platelet adhesion and platelet activation. These events significantly affect the subsequent events that occur after. Surface characteristics of the material can influence the initial events of the immune response, and thus can improve the hemocompatibility of materials.

In this study, static methods were used to characterize the protein adsorption, platelet adhesion and activation, and whole blood clotting kinetics on ePTFE, LLDPE and PET. Static methods eliminated any confounding effects from material-blood flow interaction, thus providing knowledge of the response generated by the surface characteristics of each material. This provides a baseline against which any future surface modifications of the materials can be compared.

REFERENCES

1. Leszczak, V., B.S. Smith, and K.C. Papat, *Hemocompatibility of polymeric nanostructured surfaces*. J Biomater Sci Polym Ed, 2013. **24**(13): p. 1529-48.
2. Smith, B.S. and K.C. Papat, *Titania Nanotube Arrays as Interfaces for Blood-Contacting Implantable Devices: A Study Evaluating the Nanotopography-Associated Activation and Expression of Blood Plasma Components*. Journal of Biomedical Nanotechnology, 2012. **8**(4): p. 1-17.
3. Leszczak, V. and K.C. Papat, *Improved in Vitro Blood Compatibility of Polycaprolactone Nanowire Surfaces*. ACS Appl Mater Interfaces, 2014.
4. Prawel, D.A., et al., *Hemocompatibility and Hemodynamics of Novel Hyaluronan-Polyethylene Materials for Flexible Heart Valve Leaflets*. Cardiovasc Eng Technol, 2014. **5**(1): p. 70-81.
5. Shtansky, D.V., et al., *A comparative study of the structure and cytotoxicity of polytetrafluoroethylene after ion etching and ion implantation*. Physics of the Solid State, 2011. **53**(3): p. 638-642.
6. Srinivasan, S., Q. Yang, and V.N. Vasilets, *Nitrogen Doped Diamond Like Carbon Thin Films on PTFE for Enhanced Hemocompatibility*, in *Nanostructured Materials and Nanotechnology II: Ceramic Engineering and Science Proceedings, Volume 29, Issue 8*. 2009, John Wiley & Sons, Inc. p. 233-242.
7. VARCO, T.C., et al., *Hydrogen/ Liquid Vapor Radio Frequency Glow Discharge Plasma Oxidation/ Hydrolysis of Expanded Poly (tetrafluoroethylene) (ePTFE) and Poly (vinylidene Fluoride) (PVDF) Surfaces* Journal of Polymer Science, 1991. **29**: p. 555-570.
8. Scardino, M.S., et al., *Evaluation of fibrin sealants in cutaneous wound closure*. J Biomed Mater Res, 1999. **48**(3): p. 315-21.
9. Siedentop, K.H., et al., *Safety and efficacy of currently available fibrin tissue adhesives*. Am J Otolaryngol, 2001. **22**(4): p. 230-5.

10. Saygun, O., et al., *Reinforcement of the suture line with an ePTFE graft attached with histoacryl glue in duodenal trauma*. *Can J Surg*, 2006. **49**(2): p. 107-12.
11. Reece, T.B., T.S. Maxey, and I.L. Kron, *A prospectus on tissue adhesives*. *The American Journal of Surgery*, 2001. **182**(2, Supplement 1): p. S40-S44.
12. Srinivasan, S., G.H. McKinley, and R.E. Cohen, *Assessing the accuracy of contact angle measurements for sessile drops on liquid-repellent surfaces*. *Langmuir*, 2011. **27**(22): p. 13582-9.
13. D.Y.Kwok and A.W.Neumann, *Contact angle measurement and contact angle interpretation*. *Advances in Colloid and Interface Science* 1999. **81**.
14. Han, X., et al., *Validation of an LDH assay for assessing nanoparticle toxicity*. *Toxicology*, 2011. **287**(1-3): p. 99-104.
15. Smith, P.K., et al., *Measurement of protein using bicinchoninic acid*. *Analytical Biochemistry*, 1985. **150**(1): p. 76-85.
16. Hamada, S. and S. Fujita, *DAPI staining improved for quantitative cytofluorometry*. *Histochemistry*, 1983. **79**(2): p. 219-226.
17. Kapuscinski, J., *DAPI: a DNA-specific fluorescent probe*. *Biotech Histochem*, 1995. **70**(5): p. 220-33.
18. Hayashi, S.-i., et al., *Roles of P-Selectin in Inflammation, Neointimal Formation, and Vascular Remodeling in Balloon-Injured Rat Carotid Arteries*. *Circulation*, 2000. **102**(14): p. 1710-1717.
19. Yeo, E., J. Sheppard, and I. Feuerstein, *Role of P-selectin and leukocyte activation in polymorphonuclear cell adhesion to surface adherent activated platelets under physiologic shear conditions (an injury vessel wall model)*. Vol. 83. 1994. 2498-2507.
20. Tchilian, E.Z. and P.C.L. Beverley, *Altered CD45 expression and disease*. *Trends in Immunology*, 2006. **27**(3): p. 146-153.

21. Altin, J.G. and E.K. Sloan, *The Role of CD45 and CD45-Associated Molecules in T Cell Activation*. *Immunology and Cell Biology*, 1997. **75**: p. 430-445.

CHAPTER 3

RESULTS AND DISCUSSION

3.1 Introduction

The aim of this study was to characterize the initial response of potential blood-contacting materials when they come in contact with blood. Short-term hemocompatibility of ePTFE, LLDPE and PET was investigated and compared to that of TCPS. Specifically, we characterized the responses related to protein adsorption, platelet adhesion, adhered platelet activation and whole blood clotting. The surface structure of each material was also characterized to potentially provide an explanation for the results.

3.2 Analysis of the Effect of the Carbon Tape and PTFE Disc

When these experiments began, it became obvious that ePTFE and LLDPE would float in all of the liquids used. This became problematic because these two materials were not exposed to the plasma in the same manner as TCPS and PET, which both sank. The solution to this problem was to attach ePTFE and LLDPE to PTFE discs with carbon tape circles, which would ensure they sink consistently. TCPS and PET were also taped to PTFE discs to eliminate any factors that would skew the results. Before this solution could be implemented, an analysis of the effect of the addition of the carbon tape and PTFE discs needed to be completed. This study entailed a cytotoxicity assay and characterization of platelet adhesion and activation, the specifics of which are described in subsequent sections of this chapter. The cytotoxicity assay would verify the tape and PTFE discs do not cause cell death. This was important to verify to avoid concluding a material is hemocompatible due to the lack of platelet adhesion, when in reality no platelets

adhered because the material is cytotoxic. The characterization of platelet adhesion and activation would ensure that the addition of the carbon tape and PTFE disc does not cause a significant increase in activation in those platelets that adhere to the surfaces. The experiments compared three different groups of TCPS. The first group (No Tape) did not include tape or PTFE discs. Groups two (Tape 1) and three (Tape 2) both included tape and PTFE discs, but were prepared in slightly different ways. The results showed that the tape and the PTFE do not induce cell death, so they can be considered non-cytotoxic. The presence of the tape and PTFE does promote a greater amount of platelet adhesion, but not platelet activation. Platelet activation, and not platelet adhesion, is the event that will cause a more severe immune response. Therefore, the solution was deemed acceptable to use. The results of each individual test are discussed in detail below.

3.2.1 Cytotoxicity Study

Cytotoxicity is an important material characteristic, as a material should not induce cell death, either through apoptosis or necrosis¹. Both mechanisms cause an increase in cell membrane permeability, therefore, most available assays assess cytotoxicity based on membrane integrity². In this study, the cytotoxicity of each group was measured using the LDH assay. LDH is an enzyme found within the cytosol. Upon cell damage or lysis, it is released into the culture medium. Thus, LDH activity is related to membrane permeability and can be used as an indicator of cytotoxicity². The LDH assay measures the amount of LDH activity in the substrate-exposed plasma. The results, shown in **Figure 3.2.1**, indicate that no significant differences in cytotoxicity exist between the three groups. This means that the addition of the tape and PTFE did not cause cell death, and any absence of platelet adhesion could not be attributed to the addition of the tape and PTFE disc.

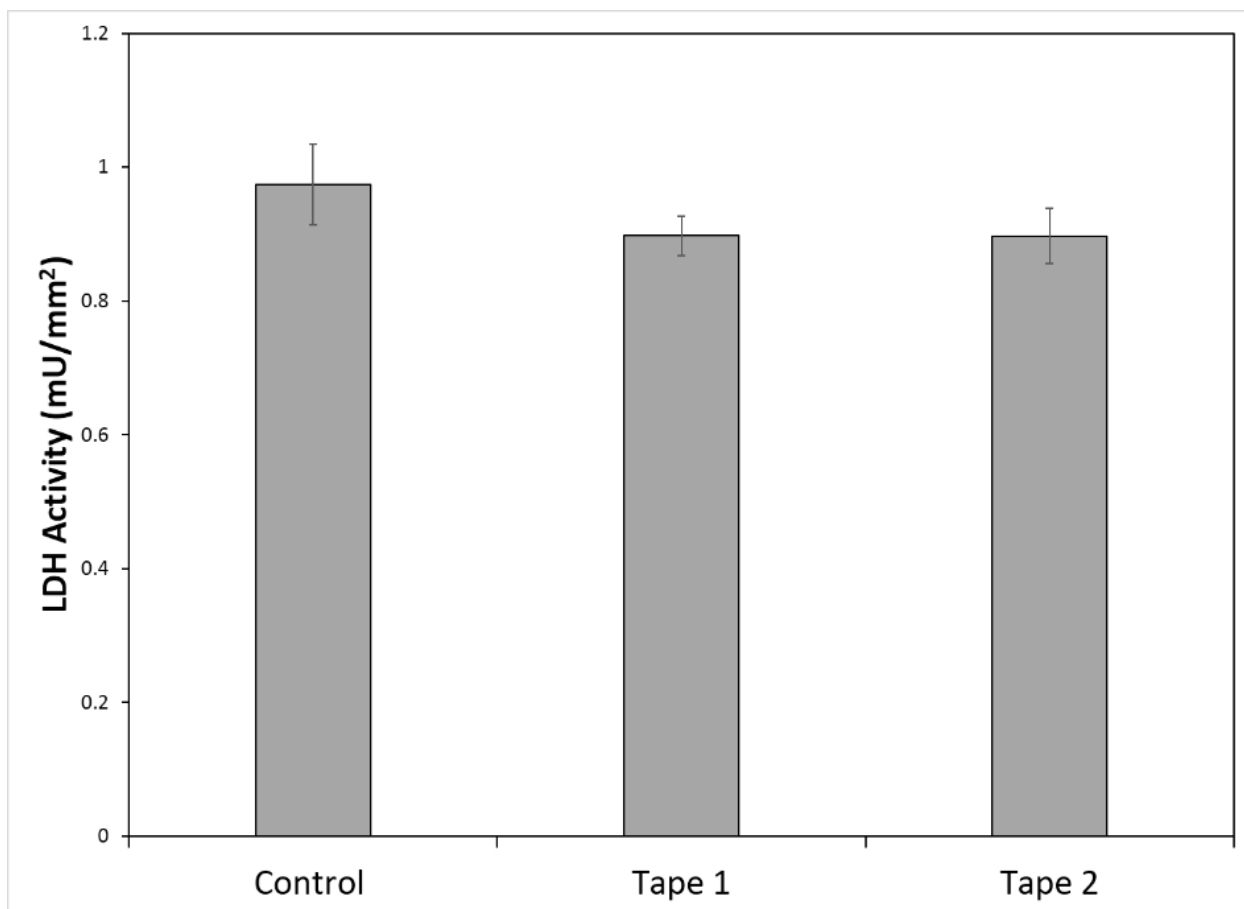


Figure 3.2.1: The cytotoxicity of the 3 groups of TCPS. The results indicate no statistical difference between the control group and the test groups.

3.2.2 Platelet and Leukocyte Adhesion – Calcein-AM Staining

Platelet adhesion was characterized by staining adhered cells with calcein-AM. Representative images are shown in **Figure 3.2.2**. The results show a visual difference in amount of adhered cells on the No Tape substrates, versus the Tape 1 and Tape 2 substrates. No obvious difference could be seen between the Tape 1 and Tape 2 groups.

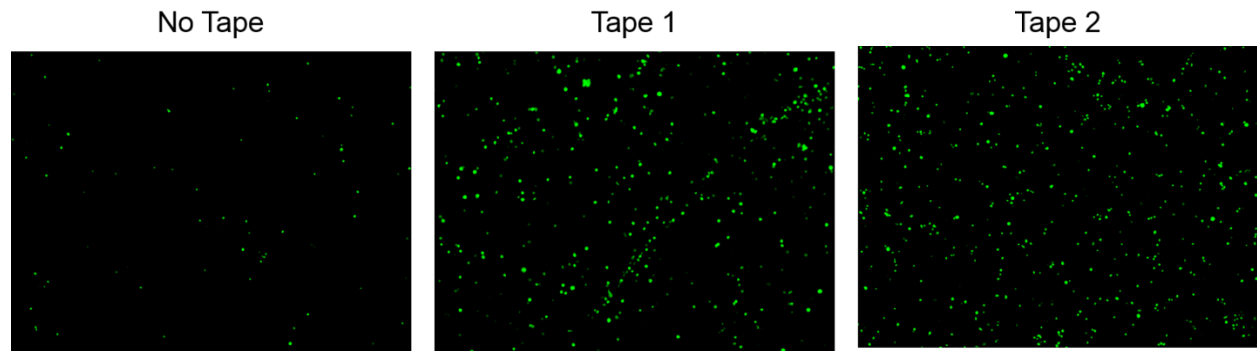


Figure 3.2.2: Fluorescence microscopy images of platelets stained with calcein AM on different groups, showing visual difference between the control and test groups.

The images were then analyzed with ImageJ software to determine the percent coverage of platelets on the surfaces. The results are presented in **Figure 3.2.3**. They correlate with the visual observations. The amount of platelets that adhered to the No Tape surfaces is significantly lower than the amount of platelets that adhered to the Tape 1 and Tape 2 surfaces. There is no significant difference between Tape 1 and Tape 2 groups. This indicates that the presence of the tape and the PTFE discs promotes greater platelet adhesion.

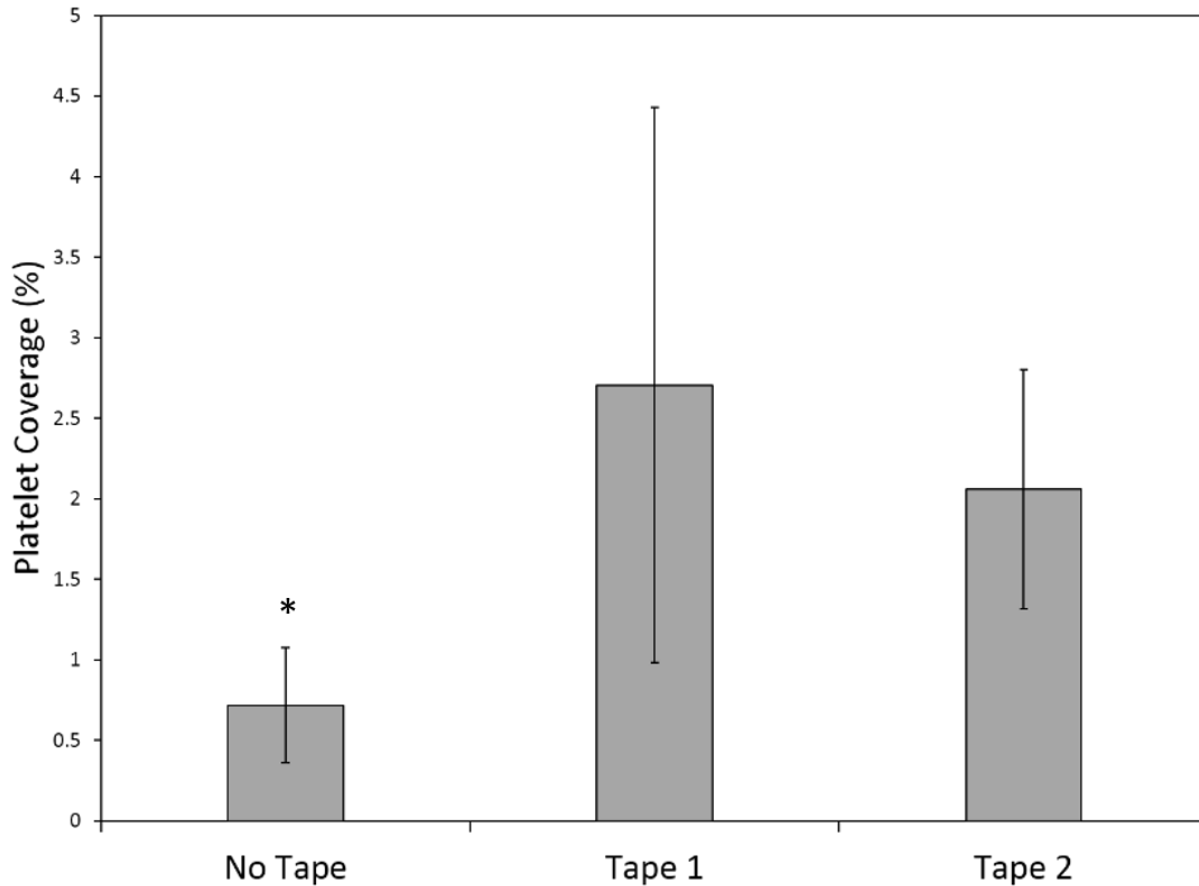


Figure 3.2.3: Platelet coverage of the different groups. There are significantly less platelets adhered to the control group as compared to the test groups (* \rightarrow $p < 0.05$).

3.2.3 Platelet Activation – SEM imaging

Platelet adhesion does not equate to platelet activation. Although a high number of platelets may adhere to a surface, if they do not become activated, the clotting process will not progress^{3,4}. Therefore, the activation of the adhered platelets onto each of the substrates in these groups was quantified using SEM imaging. The initial images showed a similar trend to the fluorescent images, in terms of the number of platelets adhered. The percentage of activated platelets was determined from the images found in **Figure 3.2.4**. The results are presented in **Figure 3.2.5**. They show that there are no significant differences in the percentage of activated platelets between all three groups.

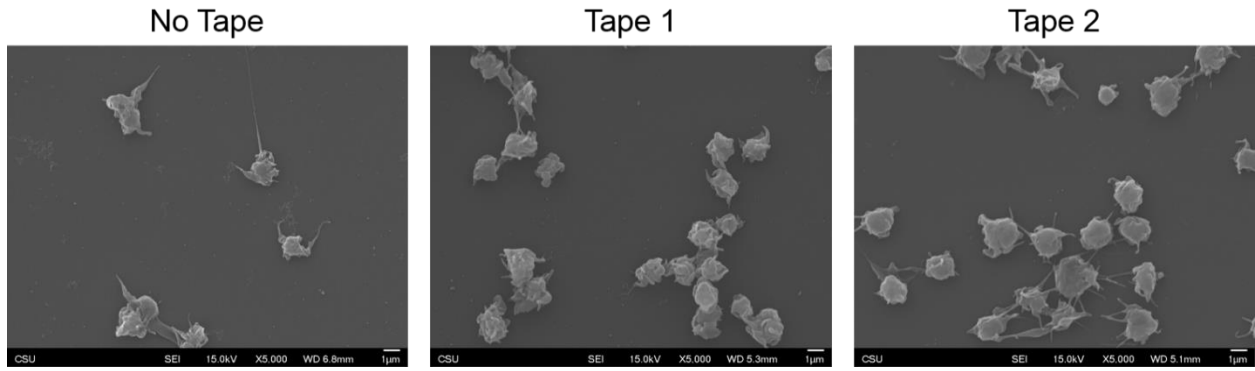


Figure 3.2.4: SEM images of adhered platelets, showing a similar trend to that found in the fluorescence microscopy images.

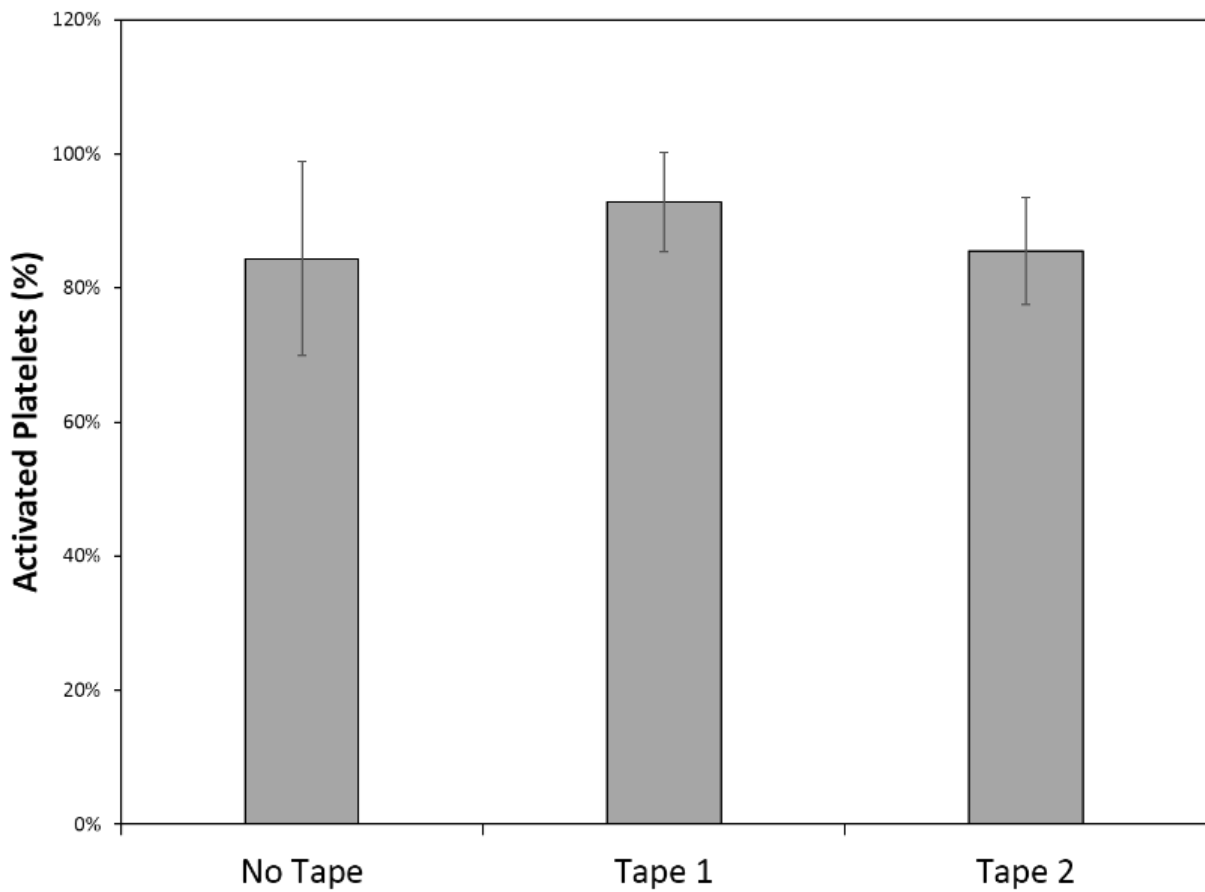


Figure 3.2.5: Percentage of activated platelets on the substrates in each of the three groups. No statistical differences exist.

3.3 Surface Characterization

3.3.1 Surface Structure – SEM imaging

In order to characterize the surface structure of each material, SEM imaging was done. Representative images are shown in **Figure 3.3.1**. The images show varying morphologies on different materials. The surface structures of TCPS and LLDPE are uniform and non-porous, lacking any apparent features that would promote platelet adhesion and activation. The surface structure of ePTFE consists of a porous network of fibers oriented in varying directions, while that of PET shows a network of uniformly oriented fibers that are much larger than those found in ePTFE. The images of TCPS, ePTFE, LLDPE, and PET show results similar to those found in literature⁵.

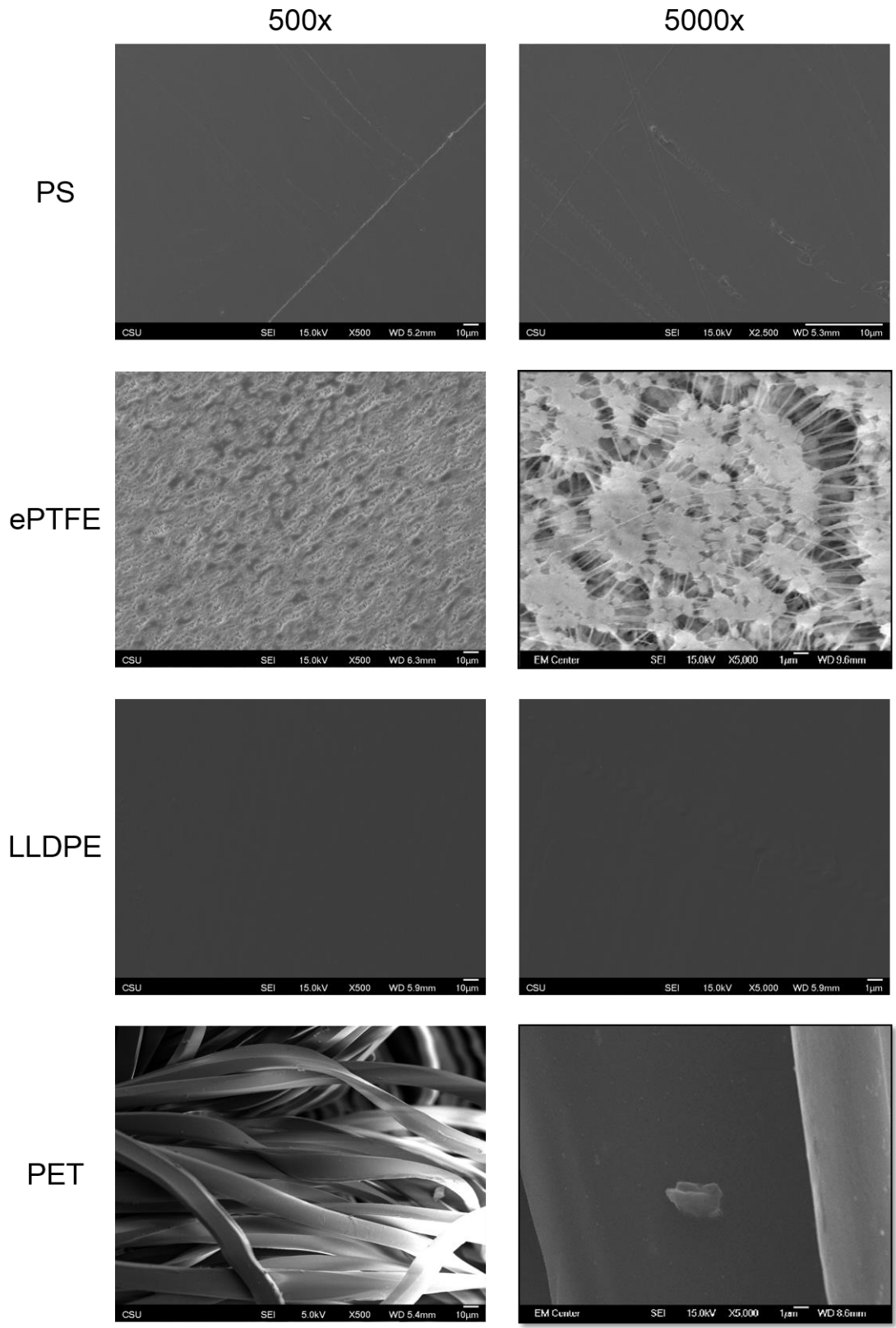


Figure 3.3.1: SEM images showing the surface structure of different materials.

3.3.2 *Surface Wettability – Contact Angle Measurements*

The wettability of each material was characterized by static contact angle measurements of DI water droplets using a sessile drop measurement technique^{6, 7}. Contact angle is defined as the angle between the substrate surface and the line tangent to the water droplet at the point of contact on the substrate. Higher contact angles are correlated to lower levels of surface energy and indicate a hydrophobic surface, whereas lower contact angles are correlated to higher levels of surface energy and indicate a more hydrophilic surface^{7, 8}. Contact angles are dependent on several surface-specific characteristics, such as surface porosity, surface roughness and polarity. Increasing surface roughness will increase contact angles on inherently hydrophobic surfaces, but it will decrease contact angles on surfaces with contact angle less than 60°⁹. The magnitude of the surface dipole moment determines the hydrophobicity or hydrophilicity of a material. Increasing surface polarity will decrease contact angles¹⁰. **Figure 3.3.2** presents the results of the contact angle measurements.

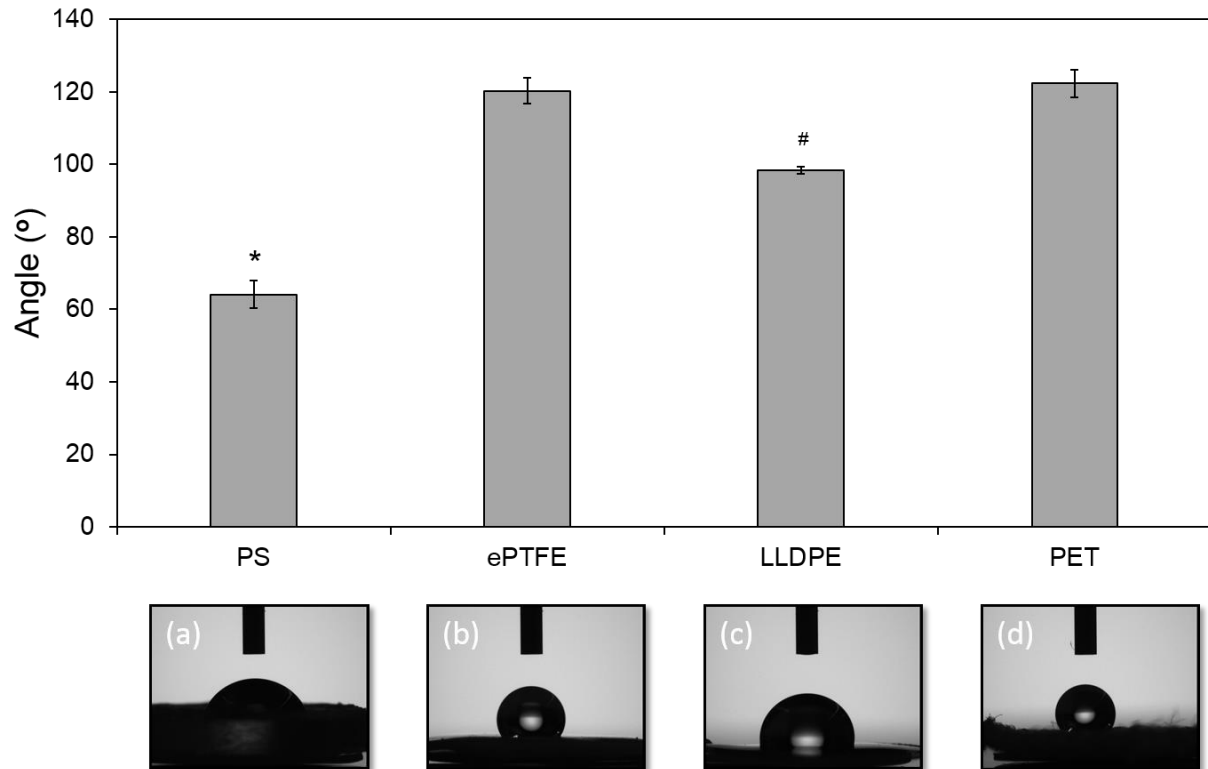


Figure 3.3.2: Contact angle measurements on different surfaces. The contact angle of TCPS is statistically different than that of ePTFE, LLDPE and PET (* \rightarrow $p < 0.05$) and that of LLDPE was statistically different than that of ePTFE and PET (# \rightarrow $p < 0.05$).

The contact angles measured were highest for ePTFE and PET with no statistically significant differences between the two. The contact angles obtained for TCPS and LLDPE were significantly less than those of ePTFE and PET, although LLDPE is still significantly higher than TCPS. These results indicate that ePTFE, LLDPE and PET are all hydrophobic materials with contact angles greater than 90° , although LLDPE is much less hydrophobic than ePTFE and PET. TCPS is a hydrophilic material with a contact angle less than 90° ¹¹. Previous studies have linked surface energy to material hemocompatibility¹²⁻¹⁷. As surface energy increases, protein adsorption increases. Furthermore, increased surface energy also has an effect on adsorbed protein

conformation¹⁸. Thus, controlling surface characteristics is a possible way to improve blood-material interactions.

3.4 Cytotoxicity

A blood-contacting biomaterial should not cause cell death. To ensure that none of these materials would cause cell death, the cytotoxicity of each material was determined using an LDH assay. The assay measured the LDH activity in substrate-exposed plasma. The results can be seen in **Figure 3.4.1**. LDH is an enzyme that is released through the cell membrane upon cell death. As discussed previously, a high level of LDH activity would indicate high levels of cell death. In this case, TCPS, a known non-cytotoxic material, was used as a positive control. All other materials were compared to it.

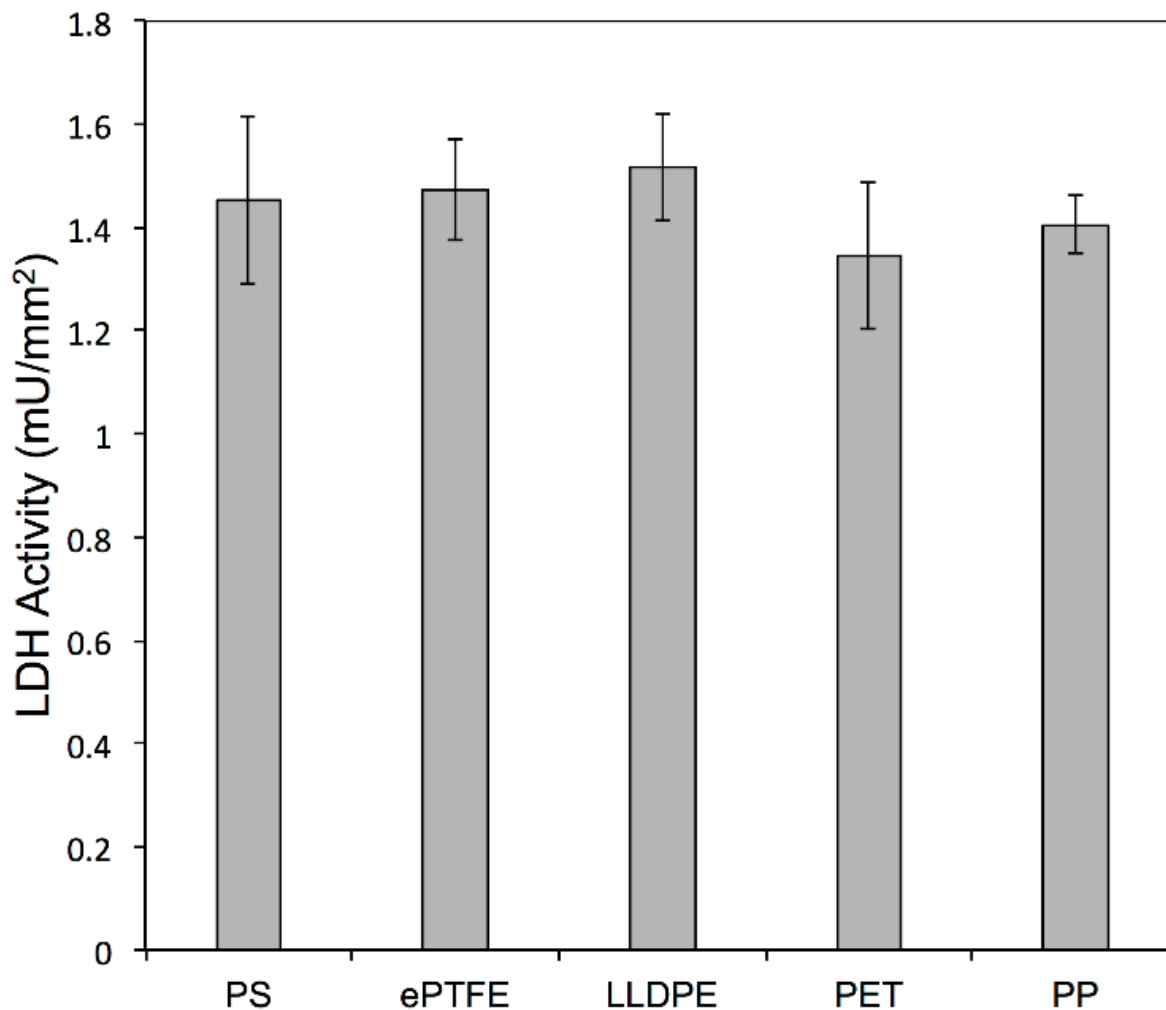


Figure 3.4.1: Cytotoxicity analysis of different materials using LDH assay. The results indicate no statistical differences in the cytotoxicity of all the materials.

The results indicate no statistically significant differences in LDH activity in the plasma exposed to the different materials. Since TCPS is generally considered to be a non-cytotoxic material, the lack of statistically significant differences indicates that none of the materials are cytotoxic.

3.5 Protein Adsorption

3.5.1 *Micro-BCA Assay*

Protein adsorption is the first step that occurs in the clotting cascade. Once a material comes into contact with blood, proteins almost immediately adsorb to its surface and begin conformational changes¹⁹⁻²². They form a layer on the material, which effectively translates its surface into a biological language. Other cells in the blood, such as platelets and leukocytes, interact with the protein layer and never come into contact with the surface of the material^{19,23}. This may be the most critical step in the blood-material interaction, as without this layer of proteins, no other cells can adhere. Indeed, the entire response of blood to a biomaterial can be viewed as the occurrence of protein adsorption, followed by platelet reactions²⁴. Previous studies have shown that the surface characteristics of a material, such as the polarity, structure and wettability, plays a pivotal role in protein adsorption^{19,25}. Thus, controlling the type and quantity of proteins which adhere to a material through its surface properties can heavily influence all subsequent steps in the clotting cascade. The adsorption of albumin (ALB), immunoglobulin (IgG) and fibrinogen (FIB) onto the material surface was characterized utilizing the micro-BCA assay. These are common proteins found in whole blood and play important roles in the clotting cascade and immune response. ALB and IgG are globular proteins, whereas FIB is a tubular protein^{21,26,27}. The main function of ALB in blood is to regulate osmotic pressure, but it aids in the transport of several substances, including enzymes, amino acids, hormones and drugs²⁶. IgG is the most common antibody found in blood that helps in controlling infection²¹. During immune response, FIB will be converted to fibrin, and becomes a major component of blood clots²⁸. In these studies, proteins were not isolated from plasma; instead, protein solutions were made of ALB, IgG and FIB at 100 µg/mL. The results of the assay are shown in **Figure 3.5.1**.

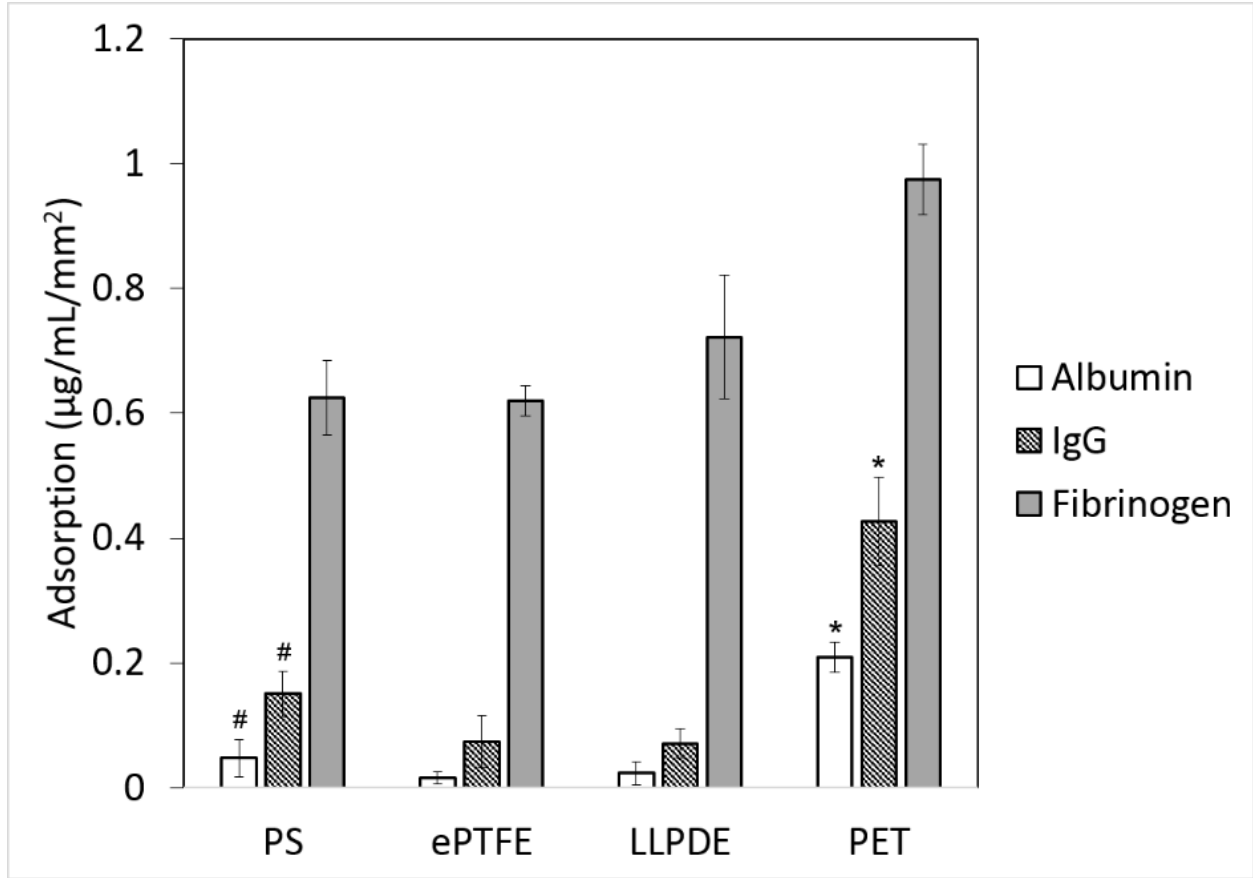


Figure 3.5.1: ALB, IgG and FIB adsorption on different materials measured with micro-BCA assay. The results indicate no statistical difference in FIB adsorption on all the materials; however, FIB adsorption was statistically higher compared to ALB and IgG adsorption on all the materials (statistical symbol for this is not shown on the graph). ALB and IgG adsorption on PET was significantly higher than that on PS, ePTFE, and LLDPE (* → $p < 0.05$). ALB and IgG adsorption on PS was significantly higher than that on ePTFE and LLDPE (# → $p < 0.05$).

FIB adsorption was statistically higher than the other proteins on all surfaces. This was followed by IgG and then ALB, although the difference between these two was not significant on all surfaces. This may be due to globular nature of ALB and IgG. Globular proteins would take up more surface area than a tubular protein once bound to a surface, thus ALB and IgG could not bind in as great of quantities as FIB. This result is not unexpected, as materials exposed to blood typically present higher levels of FIB adsorption compared to ALB and IgG adsorption²⁹. Further,

ALB and IgG adsorption on PET was significantly higher than that on all the other surfaces. The porosity of PET may promote higher protein adsorption because the increased surface area provides more binding sites for the proteins. The adsorption of ALB and IgG was significantly higher on PS than that on ePTFE and LLDPE, but it was still significantly lower than the adsorption of these proteins onto PET. Blood plasma proteins show a higher affinity for binding to hydrophobic surfaces^{20,30}, thus the fact that PET showed the significantly highest level of protein adsorption of all three proteins is expected. The adsorption of FIB was slightly higher on PET than on PS, ePTFE or LLDPE, although the difference was not statistically significant. Fibrinogen has both hydrophobic and hydrophilic regions, so it can bind easily to hydrophobic and hydrophilic materials^{20,27}. Hence, it is not surprising that FIB adsorption is not statistically different on any surface. Since FIB is the most important blood plasma protein for platelet adhesion³⁰, these results do not indicate that ePTFE, LLDPE or PET are superior to TCPS in terms of protein adsorption.

3.5.2 Visualization of Adsorbed Proteins

The adsorption of the proteins onto the surfaces of the materials was visualized with SEM, shown in **Figure 3.5.2**. The proteins were crystallized on the surfaces of TCPS, ePTFE and LLDPE, however, it appears as though they infiltrated into the PET. This could help explain why the protein adsorption was significantly higher with PET than any of the other materials. The micro-BCA assay measures complete protein adsorption, which includes proteins that may have infiltrated into the material and not just adsorbed onto the surface^{20,31}. Based on the SEM images, it is not likely that any protein was able to infiltrate the TCPS, ePTFE or LLDPE. This could provide another explanation as to why the adsorption of all three proteins was the highest on PET.

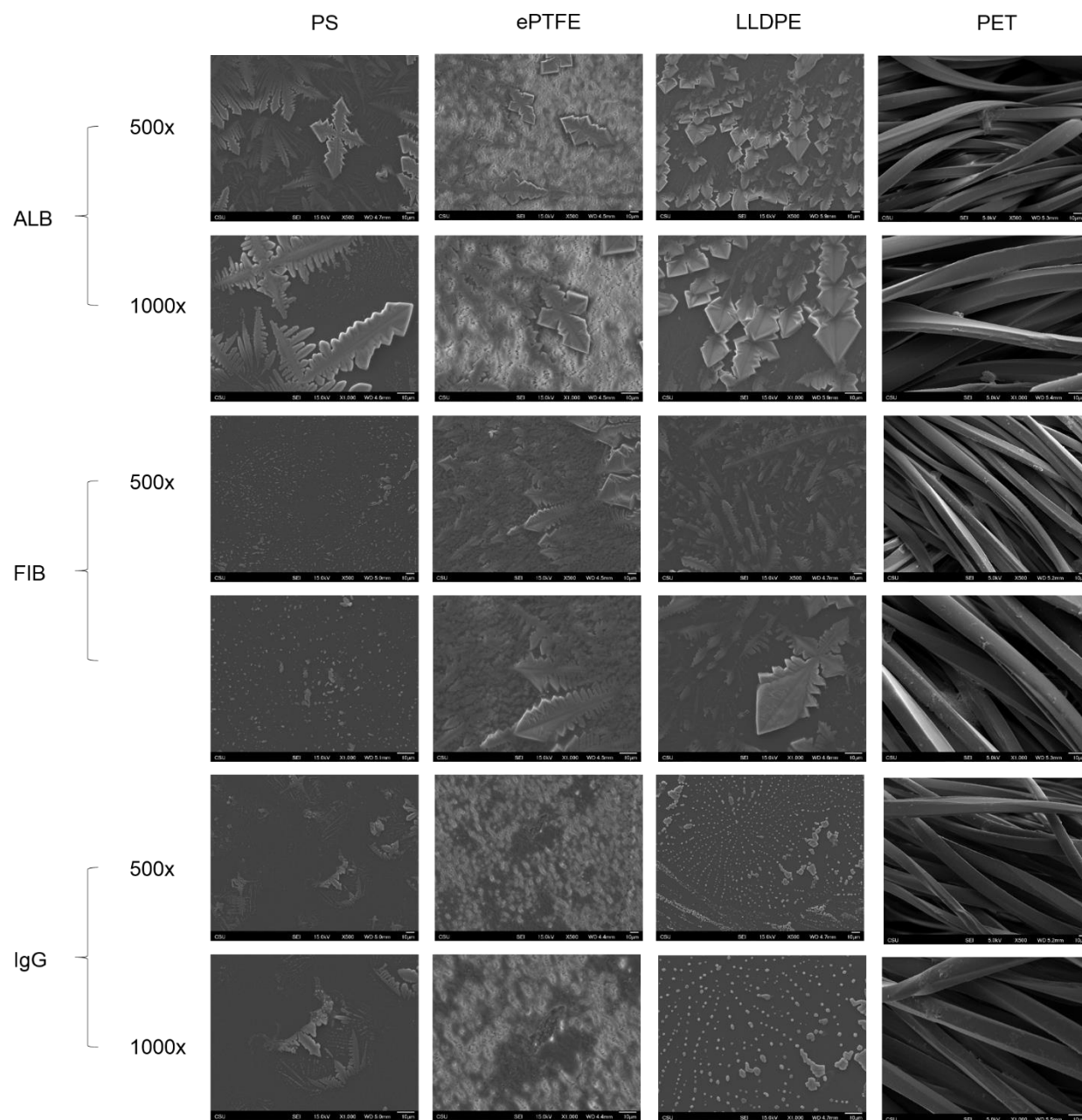


Figure 3.5.2: SEM images of ALB, IgG and FIB adsorbed to the surfaces of TCPS, ePTFE, LLDPE and PET.

3.6 Platelet and Leukocyte Adhesion

3.6.1 Fluorescence Microscopy – Calcein AM Staining

The next step in the clotting cascade after protein adsorption is platelet adhesion, which can begin the coagulation process if adhered platelets become activated^{30,32}. The interface to which the platelets bind is the layer of plasma proteins that has adsorbed to the material surface^{19, 30}. Platelets are more likely to adhere to a surface that has a higher adsorption of these plasma proteins. Specifically, the protein which promotes the most platelet adhesion is FIB, as it contains the binding sites for the platelets^{20,30}. Platelet adhesion was initially characterized by staining the cells with calcein AM. This stain is a live cell probe, as both cell membrane integrity and enzymatic activity are required to retain and activate the fluorescence of the molecules³³. Once inside the cell, the initially non-fluorescent molecules are converted by intracellular esterases into fluorescent molecules, which are then retained by the cell membrane³³. Representative images are shown in **Figure 3.6.1**.

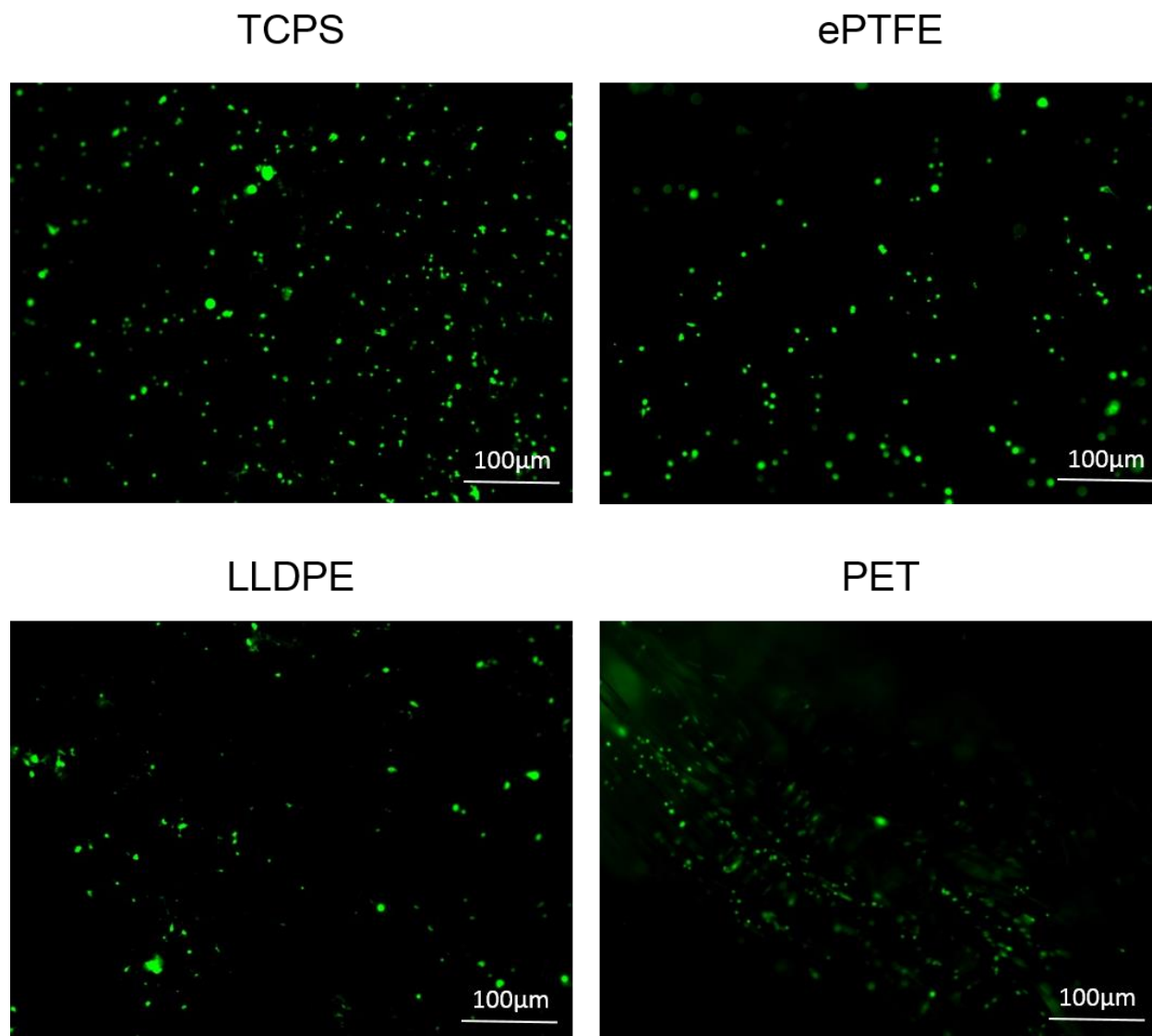


Figure 3.6.1: Fluorescence microscopy images of platelets stained with calcein AM on different materials.

The results indicate platelets adhered on all the surfaces with no apparent differences. The fluorescence microscopy images were further analyzed with ImageJ software to determine the platelet coverage on all the substrates. The results can be seen in **Figure 3.6.2**. They indicate that the percent coverage of cells was significantly higher on PET than on the other materials, while

no significant differences exist between TCPS, ePTFE and LLDPE. This result is unsurprising, as PET is the material onto which the adsorption of all three proteins was the highest.

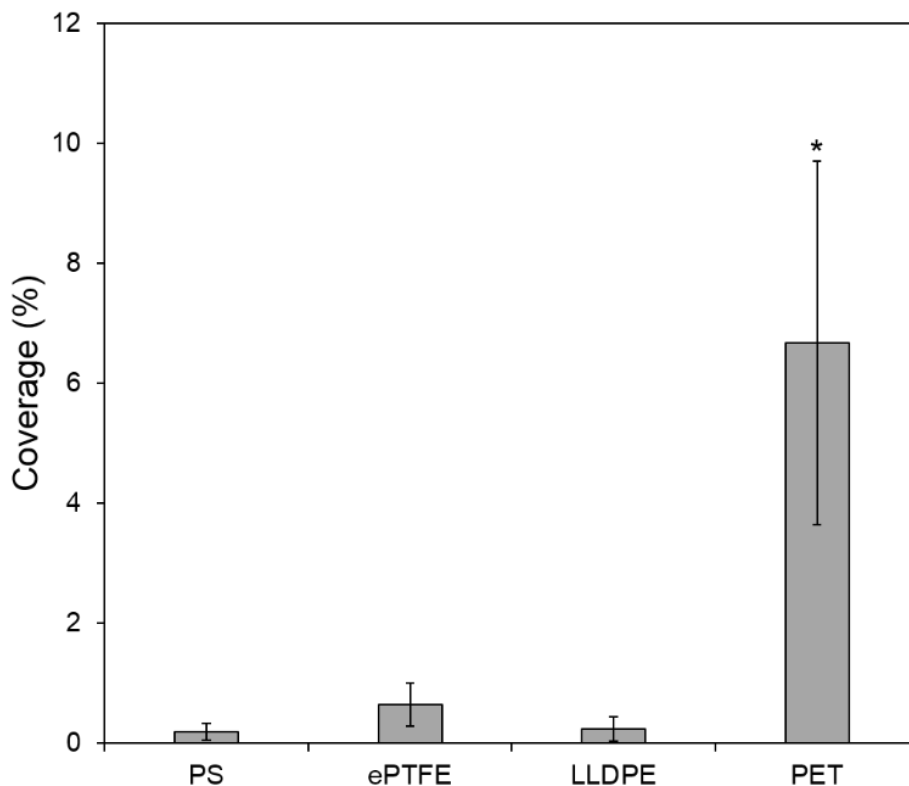


Figure 3.6.2: Platelet coverage on different surfaces calculated using ImageJ software and fluorescence microscopy images. Platelet coverage on PET is significantly higher than that on TCPS, ePTFE and LLDPE (* \rightarrow $p < 0.05$).

3.6.2 Fluorescence Microscopy – Actin and DAPI Staining

Further characterization of platelet adhesion was completed by staining the cells with actin and DAPI. DAPI selectively stains the nucleus of a cell, and thus selectively stains for leukocytes, as platelets do not contain nuclei^{22, 34, 35}. Actin stains the cytoskeleton of the cell, and will stain both platelets and leukocytes³⁶. Together, these stains identify platelet-leukocyte interactions and aggregations, as well as differentiate between platelets and leukocytes²². The role of leukocytes

in the blood-material interaction is an important one. Several studies have identified the interaction between platelets and leukocytes as a contributing factor in the formation of a thrombus around the biomaterial, which would lead to complete encapsulation of the material^{37, 38}. Platelets and leukocytes co-stimulate each other, therefore, the presence of leukocytes leads to further activation of platelets, which leads to more recruitment of platelets and leukocytes²². The fluorescent images obtained are shown in **Figure 3.6.3**.

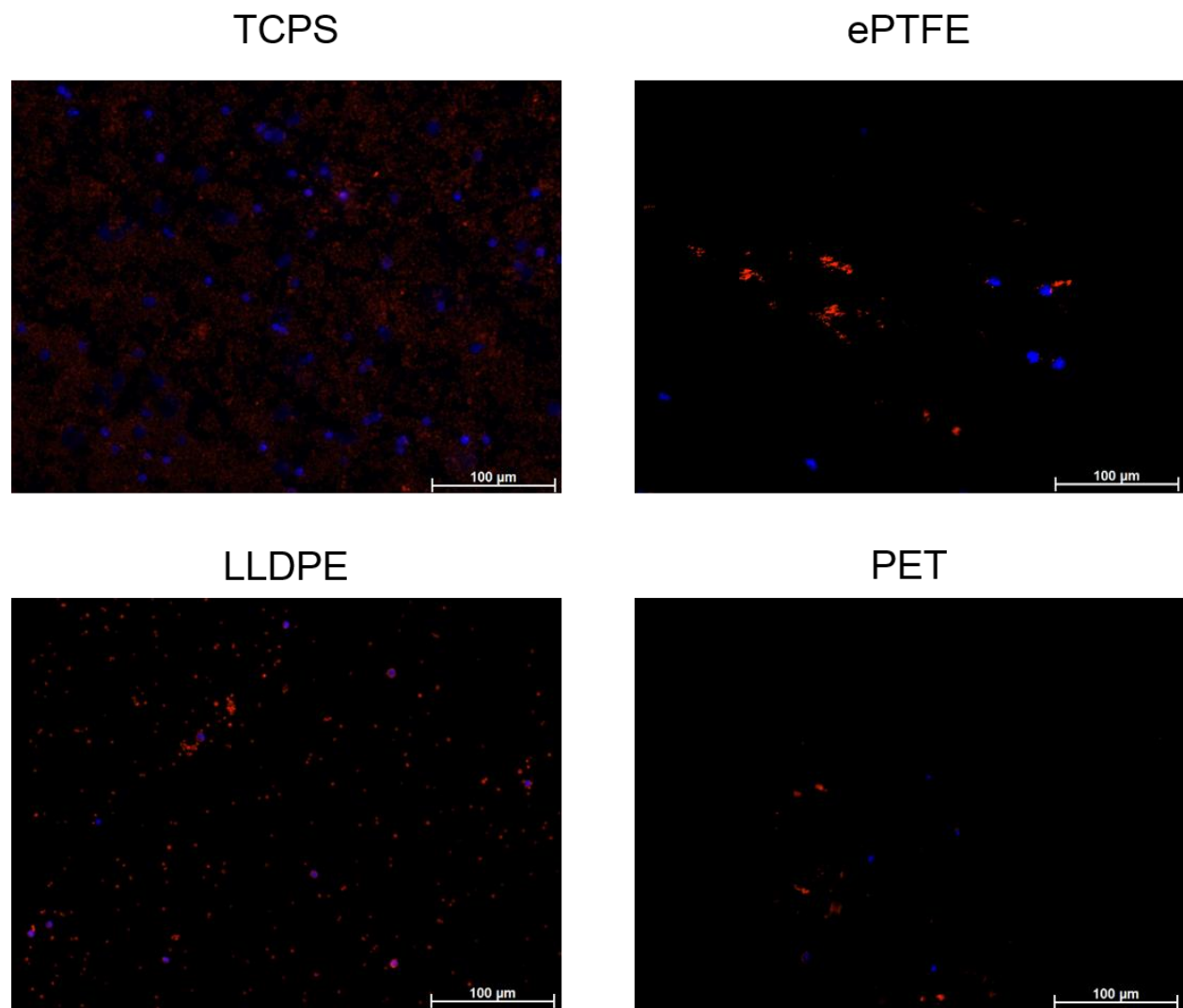


Figure 3.6.3: Fluorescence microscopy images of platelets and leukocytes stained with actin and DAPI on different materials.

The images show an obvious increase of the presence of actin cytoskeleton and nuclei on the TCPS samples. This would indicate that more platelets and leukocytes adhered to the TCPS surfaces and there were higher amounts of platelet-leukocyte interaction. The images were further analyzed with ImageJ software to determine percent coverage of the leukocytes on the materials. The results are seen in **Figure 3.6.4** and correlate to the visual analysis of the images.

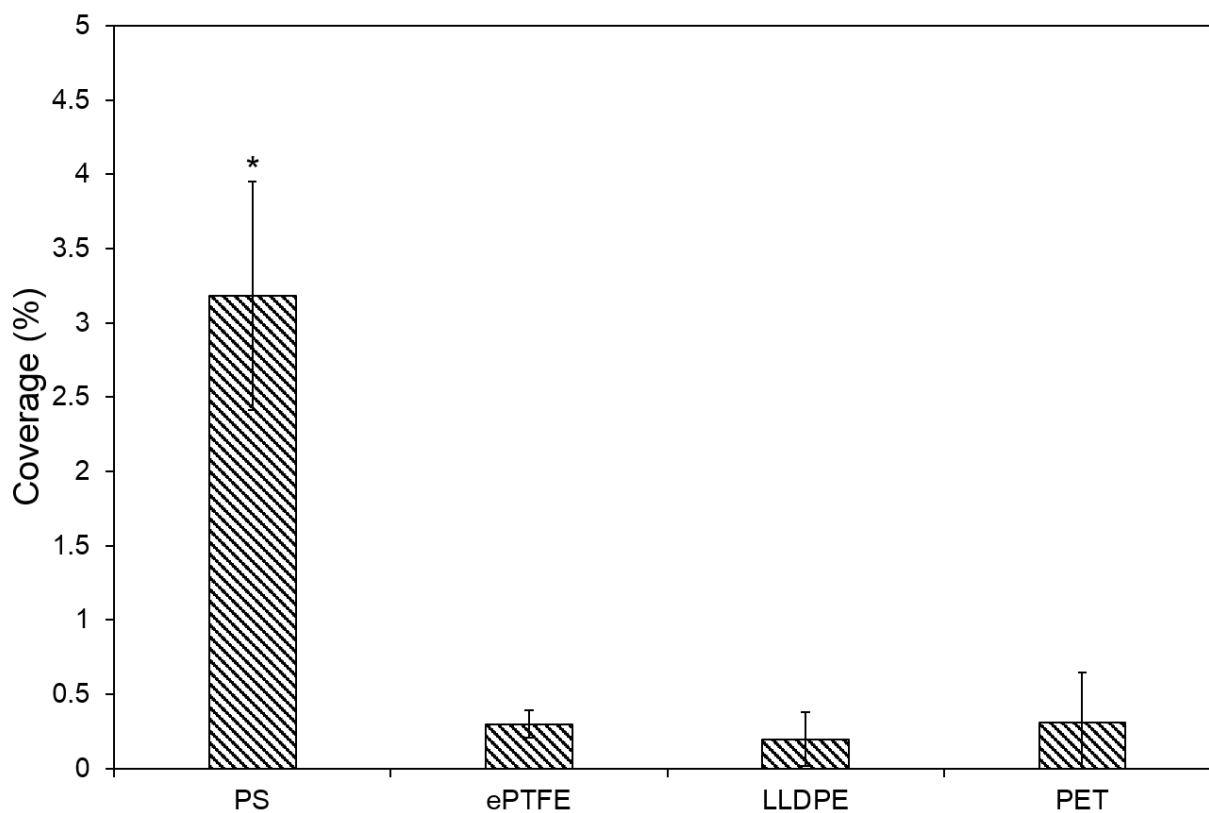


Figure 3.6.4: Leukocyte coverage on different surfaces calculated using ImageJ software and fluorescence microscopy images. Leukocyte coverage on TCPS is significantly higher than that on ePTFE, LLDPE and PET (* \rightarrow $p < 0.05$).

The percent coverage of leukocytes on TCPS is significantly higher than on ePTFE, LLDPE and PET. No statistically significant differences exist between the percent coverage of leukocytes on ePTFE, LLDPE and PET. These results seem to indicate that ePTFE, LLDPE and PET promote a

reduction of leukocyte adhesion as compared to TCPS. Reduced leukocyte adhesion would inherently reduce the amount of platelet-leukocyte interaction and platelet aggregation. This would reduce the amount of stimulation to platelets and leukocytes adhered to the surfaces, which in turn would promote the inhibition of further thrombogenic effects^{20, 22}.

3.7 Platelet and Leukocyte Activation

3.7.1 Visual Determination of Platelet Activation Through SEM imaging

Platelet adhesion does not always implicate platelet activation. Platelet activation is a crucial step in the clotting cascade, as the activated platelets signal plasma coagulation factors that lead to the formation of a thrombus^{37, 38}. The activation of adhered platelets was investigated using SEM. The substrates were imaged using SEM after a 2 hour incubation in plasma, as shown in **Figure 3.7.1**. The results indicate similar platelet coverage as observed from the fluorescence microscopy images. The SEM images were used in conjunction with the morphology criteria listed previously to determine percentage of activated platelets, shown in **Figure 3.7.2**.

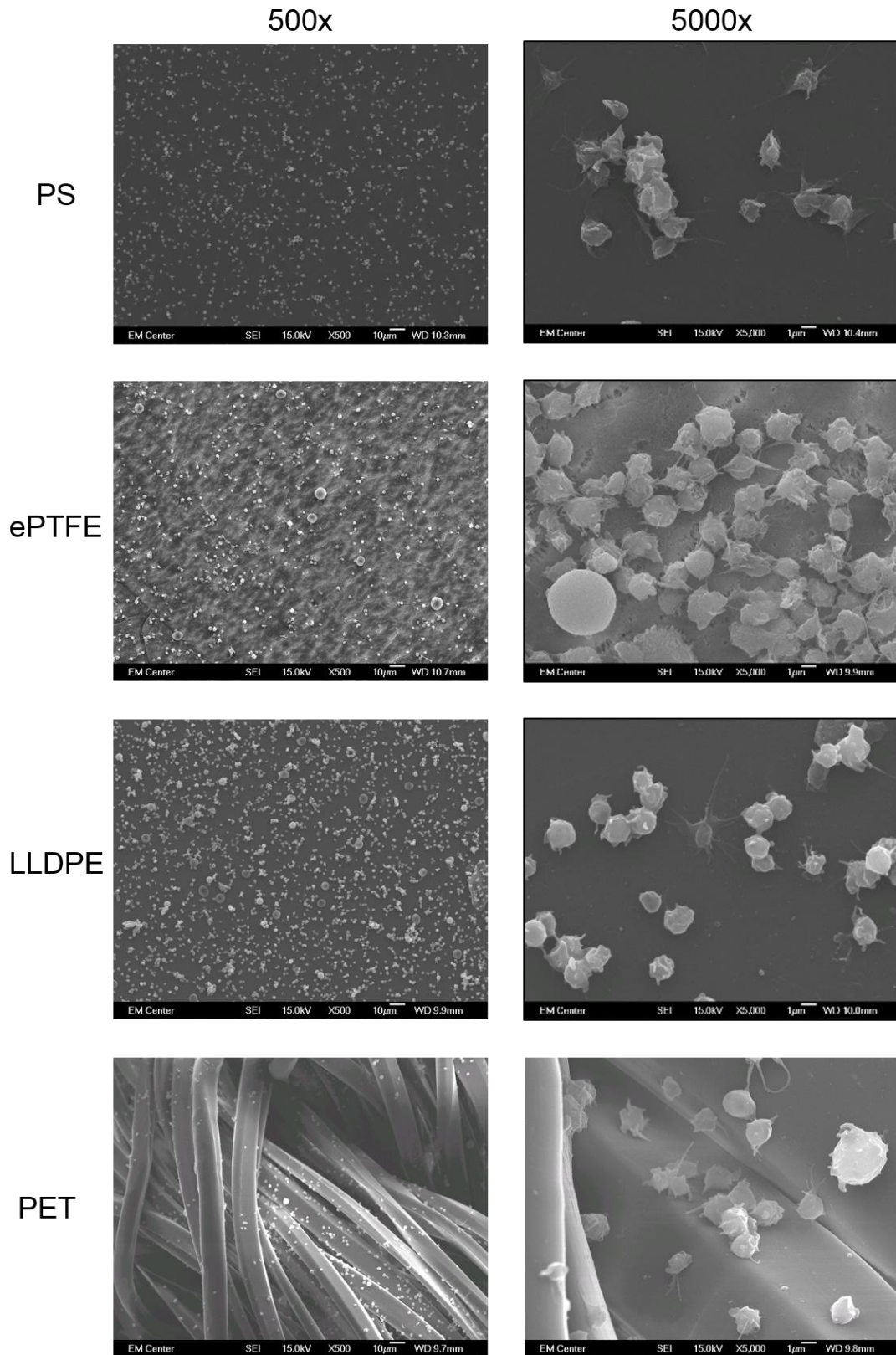


Figure 3.7.1: SEM images of platelet adhesion and activation on different materials.

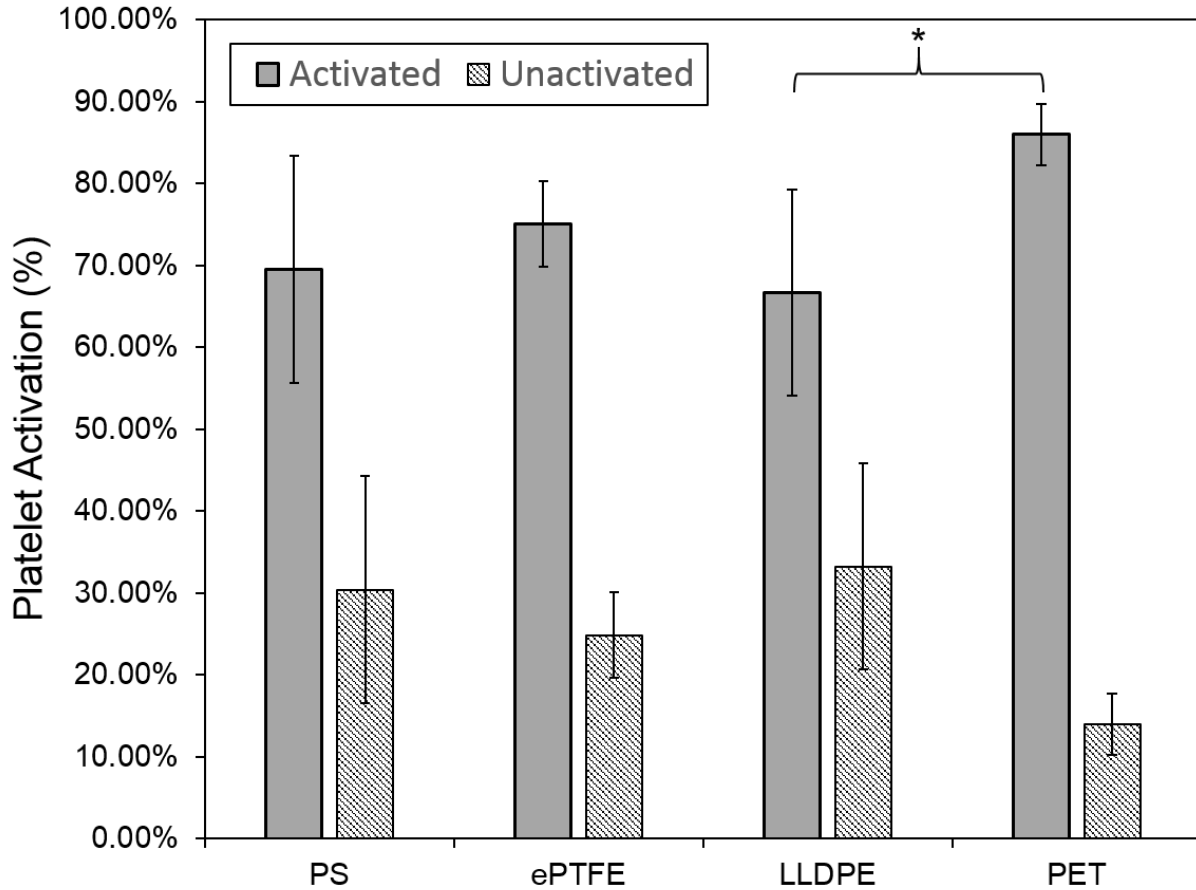


Figure 3.7.2: Percentage of activated platelets on different materials. PET has significantly higher percentage of activated platelets compared to LLDPE (* \rightarrow $p < 0.05$). No other statistical difference exist.

No significant differences exist in percentage of activated platelets between TCPS, ePTFE or LLDPE, although the percentage of activated platelets was the highest on PET. Further, the percentage of activated platelets on PET was significantly higher than on LLDPE. These results may be explained by the fact that the adhesion of platelets was the highest on PET. As more platelets adhere, they secrete signals which promote the activation and additional adhesion of more platelets.

3.7.2 Immunofluorescence Staining – P-Selectin and CD45 Expression

To further characterize platelet and leukocyte activation, immunofluorescence staining was used to determine the expression of proteins exclusive to platelets and leukocytes. Once activated, platelets and leukocytes are known to express certain proteins, specifically P-selectin and CD45, respectively. P-selectin is expressed upon the activation of platelets. It plays key roles in leukocyte recruitment and further deposition of fibrin^{22, 39, 40}. CD45 is expressed upon activation of leukocytes. It plays important roles in several immune pathways, and has not been found to be expressed by platelets^{41, 42}. Therefore, the expression of each of these proteins indicates the activation of platelets and leukocytes, and differentiates between the two. As leukocytes adhere to surfaces and become activated, they recruit increased numbers of platelets. This in turn will increase recruitment of leukocytes²⁰. Thus, materials that promote a reduction of P-selectin and CD45 expression will be more hemocompatible than materials that do not. In this study, the materials were incubated in primary antibodies (P-selectin and CD45) after a two hour incubation in plasma. Then, they were labeled with fluorescently tagged secondary antibodies and imaged with a fluorescent microscope. The fluorescent images, shown in **Figure 3.7.3**, do not show any obvious differences in the amount of P-selectin and CD45 on the surfaces of the various materials.

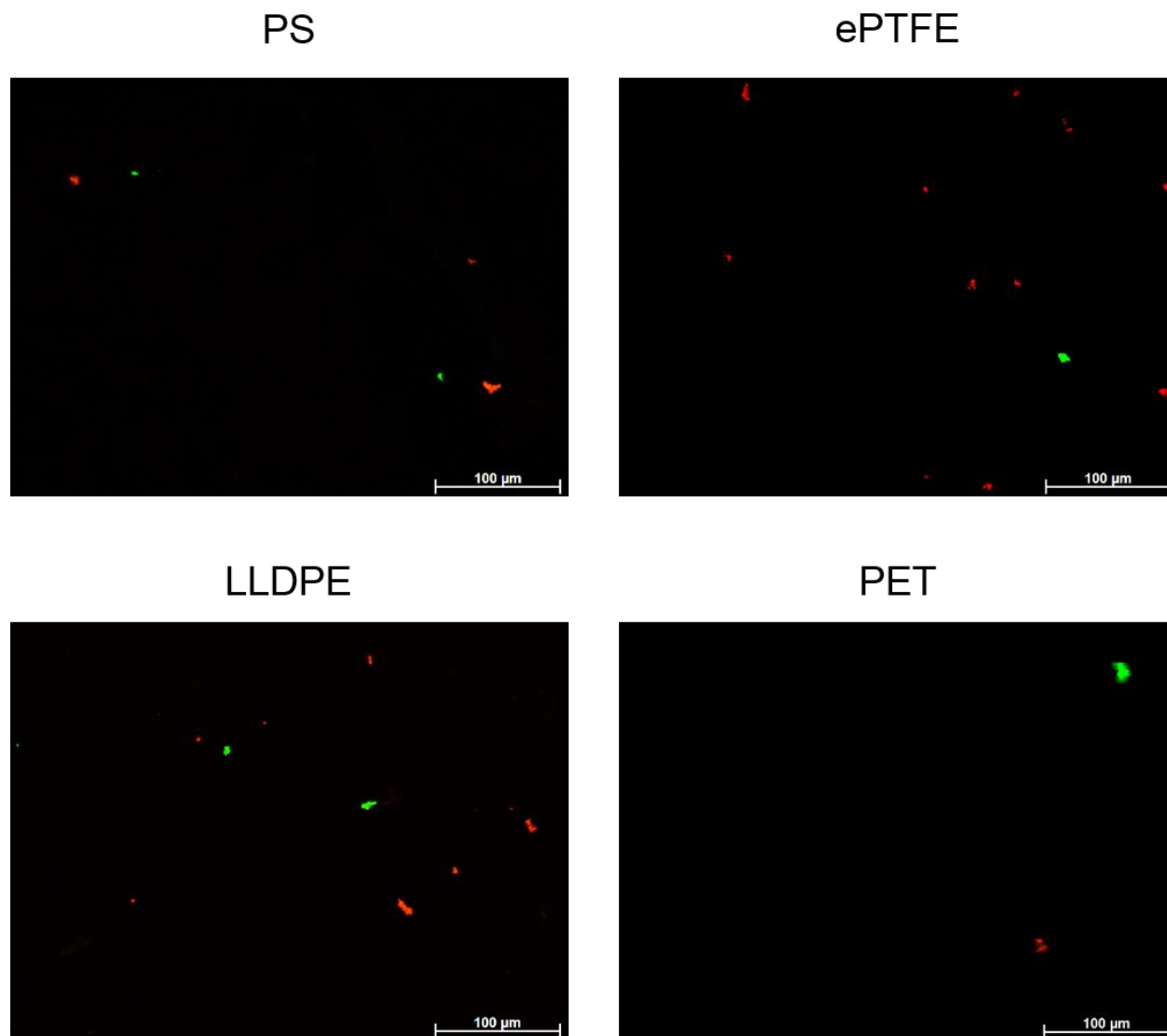


Figure 3.7.3: Fluorescence microscopy images of P-selectin and CD45 expression on different materials. The images do not indicate an obvious visual difference between the materials.

Further investigation of the images using ImageJ software supports the visual analysis. The percent coverage of both P-selectin and CD45 expression on the surfaces was calculated. The results are shown in **Figure 3.7.4**. No statistically significant differences exist in the percent coverage of P-selectin or CD45 on any of the materials.

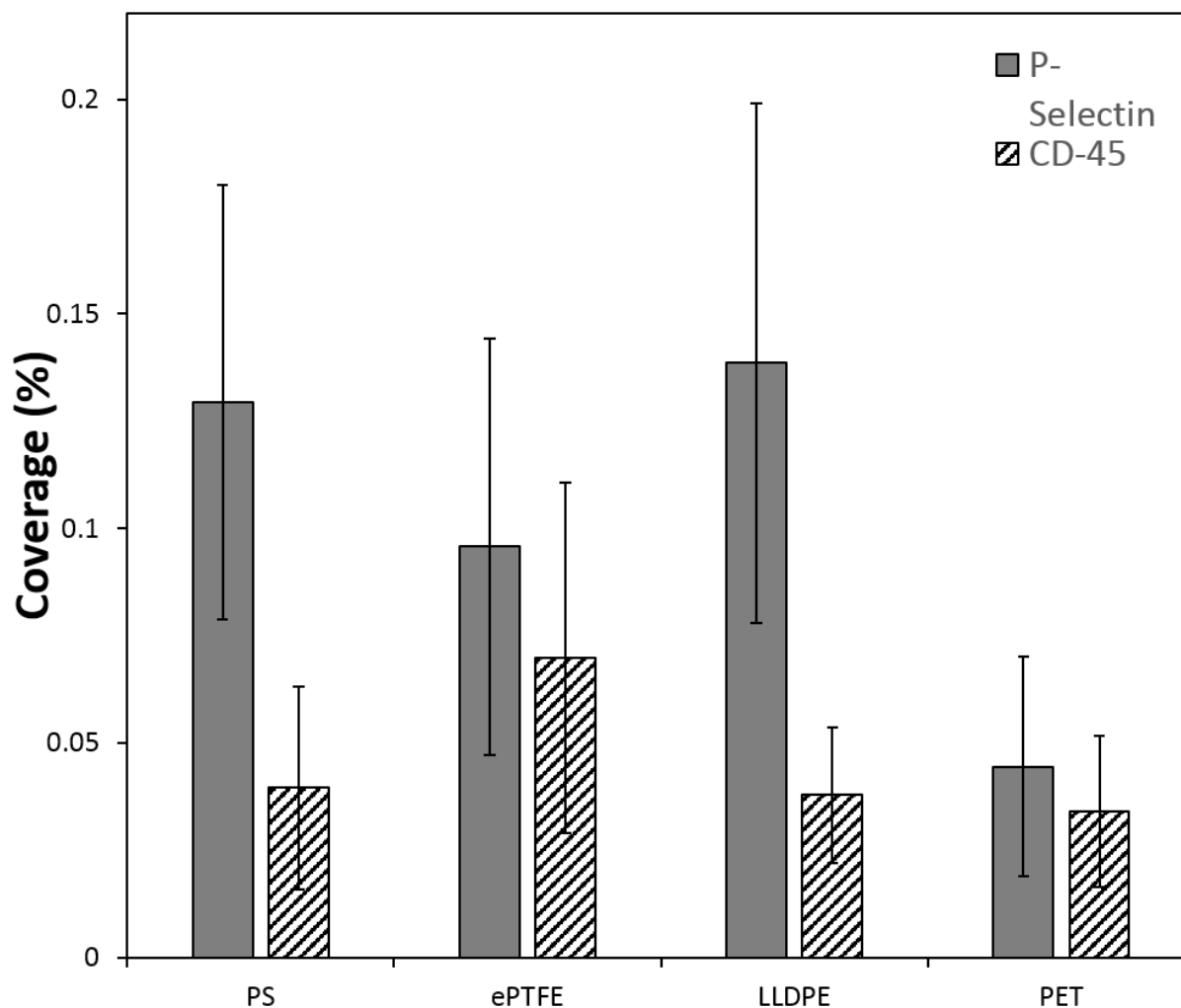


Figure 3.7.4: P-selectin and CD45 coverage on different surfaces calculated using ImageJ software and fluorescence microscopy images. No statistical differences exist for either P-selectin or CD45 on any of the materials.

This indicates that ePTFE, LLDPE and PET do not promote the expression of P-selectin and CD45, as compared to TCPS. These results contradict the results found by determining platelet activation via SEM imaging. This could be because the platelets were considered activated if they did not have spherical bodies, or if a dendritic extension was visible. It is possible that through this method, a higher number of platelets were deemed activated than actually were.

3.8 Whole Blood Clotting Kinetics

3.8.1 Hemolysis Assay

The whole blood clotting kinetics were studied on each of the materials. The formation of the fibrin matrix follows platelet adhesion and activation in the clotting cascade. The kinetics of this step is vital to the long-term success of blood-contacting biomaterials, since tissue integration is inhibited if the material becomes encapsulated^{20, 43}. The clotting kinetics were characterized using a hemolysis assay to measure the amount of free hemoglobin in each blood drop after 15, 30, 45 and 60 minutes. The results, presented in **Figure 3.8.1**, show that blood clots within 1 hour of exposure to the materials in all cases, although the rates of clotting is different for the different materials.

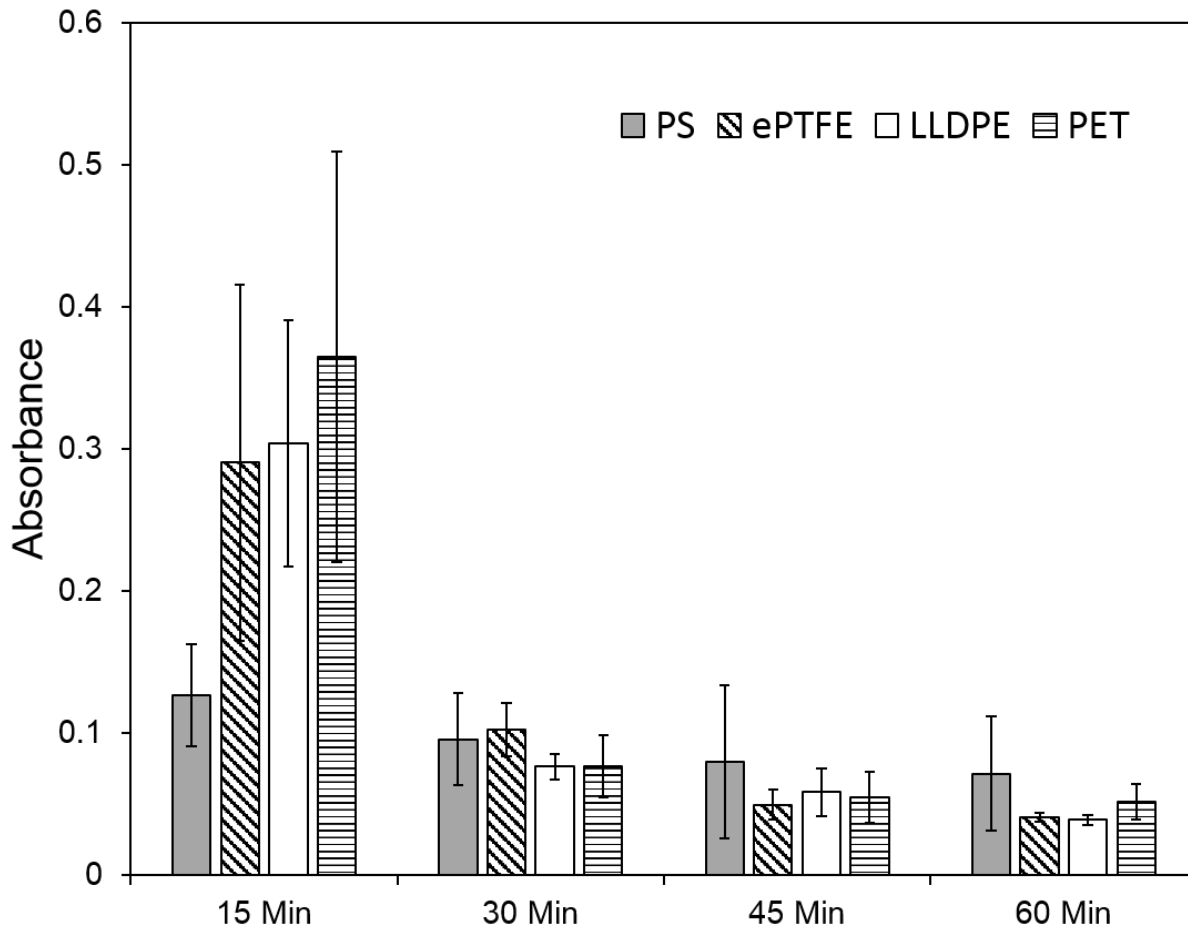


Figure 3.8.1: Absorbance due to amount of free hemoglobin in DI water after 15, 30, 45 and 60 minutes of clotting time. No statistical differences exist between the materials at any time point.

After 15 minutes, the amount of free hemoglobin was higher in ePTFE, LLDPE and PET as compared to TCPS. This indicates less clotting had occurred in those materials. However, the differences were not statistically significant. After 30 minutes, there was little to no difference in the amount of free hemoglobin across all of the materials. This indicates that the formation of the fibrin clot was not inhibited by ePTFE, LLDPE or PET, as compared to TCPS.

3.8.2 Visualization of Blood Clots on Surfaces

After the blood was allowed to clot for 60 minutes on each of the different materials, the clots were visualized with SEM. The results show that the clots are very similar on TCPS, ePTFE and LLDPE. There is a well-defined clot-material interface, as the drop of blood did not spread. In contrast, there is no well-defined interface on PET. The drop of blood spread and subsequently the clot infiltrated the material. **Figure 3.8.2** shows the images obtained.

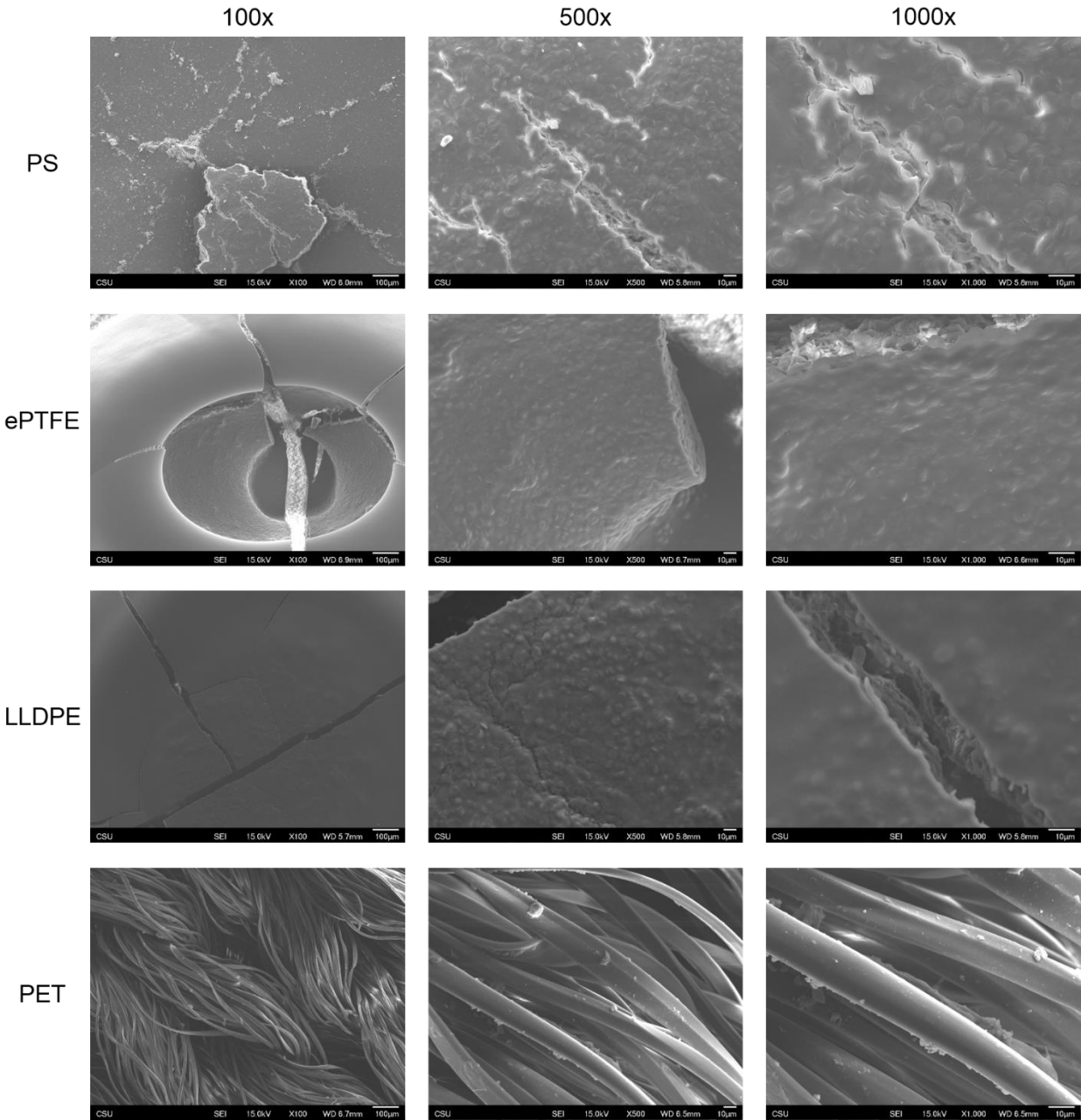


Figure 3.8.2: SEM images of blood clots on the surfaces of TCPS, ePTFE, LLDPE and PET

3.9 Conclusion

There are currently many polymeric materials used in blood-contacting applications, yet despite much research in this area, they all tend to elicit an immune response when placed in

contact with blood. The results can lead to rejection of the material by the body. In this study, we have investigated the initial events that occur after blood contact on ePTFE, LLDPE and PET, materials that may be candidates for blood-contacting applications. The results indicate that none of these materials are cytotoxic. ALB, IgG and FIB adsorption was highest on PET, and platelet adhesion was significantly higher on PET as compared to TCPS, ePTFE and LLDPE. However, the percentage of activated platelets was comparable on all materials, as measured by staining for P-selectin and CD45 expression. The whole blood clotting kinetics was also similar across all materials, with no observable differences seen after 30 minutes of clotting time.

Overall, the data show that hemocompatibility is correlated to surface morphology and other surface characteristics. The hydrophilicity/hydrophobicity of the materials directly influences the amount and type of proteins that adsorb to the surfaces. This, in turn, influences the platelet adhesion, which influences almost every other step in the clotting cascade and also is responsible for initiating an immune response^{20, 22}. Indeed, it has been well documented that controlling the surface characteristics of a material can improve the hemocompatibility of a material^{12, 20-22}.

Since this study was a static study, the experiments done do not reflect the effect that blood flow would have on the initial events that occur after implantation of a blood-contacting material. Furthermore, only the first few events of the clotting cascade were studied, and the number of plasma and whole blood donors used was small. Hence, further studies will focus on the subsequent events in the blood-material interaction, and the number of donors should be increased. Eventually, these same experiments will be completed in a dynamic study, and the feasibility of manipulation of the surface characteristics of ePTFE, LLDPE and PET will be explored.

REFERENCES

1. Fawthrop, D., A. Boobis, and D. Davies, *Mechanisms of cell death*. Archives of Toxicology, 1991. **65**(6): p. 437-444.
2. Han, X., et al., *Validation of an LDH assay for assessing nanoparticle toxicity*. Toxicology, 2011. **287**(1-3): p. 99-104.
3. Andrews, R.K., J. López, and M.C. Berndt, *Molecular mechanisms of platelet adhesion and activation*. The International Journal of Biochemistry & Cell Biology, 1997. **29**(1): p. 91-105.
4. Jennings, L.K., *Mechanisms of platelet activation: need for new strategies to protect against platelet-mediated atherothrombosis*. Thromb Haemost, 2009. **102**(2): p. 248-257.
5. VARCO, T.C., et al., *Hydrogen/ Liquid Vapor Radio Frequency Glow Discharge Plasma Oxidation/ Hydrolysis of Expanded Poly (tetrafluoroethylene) (ePTFE) and Poly (vinylidene Fluoride) (PVDF) Surfaces* Journal of Polymer Science, 1991. **29**: p. 555-570.
6. Srinivasan, S., G.H. McKinley, and R.E. Cohen, *Assessing the accuracy of contact angle measurements for sessile drops on liquid-repellent surfaces*. Langmuir, 2011. **27**(22): p. 13582-9.
7. Yuan, Y. and T.R. Lee, *Contact Angle and Wetting Properties*, in *Surface Science Technologies*, G. Bracco and B. Holst, Editors. 2013, Springer.
8. D.Y.Kwok and A.W.Neumann, *Contact angle measurement and contact angle interpretation*. Advances in Colloid and Interface Science 1999. **81**.
9. Busscher, H.J., et al., *The effect of surface roughening of polymers on measured contact angles of liquids*. Colloids and Surfaces, 1984. **9**(4): p. 319-331.

10. Giovambattista, N., P.G. Debenedetti, and P.J. Rossky, *Effect of Surface Polarity on Water Contact Angle and Interfacial Hydration Structure*. The Journal of Physical Chemistry B, 2007. **111**(32): p. 9581-9587.
11. Sorkin, J.A., *TITANIA NANOTUBE ARRAYS AS POTENTIAL INTERFACES FOR NEUROLOGICAL PROSTHESES* in *Department of Mechanical Engineering*. 2014, Colorado State University. p. 140.
12. Prawel, D.A., et al., *Hemocompatibility and Hemodynamics of Novel Hyaluronan-Polyethylene Materials for Flexible Heart Valve Leaflets*. Cardiovasc Eng Technol, 2014. **5**(1): p. 70-81.
13. Chen, J.Y., et al., *Antithrombogenic investigation of surface energy and optical bandgap and hemocompatibility mechanism of Ti(Ta(+5))O₂ thin films*. Biomaterials, 2002. **23**(12): p. 2545-52.
14. Kaelble, D.H. and J. Moacanin, *A surface energy analysis of bioadhesion*. Polymer, 1977. **18**: p. 475-482.
15. NADIM J. HALLAB, P.D., et al., *Evaluation of Metallic and Polymeric Biomaterial Surface Energy and Surface Roughness Characteristics for Directed Cell Adhesion*. Tissue Engineering, 2001. **7**(1): p. 55-71.
16. Zhao, G., et al., *High surface energy enhances cell response to titanium substrate microstructure*. J Biomed Mater Res A, 2005. **74**(1): p. 49-58.
17. Sun, T., et al., *No Platelet Can Adhere—Largely Improved Blood Compatibility on Nanostructured Superhydrophobic Surfaces*. Small, 2005. **1**(10): p. 959-963.
18. Michiardi, A., et al., *The influence of surface energy on competitive protein adsorption on oxidized NiTi surfaces*. Biomaterials, 2007. **28**(4): p. 586-594.
19. CAMERON J. WILSON, B.E., et al., *Mediation of Biomaterial–Cell Interactions by Adsorbed Proteins: A Review*. Tissue Engineering, 2005. **11**(1-2): p. 1-18.

20. Leszczak, V. and K.C. Papat, *Improved in Vitro Blood Compatibility of Polycaprolactone Nanowire Surfaces*. ACS Appl Mater Interfaces, 2014.
21. Leszczak, V., B.S. Smith, and K.C. Papat, *Hemocompatibility of polymeric nanostructured surfaces*. J Biomater Sci Polym Ed, 2013. **24**(13): p. 1529-48.
22. Smith, B.S. and K.C. Papat, *Titania Nanotube Arrays as Interfaces for Blood-Contacting Implantable Devices: A Study Evaluating the Nanotopography-Associated Activation and Expression of Blood Plasma Components*. Journal of Biomedical Nanotechnology, 2012. **8**(4): p. 1-17.
23. Gallagher, W.M., et al., *Molecular basis of cell–biomaterial interaction: Insights gained from transcriptomic and proteomic studies*. Biomaterials, 2006. **27**(35): p. 5871-5882.
24. Courtney, J.M., et al., *Biomaterials for blood-contacting applications*. Biomaterials, 1994. **15**(10): p. 737-744.
25. Roach, P., D. Farrar, and C.C. Perry, *Interpretation of Protein Adsorption: Surface-Induced Conformational Changes*. Journal of the American Chemical Society, 2005. **127**(22): p. 8168-8173.
26. Judy Hankins BSN, C., *The role of albumin in fluid and electrolyte balance*. Journal of Infusion Nursing, 2006. **29**(5): p. 260-265.
27. Cecil E. Hall, P.D. and H.S. Slayter, *The Fibrinogen Molecule: Its Size, Shape, and Mode of Polymerization* Journal of Biophysical and Biochemical Cytology, 1959. **5**(1): p. 11-16.
28. Mosesson, M.W., *Fibrinogen and fibrin structure and functions*. J Thromb Haemost, 2005. **3**(8): p. 1894-904.
29. Thomas A. Horbett, P., *Principles Underlying the Role of Adsorbed Plasma Proteins in Blood Interactions With Foreign Materials* Cardiovascular Pathology, 1993. **2**(3): p. 137S-148S.

30. Corum, L.E., *Evaluating Surface Induced Platelet Adhesion and Activation With Surface Patterning and Protein Immobilization Techniques*, in *Department of Bioengineering*. 2011, University of Utah. p. 169.
31. Smith, P.K., et al., *Measurement of protein using bicinchoninic acid*. *Analytical Biochemistry*, 1985. **150**(1): p. 76-85.
32. Smith, B.S., et al., *Reduced in vitro immune response on titania nanotube arrays compared to titanium surface*. *Biomaterials Science*, 2013. **1**: p. 322-332.
33. *Viability and Cytotoxicity Assay Reagents*, in *The Molecular Probes® Handbook—A Guide to Fluorescent Probes and Labeling Technologies*, I. Johnson and M.T.Z. Spence, Editors. 2010, Life Technologies.
34. Hamada, S. and S. Fujita, *DAPI staining improved for quantitative cytofluorometry*. *Histochemistry*, 1983. **79**(2): p. 219-226.
35. Kapuscinski, J., *DAPI: a DNA-specific fluorescent probe*. *Biotech Histochem*, 1995. **70**(5): p. 220-33.
36. *Probes for Actin*, in *The Molecular Probes® Handbook—A Guide to Fluorescent Probes and Labeling Technologies*, I. Johnson and M.T.Z. Spence, Editors. 2010, Life Technologies.
37. Gorbet, M.B. and M.V. Sefton, *Biomaterial-associated thrombosis: roles of coagulation factors, complement, platelets and leukocytes*. *Biomaterials*, 2004. **25**(26): p. 5681-5703.
38. Hong, J., et al., *A new in vitro model to study interaction between whole blood and biomaterials. Studies of platelet and coagulation activation and the effect of aspirin*. *Biomaterials*, 1999. **20**(7): p. 603-611.
39. Hayashi, S.-i., et al., *Roles of P-Selectin in Inflammation, Neointimal Formation, and Vascular Remodeling in Balloon-Injured Rat Carotid Arteries*. *Circulation*, 2000. **102**(14): p. 1710-1717.

40. Yeo, E., J. Sheppard, and I. Feuerstein, *Role of P-selectin and leukocyte activation in polymorphonuclear cell adhesion to surface adherent activated platelets under physiologic shear conditions (an injury vessel wall model)*. Vol. 83. 1994. 2498-2507.
41. Tchilian, E.Z. and P.C.L. Beverley, *Altered CD45 expression and disease*. Trends in Immunology, 2006. **27**(3): p. 146-153.
42. Altin, J.G. and E.K. Sloan, *The Role of CD45 and CD45-Associated Molecules in T Cell Activation*. Immunology and Cell Biology, 1997. **75**: p. 430-445.
43. Davie, E.W., K. Fujikawa, and W. Kisiel, *The coagulation cascade: initiation, maintenance, and regulation*. Biochemistry, 1991. **30**(43): p. 10363-10370.

CHAPTER 4

OVERALL CONCLUSIONS AND RECOMMENDATIONS FOR FUTURE WORK

4.1 Summary and Overall Conclusions

The potential of implantable blood-contacting biomaterials to improve quality of life for patients who receive them is enormous. Oftentimes, patients who receive these implants cannot survive without them, especially in cases of heart valve replacement. This is why their use is so prevalent, despite the complications associated with them. Artificial heart valves are urgently needed, and that need is only expected to increase as the world's population ages. However, the complications are quite serious. The two types of commercially available heart valve prosthesis are mechanical and bioprosthetic heart valves. Mechanical heart valves are prone to thrombosis, requiring lifelong anticoagulants for the recipients. Anticoagulant therapy drastically increases risk of hemorrhage and other bleeding complications. Bioprosthetic valves are prone to calcification and other forms of mechanical failure, and do not last as long as mechanical valves. Much of the recent research into heart valves has focused on developing new polymeric materials with which to make heart valve leaflets. A major obstacle to be overcome in these endeavors is the immune response initiated when a material is implanted into living tissue. The initial response is an inflammatory response. Eventually, the inflammatory response is intensified enough to activate the foreign body response, which usually results in complete encapsulation of the implant in dense fibrous tissue. This prevents integration and renders the implant useless. Three particular materials have been demonstrated to be promising candidates for heart valve leaflets. These materials, ePTFE, LLDPE and PET are the focus of the studies in this thesis.

The aim of the work presented in this thesis was to establish a baseline against which future studies of ePTFE, LLDPE and PET can be compared. The initial work performed was to characterize the material surface structures using contact angle measurements and SEM imaging. Following material surface characterization, protein adsorption onto the surface of each material was investigated via micro-BCA assay. Protein adsorption is a critical step in the blood-material interaction. Without this step, other cells could not adhere to the material, as the monolayer of blood plasma proteins provide the interface with which other cells interact. This effect can be undesired, as in the context of platelet adhesion. However, complete lack of protein adsorption would also inhibit complete integration of the material. Integration of a biomaterial into the body requires a layer of endothelial cells to adhere to the surface, which could not happen without a layer of proteins with which to interact. Hence, protein adsorption holds key to the ultimate success or failure of any biomaterial used for implantation. The results of the micro-BCA assay indicated similar amounts of adsorption of FIB on all surfaces, although this amount was significantly higher than the amount of ALB and IgG adsorption in all cases. IgG and ALB adsorption onto PET was significantly higher than the adsorption of these proteins on the other surfaces. On all of the materials, the adsorption of ALB was the lowest of the three proteins. These results do not indicate an obvious difference between ePTFE, LLDPE, PET and TCPS. FIB is the protein which is crucial to platelet adhesion, and the adsorption of this protein is not statistically different between the four materials.

The next event studied was platelet and leukocytes adhesion to the materials. This step in the blood-material interaction is what eventually leads to the formation of a thrombus. As platelets adhere to the layer of adsorbed blood plasma proteins, they become activated and begin to send out signals which stimulates and intensifies the coagulation cascades, and also increases

recruitment of additional platelets and leukocytes. The interaction between leukocytes and platelets further stimulates both cell types, which leads to increased activation and recruitment of both platelets and leukocytes. Therefore, reducing or avoiding the initial adhesion of platelets has a significant impact on subsequent events in the blood-material interaction. In these studies, live cell adhesion was initially characterized using calcein AM staining. The results show comparable levels of live cell adhesion between TCPS, ePTFE and LLDPE. However, the amount of live cell adhesion on PET was significantly higher than the other materials. This correlates to the protein adsorption data, as PET was the materials onto which protein adsorption, specifically FIB, was the highest. The live cell adhesion was further characterized to distinguish between platelets and leukocytes using DAPI and actin stains. The results show significantly increased leukocyte adhesion onto the surface of TCPS, as compared to ePTFE, LLDPE and PET. This indicates that ePTFE, LLDPE and PET promote a reduction of leukocyte adhesion. Reduced leukocyte adhesion would inherently reduce the amount of interaction with platelets, which would reduce the amount of stimulation to platelets. This would in turn reduce the amount of intensification to the coagulation cascade, which ultimately would result in the inhibition of further thrombogenic effects.

The activation of the adhered platelets and leukocytes was characterized next. As mentioned above, it is the activated platelets which release signals to stimulate leukocytes and the coagulation system. Thus, it is not the adhesion of platelets themselves, but rather their activation, that is most important to prevent. The activation of adhered platelets was first determined with SEM imaging, followed by immunofluorescence staining with P-selectin and CD45. These are two proteins expressed upon activation by platelets and leukocytes, respectively. The expression of these proteins will increase as more platelets and leukocytes become activated, providing a method

to not only quantify platelet and leukocyte activation, but also differentiate between the two. The SEM images showed similar platelet coverage as seen in the fluorescent microscopy images. To obtain a percentage of activated adhered platelets, each platelet was classified as activated or not activated based on their shape and dendritic extensions. The percentage of adhered platelet activation was the highest on PET, although it was significantly higher only compared to LLDPE. No significant difference existed between TCPS, ePTFE and LLDPE. This results contradicts slightly the result of the immunofluorescence imaging. The fluorescence images were analyzed with ImageJ to determine the percent coverage of P-selectin CD45. The result of this study indicates that there is no statistical different between any of the materials for either platelet or leukocyte activation. This slight deviation may be explained by the fact that the first method of determining platelet activation may have overestimated the number of platelets which were actually activated. Overall, these results seem to indicate that ePTFE, LLDPE and PET do not inhibit platelet and leukocyte activation when compared to TCPS.

The final event studied in this work was the whole blood clotting kinetics on each of the materials. A clot forms after activated platelets release signals which activate the coagulation cascade and recruit leukocytes. Through a series of protein reactions and the increased interactions between platelets, leukocytes and the coagulation systems, a fibrin matrix is formed. This is a vital step in the host response to a biomaterial. Clot formation is extremely dangerous for more than one reason. Not only can it obstruct blood flow, leading to heart attack or stroke, but it also can be a precursor to the foreign body response. This response would result in complete encapsulation of the implant, preventing tissue integration. The clotting kinetics were studied using a hemolysis assay to measure the amount of free hemoglobin in a drop of blood placed on each material. The blood completely clotted after one hour of exposure, although the rate of clotting was different on

all materials. After 15 minutes, the amount of free hemoglobin was higher in ePTFE, LLDPE and PET when compared to TCPS, indicating less clotting had occurred on those materials. After 30 minutes, little difference existed in the amount of free hemoglobin on all materials. No statistical difference existed between any of the materials at any of the time points, indicating that the formation of the fibrin clot was not inhibited by ePTFE, LLDE or PET.

The results of these studies do not show a significant improvement of hemocompatibility of ePTFE, LLDPE and PET when compared to TCPS. This is somewhat surprising, as results in the literature generally demonstrate ePTFE to have superior hemocompatibility to that of control materials. However, the ePTFE used in these studies was in its unmodified base form. This may help explain the lack of differences between ePTFE and TCPS. Additionally, the results which determined the expression of CD-45 on the surfaces of the materials is unexpected. Based on the results of the live cell staining, one would expect more leukocytes to adhere to the material onto which the most live cells adhered, which would have been PET. This might be explained by the difference in donors. Different blood donors have varying amounts of blood components, which could affect the results of these two assays.

The aim of the work was to establish a baseline to compare against future modifications of the materials. The studies completed in this work have characterized the surface structure of each material, the protein adsorption onto each material, the platelet and leukocyte adhesion and activation on each material, and the whole blood clotting kinetics of each material. The compilation of all of these studies provide a satisfactory foundation upon which future work can be built.

4.2 Recommendations for Future Work

4.2.1 Scope of Future Studies

Future studies should incorporate more extensive surface characterization of the material. Based upon the results obtained from the contact angle measurements, one would expect TCPS to have the lowest adsorption of protein, since they are the most hydrophilic surfaces. However, these results seem to suggest that the hydrophilicity/hydrophobicity may not be the most important factor in the mediation of proteins adsorption. Thus, further work with surface characterization should be done in order to more fully understand these results.

The results of these experiments do not take into consideration the effect of blood flow on the initial events of the host response to an implanted blood-contacting biomaterial. Furthermore, only the first few events of the immune response initiated by a biomaterial were studied, and the number of donors of plasma and whole blood was small. Future work should increase the number of donors and evaluate subsequent events in the biomaterial-initiated immune response, such as initiation of the coagulation cascade and the formation of foreign body giant cells. Eventually, these same experiments should be completed in a dynamic environment to determine the effect of blood flow on each step in the immune response.

4.2.2 Modification of Materials with Hyaluronic Acid

In future studies, the modification of these materials should be investigated. Several methods exist to modify polymeric materials to improve hemocompatibility. These include grafting hydrophilic molecules to the surface, coating with anticoagulant molecules, introduction of nanotopography to the surface or creating interpenetrating polymer networks (IPN). All of these methods of modification have been linked to a decrease protein adsorption, increase whole blood

clotting time, and a general improvement hemocompatibility. Of particular interest for these materials is the possibility of creating an IPN with hyaluronic acid (HA). HA is a naturally occurring polysaccharide that is prevalent in connective (including blood), epithelial and neural tissues. It has a number of functions, including lubrication, water homeostasis, filtering effects and regulation of plasma protein distribution¹. HA also appears to play a role in wound healing, and may prevent or reduce an inflammatory response^{2, 3}. One study in particular has demonstrated the potential of creating IPNs with HA for heart valve engineering applications⁴. Hence, future work with these materials should include creating IPNs using HA with ePTFE, LLDPE and PET.

REFERENCES

1. Fraser, J.R., T.C. Laurent, and U.B. Laurent, *Hyaluronan: its nature, distribution, functions and turnover*. J Intern Med, 1997. **242**(1): p. 27-33.
2. Day, A.J. and C.A. de la Motte, *Hyaluronan cross-linking: a protective mechanism in inflammation?* Trends in Immunology, 2005. **26**(12): p. 637-643.
3. Abatangelo, G., M. Martelli, and P. Vecchia, *Healing of hyaluronic acid-enriched wounds: Histological observations*. Journal of Surgical Research, 1983. **35**(5): p. 410-416.
4. Prawel, D.A., et al., *Hemocompatibility and Hemodynamics of Novel Hyaluronan-Polyethylene Materials for Flexible Heart Valve Leaflets*. Cardiovasc Eng Technol, 2014. **5**(1): p. 70-81.